

Interaction of Human Polyomavirus JC with cells of the hematopoietic system in the periphery

Dissertation zur Erlangung
des naturwissenschaftlichen Doktorgrades
der Bayerischen Julius-Maximilians-Universität Würzburg



vorgelegt von Silviu Sbiera
aus Suceava, Rumänien
Würzburg, September 2012

Eingereicht am:

Mitglieder der Promotionskommission:

Vorsitzender:

Gutachter:

Gutachter:

Tag des Promotionskolloquiums:

Doktorurkunde ausgehändigt am:

Eidesstattliche Erklärung

Ich, Silviu Sbiera versichere hiermit, dass ich diese Arbeit selbständig und nur unter Verwendung der angegebenen Quellen und Hilfsmittel angefertigt habe.

Weiterhin versichere ich, dass diese Dissertation nicht in gleicher oder ähnlicher Form in einem anderen Prüfungsverfahren vorgelegen hat. Außer dem Titel *Diplom Biologe* habe ich bisher keine anderen akademischen Titel erworben oder zu erwerben versucht.

Würzburg,

Danksagung

Ich möchte mich ganz herzlich bei Dr. Kristina Dörries bedanken für die Betreuung, sowie zahlreiche richtungsweisende aber auch manch kritische Diskussionen die für meine Weiterentwicklung als Wissenschaftler hilfreich waren.

Zusätzlich möchte ich mich bei Prof. Dr. Rüdiger Dörries bedanken für die Hilfestellung bei verschiedenen Fragestellungen und für die projektbezogene Diskussionen.

Insbesondere möchte ich mich bei unsere ehemalige technische Assistentin Nathalie Zobel bedanken für die praktische Hilfe im Labor und für die bis jetzt anhaltender Freundschaft.

Unseren Kooperationspartnern Prof. Dr. Ingo W. Husstedt und Dr. Gabriele Arendt für das Patientenmaterial.

Den Mitarbeitern und Mitarbeiterinnen des Instituts für Virologie und Immunbiologie für die angenehme Arbeitsatmosphäre, sowie für die Hilfestellung im Labor bei neuen und alten Fragestellungen.

Ich möchte mich auch bei alle meine neue Kollegen bedanken, die Mitarbeitern und Mitarbeiterinnen des Schwerpunkt für Endokrinologie der Universitätsklinikum Würzburg, für ihre Unterstützung die mir ermöglicht haben diesen Projekt zu ende zu bringen.

I especially want to thank all my friends for their support and understanding that kept me going especially, but not only, in difficult times.

In special multumesc parintilor si fratelui meu pentru ca nu au renuntat sa creada in mine, si m-au suportat moral pe toata durata vietii mele.

Table of Contents

1. INTRODUCTION	1
2. MATERIALS AND METHODS	6
2.1. Materials	6
2.1.1. Blood materials:	6
2.1.2 Cell-lines	6
2.1.3. Growth media for bacteria and cell cultures	7
2.1.4. Recombinant DNA and DNA ladders	8
2.1.4.1. Cloned virus DNA	8
2.1.4.2. Markers for electrophoretic separation	9
2.1.5. Buffers	9
2.1.6. Chemicals and enzymes:	12
2.1.7. Antibodies	13
2.1.8. Kits	14
2.1.9. Equipment	14
2.1.10. Miscellaneous	15
2.2. Methods	17
2.2.1. Escherichia coli bacterial culture for vector DNA expression	17
2.2.1.0. Preparation of agar plates	17
2.2.1.1. Growth on agar-plates	17
2.2.1.2. Growth in liquid LB-medium	17
2.2.1.3. Long term storage of bacteria	18
2.2.2. Cell Cultures as controls for the virus detection	18
2.2.2.1. Splitting adherent mammal cell cultures	19
2.2.2.2. Splitting suspension cell cultures	19
2.2.2.3. Splitting adherent insect cells in culture	19
2.2.2.4. Preparation of virus infected cells for single cell detection of viral products	19
2.2.2.5. Recombinant JC Virus infection in Sf-9 cells	20
2.2.3. DNA isolation and characterization	20
2.2.3.1. Preparation of plasmid DNA	20
2.2.3.2. Leukocyte DNA isolation	21
2.2.3.3. DNA ethanol precipitation	22

2.2.3.4. Preparation of carrier DNA solution	22
2.2.3.5. Agarose gel electrophoresis of nucleic acids	23
2.2.3.6. Purification of radioactive phosphor 32- and Digoxigenin-labeled PCR products by Sephadex G50 column chromatography	23
2.2.4. Isolation of blood cells and separation of haematopoietic subpopulations.	24
2.2.4.1. Isolation of peripheral blood mononuclear cells (PBMC) by Ficoll© density centrifugation	24
2.2.4.2. Isolation of granulocytes and PBMCs from peripheral blood by a two-step Percoll© gradient centrifugation	24
2.2.4.3. Erythrolysis	25
2.2.4.4. Viability and cell-count determination by trypan-blue exclusion	26
2.2.4.5. Separation of PBMC subpopulations by magnetic bead isolation	26
2.2.4.5.1. Magnetic isolation of peripheral blood B-cells, T-cells and monocytes by positive selection	26
2.2.4.6. Determination of the purity of separated subpopulations by FACS analysis	27
2.2.5. Detection of virus specific DNA in peripheral blood cells by polymerase chain reaction (PCR)	28
2.2.6. Specificity characterization of PCR amplified DNA fragments- using hybridization techniques	28
2.2.6.1. Transfer of PCR amplified DNA fragments on nitrocellulose membrane for further analysis using Southern Blot	28
2.2.6.2. Determining the specificity of the PCR amplified products using radioactive hybridization of Southern blots	29
2.2.6.2.1. Radioactive labeling of specific oligonucleotides as hybridization probes	29
2.2.6.2.2. Hybridization of membrane bound DNA with radioactive labeled oligonucleotide probes	31
2.2.6.3. Detection of virus DNA <i>in situ</i> using Fluorescence <i>in situ</i> Hybridization (FISH)	32
2.2.6.3.1. Fixation and permeabilization of cells on slides	32
2.2.6.3.2. Preparation of digoxigenin-labelled DNA probes for FISH	32
2.2.6.3.3. Fluorescence <i>in situ</i> hybridization with chemical amplification of the signal	36
2.2.6.3.4. Fluorescence <i>in situ</i> Hybridization without chemical amplification	38
2.2.6.4. Estimation of digoxigenin labeled DNA probe specificity by Dot-blot hybridization	38
2.2.6.4.1. Immunostaining detection of dot-blot hybridization products	38
2.2.8. Visualization of <i>in situ</i> fluorescent signals using microscopy	39

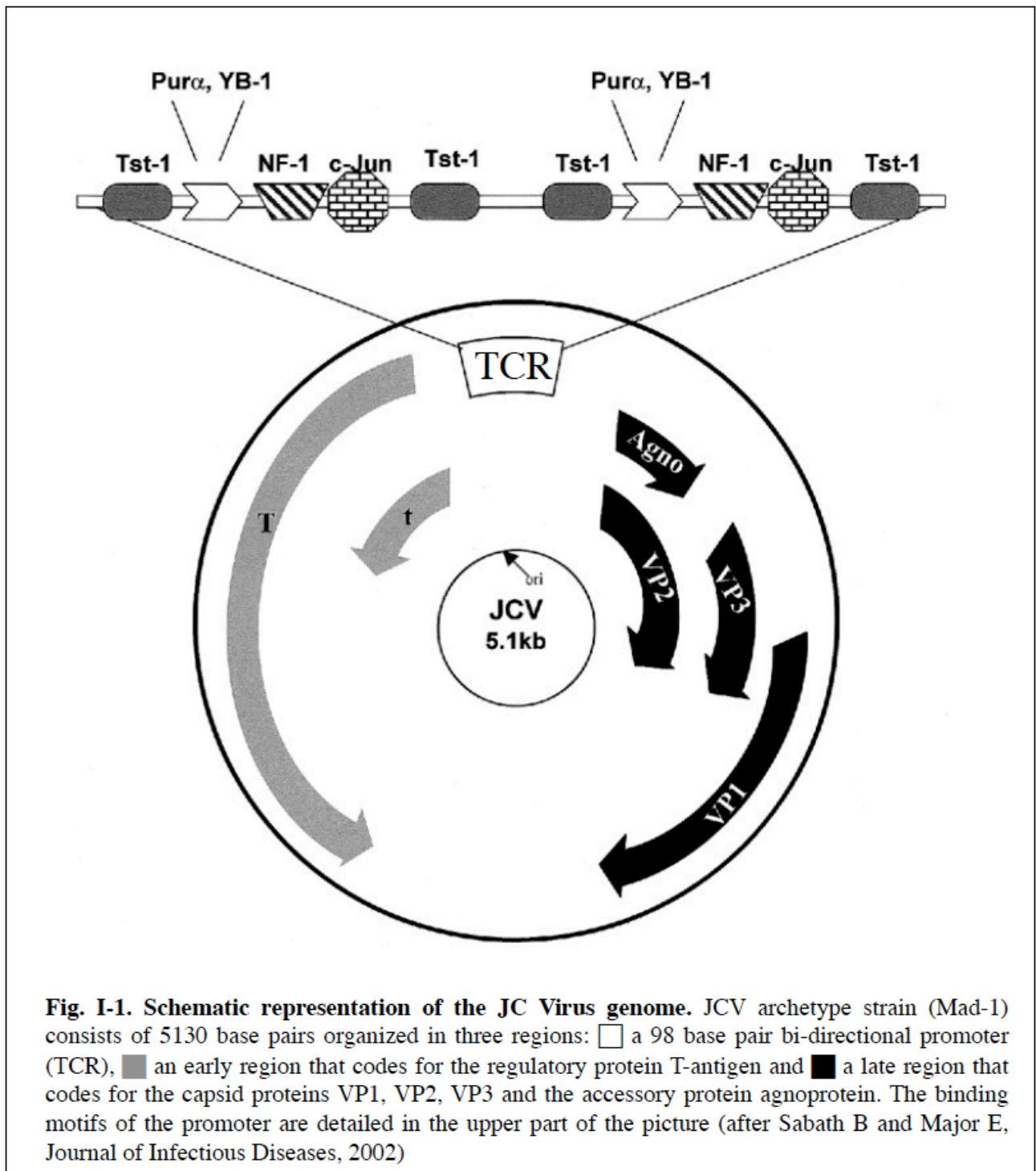
2.2.8.1. Assessing the FISH results using classical fluorescence microscopy	39
2.2.8.2. Visualization and localization of fluorescent signals using Laser Scanning Microscopy (LSM)	40
3. RESULTS	41
3.1. Aim of the study	41
3.2. Study groups for analysis of JCV infection in peripheral blood cells	41
3.3. Material collection strategy	42
3.3.1. Isolation of peripheral blood cell populations	42
3.3.1.1. Isolation of PBMCs and granulocytes by density gradient centrifugation	42
3.3.1.2. Enrichment of PBMC subpopulations by magnetic cell separation system	44
3.3.1.3. Purity of hematopoietic cell subpopulations	44
3.3.1.3.1. Purity of density gradient purified PBMCs and granulocytes	44
3.3.1.3.2. Purity of MACS isolated leukocyte subpopulations determined by FACS analysis	45
3.4. Detection of JCV DNA in peripheral blood cells	50
3.4.1. Sensitivity and specificity of the polymerase chain reaction (PCR) for the detection of JCV DNA in peripheral blood cells	50
3.4.2. Presence of JCV DNA in peripheral blood cell preparations	51
3.4.2.1. Detection of JCV DNA in peripheral blood cells of healthy blood donors	51
3.4.2.2. Detection of JCV DNA in peripheral blood cells of immune impaired patients	56
3.5. Characterization of JCV-peripheral blood cells association	60
3.5.1. Establishment of the fluorescence <i>in situ</i> hybridization technique for sub-cellular localization of JCV DNA in peripheral blood cells	60
3.5.1.1. Fixation of primary peripheral blood cells for FISH	61
3.5.1.2. Development of a highly sensitive JCV specific fluorescence probe for <i>in situ</i> hybridization	68
3.5.1.3. Detection conditions for digoxigenin-labeled hybridization probes in primary blood cells	73
3.5.1.4. JCV specificity of the FISH hybridization in single cells	79
3.5.2.1. Improvement of the in-situ visualization by deconvolution software	81
3.5.2.2. JCV localization at single cell level by confocal microscopy	83

3.5.2.3. Software based localization of JCV signals at subcellular level	83
3.5.3.1. JCV localization in peripheral blood cells	85
3.5.3.2. Rate of peripheral blood cells associated with the JCV DNA	86
3.5.3.3. Intracellular quantification of viral genomes in PBCs	92
3.5.3.4. Influence of short time immune system activation on JCV association with peripheral blood cells	96
4. SUMMARY AND DISCUSSIONS	101
5. BIBLIOGRAPHY	116
6. ABBREVIATIONS	132
7. ENGLISH ABSTRACT	134
8. GERMAN ABSTRACT	136
9. CURRICULLUM VITAE	138

1. Introduction

In 1958, Åström et al (Astrom, Mancall et al. 1958) described a CNS demyelinating disease of unknown aetiology associated with chronic lymphocytic leukaemia and lymphoma, which showed characteristic oligodendrocytopathy and giant astrocytes. This new pathological entity was named progressive multifocal leukoencephalopathy (PML). The association of the human polyomaviruses with this demyelinating disease dates from 1971 when Padgett, Walker and colleagues (Padgett, Walker et al. 1971) cultured the agent, which has first been observed in PML lesions by electron microscopy in 1965 (Zurhein and Chou 1965). The virus was named JC virus (JCV) from the name of the first PML patient.

The members of the polyomaviruses family have been isolated from a number of species, including birds, rodents, monkeys and humans. The polyomaviruses are small naked viruses with icosahedral capsids composed of three structural proteins VP1, VP2 and VP3 that tightly packs the viral DNA (Shishido-Hara, Hara et al. 2000). The DNA is double stranded, circular, supercoiled and is associated with the histones H2A, H2B, H3 and H4 in the virion and with H1 in the cells (Mueller, Graessmann et al. 1978; Zentgraf, Keller et al. 1978). The JCV genome was completely sequenced for the first time in 1984 (Frisque, Bream et al. 1984). The DNA sequence identity among the primate viruses is approximately 70%, the genomic organization of these viruses is also conserved (Schatzl, Sieger et al. 1994). The genome is divided in three regions: the noncoding transcriptional control region (TCR) containing the origin of DNA replication and the promoters, the early region encoding the regulatory proteins and a late region encoding the capsid proteins (VP1,2 and 3) (**Fig. I-1**)(Beckmann, Shah et al. 1985). The late genes encode the three structural proteins mentioned above, VP1 VP2 and VP3, are expressed from alternatively spliced mRNAs, whose transcription initiation sites are identical (Kamen, Favaloro et al. 1980). Based on *in vitro* studies it is believed that these proteins assemble first into capsid structures and then the DNA is inserted into these capsids (Salunke, Caspar et al. 1986; Forstova, Krauzewicz et al. 1993; Sandalon and Oppenheim 1997). The late region also encodes for a small multifunctional phosphoprotein, agnoprotein whose regulatory functions are still largely unknown. It has been generally attributed viroporin functions (Suzuki, Orba et al. 2010) with involvement in the virus release and propagation. Several *in vitro* studies have shown that agnoprotein deletion mutants or silencing RNA (siRNA) induced underexpression in infected cells leading to defective viral release, most of the virions released being deficient in DNA content (Matoba, Orba et al. 2008; Saribas, Arachea et al. 2011; Sariyer, Saribas et al. 2011). Involvement of agnoprotein with DNA damage and repair mechanisms has been also confirmed in the oligodendrocytes of the PML lesions and in tumor



tissues associated with JCV (Merabova, Kaniowska et al. 2008; Del Valle and Khalili 2010).

The early genes are transcribed from one strand of the genome and the late genes are transcribed in the opposite direction from the complementary strand. The early genes of the human polyomaviruses encode two major proteins, the large tumor antigen (TAg) and the small tumor antigen (tAg), the first with three different extra splice forms, T'135, T'136 and T'165, whose role is unknown (Ishaq and Stoner 1994). The early proteins are expressed from two mRNAs that derive by alternative splicing of a single primary transcript (Norbury and Fried 1987). These proteins are so named because of the early finding that they were dominant tumor antigens in animals (Black,

Rowe et al. 1963). TAg plays a major role during the early phase of infection by inducing the infected cell to enter in the S phase. This is necessary for virus multiplication because JCV does not encode for any DNA replication molecules, therefore it relies on the cellular machinery. Once DNA replication begins, TAg acts to stimulate transcription of the late genes by interacting with components of the cellular basal transcription machinery (Gruda, Zabolotny et al. 1993; Berger, Smith et al. 1996). An important player in the regulation of the JC virus life cycle is the transcriptional control region (TCR). The best described promoter is the 293bp promoter region from the JCV strain Mad-1 isolated from PML brain tissue (Tada, Lashgari et al. 1991). The Mad-1 promoter contains two characteristic tandem 98bp repeats and functions in opposite orientations to regulate early and late gene expression, respectively. In this region the expression of JCV is regulated by a series of transcription factors, including both activators and silencers (Tada, Lashgari et al. 1989). Interestingly, among the JCV activators the TCR contains consensus binding motifs for factors implicated in the lymphocytic activation pathways as nuclear factor 1 (NF-1) (Tamura, Inoue et al. 1988; Major, Amemiya et al. 1990; Sock, Wegner et al. 1991), activating transcription factor 1(AP-1) (Sadowska, Barrucco et al. 2003), nuclear factor kappa B (NFkB) (Ranganathan and Khalili 1993; Atwood, Wang et al. 1995; Safak, Gallia et al. 1999), single stranded DNA binding proteins Puralpha and cellular Y-box binding transcription factor (YB-1) (Chen, Chang et al. 1995; Safak, Gallia et al. 1999; Safak, Gallia et al. 1999) (**Fig. I-1** upper side) and a series of viral transactivators of human immunodeficiency virus-1 (HIV-1) (Tada, Rappaport et al. 1990; Daniel, Wortman et al. 2001) and human herpes virus-6 (HHV-6) (Blumberg, Mock et al. 2000).

Originally, JCV was thought to have a very restricted host and celltype specificity, replicating only in oligodendrocytes (Padgett, Rogers et al. 1977; Walker and Padgett 1983). Because of its capacity to cause demyelination in the CNS and to multiply mainly in human glial cells in culture, JCV was considered to be a neurotropic virus. However, with increasing knowledge on epidemiology and virology of the virus cell specificity had to be expanded considerably.

On the basis of the detection of JCV specific antibodies, it is estimated that more than 80% of the human population is infected by JCV (Major, Amemiya et al. 1992; Viscidi, Rollison et al. 2003). Seroconversion generally occurs during childhood, since 65% of adolescents produce JCV specific antibodies (Major, Amemiya et al. 1992; Kunitake, Kitamura et al. 1995). After asymptomatic primary infection, lifelong persistent infection is established with basic expression in immunocompetent individuals. Persistent JCV DNA was first described by PCR in kidney and other renal tissues (McCance 1983; Kitamura, Sugimoto et al. 1997; Elsner and Dorries 1998) then in colon and colorectal tissues (Laghi, Randolph et al. 1999; Altschuler 2000; Shadan, Cunningham et al. 2002), in the upper gastrointestinal tract (Ricciardiello, Laghi et al. 2000) and although

seldomly also reported in the prostate (Zambrano, Kalantari et al. 2002). Its presence in the brain of healthy individuals is still disputed (McCance 1983; Elsner and Dorries 1992; White, Ishaq et al. 1992; Vago, Cinque et al. 1996; Caldarelli-Stefano, Vago et al. 1999). A recent discovery was the detection of JCV in cells of the hematopoietic system, both in lymphoid tissues like hematopoietic progenitor cells and tonsillar stromal cells (Monaco, Atwood et al. 1996; Monaco, Jensen et al. 1998), but also in peripheral blood leukocytes (PBL). Using PCR, JCV DNA presence was demonstrated in the PBLs (Tornatore, Berger et al. 1992; Dorries, Vogel et al. 1994; Azzi, De Santis et al. 1996; Dubois, Dutronc et al. 1997), peripheral blood mononuclear cells (PBMC) (Koralnik, Schmitz et al. 1999; Dolei, Pietropaolo et al. 2000) or, more specific, in B and T cell subpopulations (Shimizu, Imamura et al. 1999; Dorries, Sbiera et al. 2003). This finding may play a crucial role in the understanding of JCV trafficking in the human organism, its transport from the entrance site to the site of lytic infection, the CNS, irrespective whether this is the gastrointestinal (Sundsford, Flaegstad et al. 1994; Bofill-Mas, Formiga-Cruz et al. 2001; Bofill-Mas and Girones 2001) or the nasopharyngeal tract (Sundsford, Spein et al. 1994). Together with the discovery of transcription activator sites with consensus binding motifs for immunological factors this is pointing to an involvement of PBC in transport and also in activation of JC virus in the human host.

JCV viraemia is closely associated with immunological disturbances. Temporary virus activation occurs under limited disturbance of the immune system as found in pregnancy (Andrews, Daniel et al. 1983) or under transplantation conditions (Andrews, Shah et al. 1988; Arthur, Shah et al. 1988; Arthur, Dagostin et al. 1989), where it was reported to be associated with nephropathy (Randhawa, Baksh et al. 2001; Hirsch, Drachenberg et al. 2006) and nephritis (Boubenider, Hiesse et al. 1999).

However, under severe immunodeficient conditions as found in lymphoproliferative diseases or in acquired immunodeficiency syndrome (AIDS), unrestricted virus growth in the CNS leads to the most prominent disease associated with human polyomaviruses, progressive multifocal leukoencephalopathy (PML) (Weber and Major 1997; Hou and Major 2000). PML is a disorder of the brain induced by lytic infection of the myelin producing oligodendrocytes by JCV (Brew, Davies et al. 2010; White and Khalili 2011). Initially as multiple foci mainly around blood vessels (Houff, Major et al. 1988) with disease progression they coalesce into plaque lesions of more than one centimeter in diameter (Sabath and Major 2002). After establishment, disease progression is very rapid, most of the patients dying within months after diagnosis (Weissert 2011). Establishment of PML is tightly associated with deficiencies of the lymphoid system. While initially associated with leukaemia and lymphoma (Astrom, Mancall et al. 1958; Major, Amemiya et al. 1992), with an increase of worldwide HIV-1 infections incidence the number of PML cases increased also, with 5-

10% of all AIDS patients developing PML (Berger and Major 1999; Cinque, Koralnik et al. 2009; Major 2010). In the last decade the number of PML associated causes increased again in the aftermath of immunosuppressive antibody therapies of autoimmune diseases (Tavazzi, Ferrante et al. 2011). While no therapeutic agent has been found to specifically affect JCV infection, in many PML cases it has been demonstrated that rapid restoration of immune function leads to stabilization and clinical improvement of PML (Khatri, Man et al. 2009; Linda, von Heijne et al. 2009) underlining the crucial importance of the immune system in the pathogenesis of JCV.

In contrast to PML, the knowledge on JCV persistent infection in healthy individuals and especially in peripheral blood cells is limited. As shown before, the cells of the peripheral blood are widely held responsible for dissemination of the virus between different sites of persistence and maybe also playing an important role in the establishment of PML as JCV DNA has been also found in the brain of non-PML patients. Most of the studies on JCV persistence have been made using PCR. However, PCR alone cannot provide any data regarding the nature of virus-cell association, whether it is an unspecific membrane association or whether there is evidence of episomal presence of viral DNA in cell nuclei, a prerequisite of JCV persistent infection. Therefore our aim was to first identify the peripheral blood cell populations more frequently associated with JC virus in healthy blood donors by PCR, and then to more intimately characterize the type of JCV interaction with these cells by localization of JCV DNA intracellularly using fluorescence *in situ* hybridization (FISH). Secondly, using the same methods, we aimed to understand the modulation of JCV-cell associations by short activation of the immune system in a subset of healthy subjects who received influenza vaccination. We further analyzed the association and intracellular distribution of JCV in the peripheral blood cell subpopulations of AIDS patients with and without established PML for a better understanding of the possible role played by leukocyte associated JCV in the establishment of PML.

2. Materials and Methods

2.1. Materials

2.1.1. Blood materials:

Buffy Coats (BC), Leukocytes Removing Filters (LRF) and Leukopheresis (LKF) from healthy blood donors (Abteilung für Transfusionmedizin und Immunhämatologie der Universitätsklinikum Würzburg)

Natrium citrate treated blood from healthy laboratory personnel (Institut für Virologie und Immunbiologie der Universität Würzburg - Abteilung Virusdiagnostik),

Natrium citrate treated blood from HIV-1 patients with and without established progressive multifocal leukoencephalopathy (PML) were kindly provided by Professor Dr. Ingo W. Husstedt, Neurologische Klinik, Universitätsklinikum Münster and Professor Dr. Gabriele Arendt, Neurologische Klinik, Universitätsklinikum Düsseldorf. HIV-1 diagnosis and classification were performed according to the international standard recommendation by the Centers of Disease Control and Prevention (CDC)/World Health Organization (WHO) (Schneider, Whitmore et al. 2008) and PML diagnosis according to established clinical procedures (von Giesen, Neuen-Jacob et al. 1997; Weber 2008)

2.1.2 Cell-lines

HJC-15 permanent cell-line from a hamster glioma which expresses JCV-T-Antigen (Walker, Padgett et al. 1973)

H7BK permanent cell-line from a Syrian hamster choroid plexus papilloma, which expresses BKV-T-Antigen (Greenlee, Narayan et al. 1977)

Vero permanent cell-line from an African green-monkey kidney cells (Yasumura and Kawakita 1963)

CV1 permanent cell-line from an African green-monkey kidney cells (Jensen, Girardi et al. 1964)

Sf9 permanent cell-line derived from pupal ovarian tissue of the fall armyworm, *Spodoptera frugiperda* (Smith, Summers et al. 1983)

FL4	permanent feline lymphoblastoid cell-line persistantly infected with Feline Immunodefficiency Virus (FIV) strain Petaluma (Yamamoto, Ho et al. 1986)
293	permanent cell-line from Adenovirus type 5 transformed human embryonal kidney cells (Graham, Smiley et al. 1977)
Raji	permanent cell-line from an Epstein-Barr Virus (EBV) transformed human B-cell lymphoma (Pulvertaft 1965)
Jurkat	permanent cell-line from an Epstein-Barr Virus (EBV) transformed human T-cell lymphoma (Schneider, Schwenk et al. 1977)
P3HR1	permanent cell-line from an Epstein-Barr Virus (EBV) transformed human B-cell lymphoma (Hinuma and Grace 1967)
BJAB	permanent cell-line from an Epstein-Barr Virus (EBV) transformed human B-cell lymphoma (Menezes, Leibold et al. 1975)
HEL	human erythroleukemia cell line with spontaneous and induced globin expression (Martin and Papayannopoulou 1982)

2.1.3. Growth media for bacteria and cell cultures

LB-Medium	Bacto-Trypton	1%
	Yeast extract	0.5%
	NaCl	0.5%
	pH value	7.3
MEM medium (Gibco BRL)	Modified Eagle's Medium (MEM)	
	NaHCO ₃	2.2 g/l
	FCS (PAN)	10%
	L-Glutamine	2.5mM
	Penicillin/Streptomycin	0.001%

RPMI medium (Gibco BRL)	RPMI 1640	
	FCS (PAN)	10%
	L-Glutamine	2.5mM
	Penicillin/Streptomycin	0.001%
TC100 medium (Biochrom)	TC100 medium	
	FCS Gold (PAA)	10%
	L-Glutamine	2.5mM
	Penicillin/Streptomycin	0.001%
	Refobacin	50µg/ml
	Amphotericin	2.5µg/ml

2.1.4. Recombinant DNA and DNA ladders

2.1.4.1. Cloned virus DNA

Plasmid	Characterization	Reference
pJCV-GS/B clone 211	entire JCV-GS/B genome cloned in BamHI restriction site of pBluescript SK(+); JCV-GS/B variant was isolated from neuronal tissue of a PML patient	(Loeber and Dorries 1988)
pJCV-GS/B clone 19	entire JCV-GS/B genome cloned in EcoRI restriction site of pUC	(Loeber and Dorries 1988)
pJCV-GS/K clone 9	entire JCV-GS/K genome cloned in EcoRI restriction site of pUC12 ; JCV-GS/K variant was isolated from kidney tissue of a PML patient	(Loeber and Dorries 1988)
pJCV-Mad-1 clone 99	entire JCV-Mad-1 genome cloned in BamHI restriction site of pBR322 ; JCV-Mad-1 variant was isolated from brain of a PML patient	(Frisque, Bream et al. 1984)
pBKV clone 733	entire BKV genome cloned in BamHI restriction site of the pBluescript	(Dorries, Vogel et al. 1994)

2.1.4.2. Markers for electrophoretic separation

Number	Plasmid	Provenience	Fragments length
M31	pBluescript KS(+)	Restriction with <i>MspI</i>	710, 489, 404, 367, 242, 190, 157, 147, 110 bp
M30	pMal-c2	Restriction with <i>MspI</i>	1264, 763, 527, 443, 392, 381, 316, 309, 242, 241, 202, 190, 180, 156, 147, 123 bp
M19	l-DNA	Restriction with HindIII and EcoRI	21226, 5148, 4973, 4268, 3530, 2027, 1904, 1584, 1375, 947, 831 bp
L100	-	Gibco, Rockville, USA	100 bp ladder from 100 to 1500bp and an extra band at 2072bp

2.1.5. Buffers

PBS (-)	NaCl	154mM
	Na ₂ HPO ₄	8.1mM
	NaH ₂ PO ₄	1.2 mM
	pH	7.4

This buffer was prepared at the core facility of the institute

PBS (+)	NaCl	154mM
	Na ₂ HPO ₄	8.1mM
	NaH ₂ PO ₄	1.2 mM
	CaCl ₂	0.9mM
	MgCl ₂	0.5mM
	pH	7.4

This buffer was prepared at the core facility of the institute

20xSSC	NaCl	3M
	Na ₃ Citrate	0.3M
	pH	7.0

5xTBE	Tris	0.5M
	H ₃ BO ₃	0.5M

Materials and Methods: Materials

	EDTA	10mM
	pH	8.3
50xTAE	Tris	2M
	Acetic acid	5.7%
	EDTA	0.5M
	pH	8.0
Denaturation buffer for Southern Blot	NaCl	1.5M
	NaOH	0.5M
Neutralization buffer for Southern Blot	NaCl	3M
	Tris-HCl	0.5M
	pH	5.0
DNA Loading buffer for electrophoreis	Glycerine	75%
	Bromphenol Blue	0.25%
	Xylencyanol	0.25%
DNA Lysis buffer 1(-SDS) for leukocyte DNA isolation	NaCl	0.5M
	Tris	0.1M
	pH	8.1
	Proteinase K	200µg/ml
2xDNA Lysis buffer 2 (+SDS) for leukocyte DNA isolation	NaCl	0.5M
	Tris	0.1M
	pH	8.1
	Proteinase K	200µg/ml
	SDS	2%
5xSTE buffer for Sephadex DNA purification	Tris/HCl	100mM
	NaCl	0.5M
	EDTA	5mM
	pH	8.0

Erythrolysis buffer: (LRF washing buffer)	NH ₄ Cl	155mM
	KHCO ₃	10mM
	EDTA	10μM
	pH	8
MB buffer for immuno-magnetic separation of PBMC subpopulations	BSA	0.5%
	EDTA	2mM
	NaN ₃	0.02% (w/v)
	in PBS (-)	
Flow Cytometry (FACS) buffer	BSA	0.1% (w/v)
	NaN ₃	3mM
	in PBS (+)	
TN buffer for Fluorescence <i>in situ</i> Hybridization (FISH)	Tris-HCl	100mM
	NaCl	150mM
	pH	7.5
TNB buffer for FISH	Tris-HCl	100mM
	NaCl	150mM
	casein	0.5%
	pH	7.5
TNT buffer for FISH	Tris-HCl	100mM
	NaCl	150mM
	Tween 20	0.05%
	pH	7.5
DNA-DNA hybridization buffer for FISH	Formamide	50%
	SSC	5x
	Denhardt solution	1x

	HSP-DNA (denat)	200µg/ml
Radioactive hybridization buffer	SSC	6x
	Denhardt solution	5x
	SDS	0.5%
	HSP DNA	100 ng/ml

2.1.6. Chemicals and enzymes:

Acetic anhydride	Merck, Darmstadt, Germany
Agar	Difco, Detroit, USA
Agarose (electrophoresis grade)	Invitrogen, Karlsruhe, Germany
Ammoniumchlorid	Merck, Darmstadt, Germany
Bromphenyl blue	Merck, Darmstadt, Germany
BSA	Sigma-Aldrich, Taufkirchen, Germany
Buthanol	Merck, Darmstadt, Germany
Chloroform	Roth, Karlsruhe, Germany
Denhardt	Sigma-Aldrich, Taufkirchen, Germany
Deoxynucleotide triphosphates	Invitrogen, Karlsruhe, Germany
Diethylether	Ferak, Berlin, Germany
Digoxigenin-11-dUTP	Roche Diagnostics, Mannheim, Germany
Dimethylsulfoxid (DMSO)	Merck, Darmstadt, Germany
Ethanol	Roth, Karlsruhe, Germany
Ethidium bromide	Serva, Heidelberg, Germany
EDTA	Roth, Karlsruhe, Germany
Ficoll Paque Plus	Amersham Biosciences, Freiburg, Germany
FCS	PAN, Aidenbach, Germany
FCS Gold	PAA Laboratories, Linz, Austria
Glycine	Merck, Darmstadt, Germany
Glycerine	Roth, Karlsruhe, Germany
Herring sperm (HSP) DNA	Sigma-Aldrich, Taufkirchen, Germany
Isopropanol	Merck, Darmstadt, Germany
MEM	Invitrogen, Karlsruhe, Germany
Natrium acetate	Merck, Darmstadt, Germany

Natrium azide (NaN ₃)	Merck, Darmstadt, Germany
tri-Natrium citrate	Roth, Karlsruhe, Germany
Natrium chloride (NaCl)	Roth, Karlsruhe, Germany
Natrium hydrogencarbonate (NaHCO ₃)	Merck, Darmstadt, Germany
Natrium hydroxide (NaOH)	Merck, Darmstadt, Germany
Paraformaldehyde	Science Services, Munich, Germany
Pepsine	Kreatech, Amsterdam, The Netherlands
Percoll	Amersham Biosciences, Freiburg, Germany
(saturated with Tris, pH 7.4)	Phenol Roth, Karlsruhe, Germany
Proteinase K	Roche Diagnostics, Mannheim, Germany
α-[³² P]-dATP	Amersham Biosciences, Freiburg, Germany
Restriction endonucleases	New England Biolabs, Beverly, USA
RPMI 1640	Gibco, Rockville, USA
Autoradiographic films	Sterling Diagnostics Imaging, Newark, USA
Sephadex G 50	Pharmacia, Uppsala, Sweden
Streptavidin-Texas Red	Molecular Probes, Eugene, USA
Sytox-blue	Molecular Probes, Eugene, USA
Taq Polymerase	Invitrogen, Karlsruhe, Germany
Terminal Transferase (TdT)	Roche Diagnostics, Mannheim, Germany MBI Fermentas, Vilnius, Lithuania
TO-PRO-3 iodide	Molecular Probes, Eugene, USA
Triethanol amine	Merck, Darmstadt, Germany
Tris	Roth, Karlsruhe, Germany
Triton X-100	Sigma-Aldrich, Taufkirchen, Germany
Trypan blue	Sigma-Aldrich, Taufkirchen, Germany
Trypton	Difco, Detroit, USA
Tween 20	Sigma-Aldrich, Taufkirchen, Germany

2.1.7. Antibodies

Anti Digoxigenin, monoclonal mouse	Roche Diagnostics, Mannheim, Germany
Anti mouse from goat, HRP labeled	Dako A/S, Glostrup; Denmark
Anti mouse from goat, Texas Red labeled	Molecular Probes, Eugene, USA Jackson ImmunoResearch, West Grove, USA

Anti Digoxigenin from goat, FITC labeled	Roche Diagnostics, Mannheim, Germany
Anti SV40 Tag, monoclonal mouse	Oncogene, Boston, USA
Anti Dinitrophenyl from rabbit, KLH- -labeled	Molecular Probes, Eugene, USA
Anti JCV capsid proteins from rat	Laboratory made
Anti BKV capsid proteins from rat	Laboratory made
Anti rat IgG from rabbit, HRP labeled	Jackson Immunoresearch, West Grove, USA
Normal Goat serum	PAA Laboratories, Linz, Austria
Normal Rabbit serum	PAA Laboratories, Linz, Austria
Anti human CD3, mouse, FITC labeled	Immunotech, Marseille, France
Anti human CD14, mouse, PE labeled	Immunotech, Marseille, France
Anti human CD19, mouse, FITC labeled	Immunotech, Marseille, France
Simultest human CD3-FITC/CD19-PE	BD Biosciences, San Jose, USA
Anti human CD3,CD14,CD19, CD66b monoclonal mouse, magnetic beads coupled	Miltenyi Biotech, Bergisch Gladbach, Germany

2.1.8. Kits

Situs Control Kit	Situs Chemicals, Düsseldorf, Germany
Ulyses DNP Labeling Kit	Kreatech, Amsterdam, The Netherlands
TSA Amplification Kit	NEN Life Science Products, Boston, USA
Jet-Star Plasmid Midi-Prep Kit	Genomed, USA
Midi-MACS separation Kit	Miltenyi Biotech, Bergisch Gladbach, Germany

2.1.9. Equipment

Automatical Pipette-Boy	Hirschmann,
Automatical Pipettes	Gilson, Middleton, USA
Bacterial Incubator	Heraeus, Hanau, Germany
Bacterial Shaker	Infors ITE, Bottmingen, Switzerland
Centrifuges	
Rotanta RSC	Hettich, Kirchlengern, Germany
EBA 20	Hettich, Kirchlengern, Germany
RC5	Sorvall, Newtown, USA

Microfuge 18	Beckmann Coulter, Krefeld, Germany
FACS-Calibur cytometer	BD Biosciences, San Jose, USA
Hybridization water baths	Julabo, Seelbach, Germany
	Heinse Ziller, Würzburg, Germany
Microscopes	
LSM Meta 510	Zeiss, Jena, Germany
Aristoplan	Leica, Wetzlar, Germany
PCR Hood	Appligene, Illkirch, France
PCR machine	MJ Research, Watertown, USA
pH Meter	WTW, Weilheim, Germany
Photometers	Zeiss, Jena, Germany
	Pharmacia, Uppsala, Sweden
Sterile Bank	Gelaire Flow Laboratories, Opera, Italy

2.1.10. Miscellaneous

Cell-culture bottles	Greiner Bio-One, Frickenhausen, Germany
Chromatography paper	Whatmann, Maidstone, England
Cover slips	Langenbrinck, Teningen, Germany
	Knittel Gläser, Braunschweig, Germany
Flow cytometry tubes	BD Biosciences, San Jose, USA
Glass slides	Knittel Gläser, Braunschweig, Germany
Injection needles	Dispomed, Gelnhausen, Germany
ISPCR slides, discs and clips	Applied Biosystems, Foster City, USA
Kryotubes	Greiner Bio-One, Frickenhausen, Germany
Nylon membrane Hybond-N	Amersham Biosciences, Freiburg, Germany
Nitrocellulose membrane Protran	Schleicher&Schuell, Dassel, Germany
PAP-pen	Dako A/S, Glostrup, Denmark
Parafilm	American National Can, Neenah, USA
PCR reaction tubes	Greiner Bio-One, Frickenhausen, Germany
Plastik Pipettes	Corning Inc., Corning, USA
	Sarstedt, Nümbrecht, Germany
Plastic tubes Falcon 15 and 50 ml	BD Biosciences, San Jose, USA
Syringes	BD Biosciences, San Jose, USA

Ultracentrifugation tubes Corex 15 ml Cole-Parmer, Vernon Hills, USA

2.2. Methods

2.2.1. Escherichia coli bacterial culture for vector DNA expression

2.2.1.0. Preparation of agar plates

LB Medium:	Bacto-Trypton	1%
	Yeast extract	0.5%
	NaCl	0.5%
	pH value	7.3
LB-Agar:	Bacto-agar	2%
	Ampicillin	50µg/ml
	in LB Medium	

Agar was solved in the LB medium, autoclaved and 50µg/ml ampicillin was added at 40°C, under permanent mixing. The agar was poured under sterile conditions in Petri dishes, and stored at 4°C.

2.2.1.1. Growth on agar-plates

For isolation of single colonies, bacteria were smeared on LB-agar-plates. This was done with the help of a sterile inoculation eye by successive zigzag movements on the surface of the LB-agar surface. Ampicillin insured positive selection of ampicillin resistant transformed bacteria. The bacteria were incubated over-night at 37 °C. The plates were kept at 4°C sealed with Parafilm until needed.

2.2.1.2. Growth in liquid LB-medium

LB-medium was supplemented with 50µg/ml ampicillin for bacterial growth. From the agar-plates a single colony of E.coli was transferred in 3ml LB-medium and subsequently incubated in aerobic conditions in the rotation shaker at 37°C and 220 rpm. After six hours a volume of 500 µl preculture was transferred in 50 ml LB-medium in a 250 ml Erlenmeyer beaker, and incubated over-night at 37°C and 180 rpm.

2.2.1.3. Long term storage of bacteria

For the storage of bacteria, 700 µl of liquid bacterial culture was mixed with 700µl glycerin in a sterile Kryotube (Greiner, Germany). This bacterial suspension was frozen slowly in -70°C then the tubes were transferred in liquid nitrogen. For bacterial growth a small amount was taken out with a sterile inoculation eye and seeded on a LB-agar plate.

2.2.2. Cell Cultures as controls for the virus detection

FCS	inactivated for 30 minutes at 56°C	
L-Glutamine	350mM in PBS	
Medium for adherent mammal cells	MEM/2.2 g/l NaHCO ₃	
	FCS (PAN)	10%
	L-Glutamine	2.5mM
	Penicillin/Streptomycin	0.001%
Medium for suspension cell-culture	RPMI 1640	
	FCS (PAN)	10%
	L-Glutamine	2.5mM
	Penicillin/Streptomycin	0.001%
Medium for Sf-9 insect cell-culture	TC100	
	FCS Gold (PAA)	10%
	L-Glutamine	2.5mM
	Penicillin/Streptomycin	0.001%
	Refobacin	50µg/ml
	Amphotericin	2.5µg/ml

2.2.2.1. Splitting adherent mammal cell cultures

Trypsine-EDTA	NaCl	136mM
	KCl	5.4mM
	D (+) Glucose	5.5mM
	Trypsine	0.05%(w/v)
	EDTA	0.02%(w/v)

After discarding the medium from adherent cell cultures, the cells were washed two times with trypsin 0.05%, incubated for 5 minutes at 37°C and resuspended in culture medium. Subsequently the cells were splitted 1:4 up to 1:10 depending on the rate of cell-growth, transferred in new culture bottles and refilled with the respective amount of medium.

2.2.2.2. Splitting suspension cell cultures

The cells in suspension culture were thoroughly resuspended in the medium by pipetting. Depending on the growth rate of the respective cell-type, 1:4 to 1:10 of the volume was transferred in new bottles and completed with new medium.

2.2.2.3. Splitting adherent insect cells in culture

After discarding the culture medium, cells were re-suspended by squirting 10 ml medium several times over the cells with a thin pipette and a Peleus ball. Thoroughly resuspended cells were splitted 1:2 in new culture bottles and supplemented with new medium.

2.2.2.4. Preparation of virus infected cells for single cell detection of viral products

Incubation Medium	MEM	500ml
	L-glutamine	2.5mM
	Penicillin/Streptomycin	0.001%
	Virus stock	7x10 ⁷ PFU/ml

BKV and SV40 virus infections were performed on the adherent cell-lines Vero, HEL and CV1. Glass-slides were deposited in 18cm ϕ Petri dishes and autoclaved. Under sterile conditions, 3-4x10⁷ adherent cells were seeded and the slides were incubated with standard culture medium at

37°C, 5%CO₂ until a monolayer was formed. The medium was removed and the cells were washed once with PBS. Incubation medium containing 20PFU/cell infectious virus was added and the virus was adsorbed for one hour. The Petri dishes were completed with standard culture medium and incubated at 37°C, 5%CO₂. The cells were kept under microscopic surveillance until a CPE was visible. Subsequently the slides were washed shortly in PBS and appropriately fixed.

2.2.2.5. Recombinant JC Virus infection in Sf-9 cells

Incubation Medium	TC100	500ml
Recombinant JCV VP1 in baculovirus (JCV GS/B clone 19)		5x10 ⁷ PFU/ml

Glass-slides were autoclaved in 18cm ϕ Petri dishes, 3-4x10⁷ adherent Sf-9 cells were seeded and incubated at 27°C, 5%CO₂ for 1 hour in complete culture medium, until they formed a monolayer. The culture medium was removed, the slides were covered with incubation medium containing 10PFU/cell infectious JCV VP1 recombinant baculovirus and the virus was adsorbed for one hour. The Petri dishes were completed with culture medium and incubated at 27°C, 5%CO₂. The cells were kept under microscopic surveillance until CPE was observed. Subsequently, the slides were taken out from the culture and then appropriately fixed.

2.2.3. DNA isolation and characterization

2.2.3.1. Preparation of plasmid DNA

E1 Buffer	Tris/HCl (pH 8)	50mM
	EDTA	10mM
	RNase A	100 μ g/ml
E2 Buffer	NaOH	200mM
	SDS	1% w/v
E3 Buffer	CH ₃ COOK	100mM
	pH	5.5
E4 Buffer	NaCl	600mM
	CH ₃ COONa	100mM
	Triton X-100	0.15%(v/v)
	pH	5.0

E5 Buffer	NaCl	800mM
	CH ₃ COONa	100mM
	pH	5.0
E6 Buffer	NaCl	1.25 M
	Tris/HCl (pH 8.5)	100mM
	pH	8.5

The isolation of plasmid DNA from up to 50 ml bacterial culture was performed with the Jetstar Midi-preparations system (Genomed, Germany). 50 ml suspension culture (see bacterial growth) was centrifuged at 5000g for 5 min. at 4°C in a Sorvall centrifuge. The supernatant was removed and the bacterial pellet was re-suspended in 4 ml buffer E1 and immediately 4 ml buffer E2 was added and carefully mixed together. After 5 minutes incubation at room temperature 4ml buffer E3 was added and thoroughly mixed until a precipitate appeared. The content was centrifuged at 13000 g for 10 minutes at 4°C. The elution columns were equilibrated with 10 ml buffer E4 and the supernatant from the ultracentrifugation was added. After complete flow-through the columns were washed twice with 10 ml buffer E5 and subsequently the plasmid DNA was eluted with 5 ml E6 buffer in a 15 ml Corex tube. DNA was precipitated with 3.5 ml isopropanol at room temperature and centrifuged at 10000 g for 30 minutes at 4°C. The supernatant was removed and the pellet washed with 5 ml 70% ethanol at 10000 g for 10 minutes at 4°C. After ethanol removal, the new pellet was air dried and the DNA was resuspended in 150 µl 10mM Tris buffer. The DNA concentration was determined photometrically.

2.2.3.2. Leukocyte DNA isolation

DNA Lysis Buffer 1(-SDS)	NaCl	0.5M
	Tris	0.1M
	pH	8.1
	Proteinase K	200µg/ml
2xDNA Lysis Buffer 2 (+SDS)	NaCl	0.5M
	Tris	0.1M
	pH	8.1
	Proteinase K	200µg/ml

SDS

2%

The cells were centrifuged at 800g for 10 minutes at RT, washed with 10ml PBS and re-centrifuged. The cell pellet was resuspended in Lysis buffer 1. For 5×10^7 cells 500 μ l of buffer was used. The lysate was mixed with 500 μ l Lysis Buffer 2 and incubated over night at 37°C. The cell lysate was emulsified with the same volume of phenol for 15 minutes at room temperature in a Reax (IKA, Germany). The phases were separated by centrifugation at 3000 g for 10 minutes at RT, and the water-phase was re-extracted until no interphase was visible. Subsequently, the resulting DNA solution was extracted 3 times with chloroform and the concentration of DNA was increased by extraction with 0.5 volumes of 2-butanol. The 2-butanol was removed by a double diethyl-ether extraction. Residual ether was evaporated in a vacuum centrifuge at 1000g for at least 3 hours at RT. The DNA solution was concentrated by ethanol precipitation.

2.2.3.3. DNA ethanol precipitation

The DNA solution was mixed with a tenth part of its volume 3M Natrium-acetate solution (pH 5.2) and 2.5 volumes ice cold (-20°C) ethanol absolute. The mixture was incubated over night at 4°C and centrifuged at 10000rpm for 30 minutes at 4°C in 15 ml Corex tubes (DuPont, France) in a HB-4 rotor (Sorvall, Germany). The pellet was washed with 70% ethanol and recentrifuged for 10 minutes at 10000rpm at 4°C. The supernatant was carefully removed and the DNA was air-dried and resuspended in 10mM Tris buffer, pH 7.4. The DNA concentration was determined using a GeneQuant photometer (Pharmacia, Denmark).

2.2.3.4. Preparation of carrier DNA solution

100 mg herring sperm DNA (HSP)(Sigma) was diluted in 20 ml distilled water at 37°C for 2 hours. The solution was extracted with the same volume of phenol for 15 minutes and the phases were separated at 3000 rpm (Rotanta, Hettich, Germany) for 15 min. at RT. The water phase was extracted with a phenol/chlorophorm/isoamylalcohol (25/24/1) mixture and then with chloroform alone. The DNA was precipitated at RT by adding 0.1volume of NaAcetate (pH5.2) and 2.5 volumes ethanol absolute. The precipitate was centrifuged in Corex tubes for 30 min. at 10000rpm and 4°C in a HB4 rotor (Sorvall, Germany). The supernatant was removed and the pellet was washed with 70% ethanol, recentrifuged at 10000rpm for 10min. at 4°C, then air-dried. The DNA was resuspended in 10 mM Tris at a final concentration of 10mg/ml.

2.2.3.5. Agarose gel electrophoresis of nucleic acids

Ethidium Bromide stock	Ethidium bromide in H ₂ O	1mg/ml
Loading Buffer	Glycerin	75% (v/v)
	Brome-phenol Blue	0.25% (w/v)
	Xylencyanol	0.25% (w/v)
TBE Buffer	Tris	0.1M
	H ₃ BO ₃	0.1M
	EDTA	2mM
	pH	8.3
TAE Buffer	Tris	0.02M
	Acetic acid	0.11%
	EDTA	0.01M
	pH	8.0

The electrophoretic separation of nucleic acids and labeled amplification products was performed on flat bed agarose gel electrophoresis in either TBE buffer or TAE buffer for Southern blotting with ethidium bromide at a final concentration of 0.5µg/ml. Agarose gels of 1 to 2% were used for DNA fragments at a length of 100 to 5000 bp. DNA samples were mixed with 0.2 volumes loading buffer and separation was done by applying an electrical tension of 6-9 V/cm_{gel-length}. The visualization of the DNA bands was performed by UV light (Intas, Germany).

2.2.3.6. Purification of radioactive phosphor 32- and Digoxigenin-labeled PCR products by Sephadex G50 column chromatography

1xSTE Buffer	Tris/HCl	10mM
	NaCl	100mM
	EDTA	1mM
	pH	8.0

Sephadex G-50 resin (Pharmacia, Denmark) was soaked overnight in 1xSTE buffer. 1ml syringes were used as columns after stamps were removed and the discharge openings were blocked with glass wool. They were placed in 15 ml Falcon tubes and were filled close to the edge by repeated steps of pipetting Sephadex G50 suspension following centrifugation (4 min. at 1000rpm Rotanta (Hettich, Germany)). Subsequently the columns were washed 3 times with 200µl 1xSTE and transferred in new 15ml Falcon tubes containing open 1.5ml Eppendorf tubes. 100µl of the labeled mixture was applied on the column after the last wash and centrifuged for 4 min. at 1000rpm. The solution containing labeled oligonucleotides or DNA fragments were collected in the Eppendorf tubes, while the un-incorporated nucleotides remained inside the column and were discarded. The amplicons were stored at -20°C and the labeled oligonucleotides were used immediately for radioactive hybridization.

2.2.4. Isolation of blood cells and separation of haematopoietic subpopulations.

2.2.4.1. Isolation of peripheral blood mononuclear cells (PBMC) by Ficoll© density centrifugation

Peripheral blood samples were diluted 1:1 with Versene buffer. In a 15 ml Falcon tube 5 ml Ficoll-Paque (Pharmacia, Denmark) were pipetted. 10 ml blood/Versene mixture was carefully pipetted on top of the Ficoll-Paque layer without disturbing the interface and centrifuged at room temperature at 1600 rpm for 30 minutes in a low speed centrifuge. After centrifugation the granulocytes and the erythrocytes were located at the bottom of the tube, while the PBMC formed a ring at the interface between the Ficoll cushion and the plasma. The plasma was removed, subsequently the PBMCs were recovered. The cells were washed 2 times with Versene buffer to eliminate the contaminant thrombocytes. The PBMCs were resuspended in 5 ml ice-cold Versene buffer. Before other experiments were performed, cells were counted and the percentage of living cells were determined by trypan-blue exclusion (Strober 2001).

2.2.4.2. Isolation of granulocytes and PBMCs from peripheral blood by a two-step Percoll© gradient centrifugation

Percoll 1.077 g/ml (ca. 62%)	Percoll	62% (v/v)
	NaCl	150mM
	EDTA (pH 7.4)	10mM

Percoll 1.090 g/ml (ca. 74%)	Percoll	74% (v/v)
	NaCl	150mM
	EDTA (pH 7.4)	10mM

Percoll (Pharmacia, Denmark) was diluted to densities of 1.077 (62%) and 1.090 g/ml (74%) in 150mM NaCl and 10mM EDTA. To avoid volume changes all solutions were used at room temperature.

Peripheral blood samples were diluted 1:1 with Versene Buffer. 2.5 ml of Percoll 1.077g/ml was pipetted at the bottom of a 15ml Falcon tube and 2.5ml of Percoll 1.090g/ml were underlayered. 5ml of blood/Versene mixture were pipetted on top of each Percoll gradient. The tubes were centrifuged at 600g for 35min. at RT, without brakes. The plasma was removed, the PBMCs were recovered from the upper ring at the interface between the plasma and the first Percoll layer and granulocytes from the second ring between the two Percoll solutions. Granulocytes and PBMCs were washed separately 2 times with Versene. In case of erythrocyte contamination the cells were washed with ERB Washing Buffer. Finally, the cells were resuspended in 5 ml Versene and put on wet ice. The cells were counted and the percentage of living cells was determined by trypan-blue exclusion.

2.2.4.3. Erythrolisis

Erythrocyte Removing Buffer : (ERB)	NH ₄ Cl	155mM
	KHCO ₃	10mM
	EDTA	10μM
	pH	8.0

Erythrocyte contamination of leukocyte preparations was removed by treatment with 50ml ERB buffer for a maximum of 10 minutes on ice (Casareale, Pottathil et al. 1992). The state of erythrolisis was observed as the cell-suspension became clearer. The cells were subsequently centrifuged at 400 g for 10 min. at 4°C. The supernatant was removed and in case of uncompleted removal of the erythrocytes, the lysis process was repeated. After erythrolisis, the cells were resuspended in 5 ml Versene Buffer and stored on wet ice.

2.2.4.4. Viability and cell-count determination by trypan-blue exclusion

The total cell-count (alive and dead cells) was determined using a Neubauer-Hemocytometer. 10 μ l of the cell-suspension were diluted 1:10 in PBS, and 10 μ l Trypan-blue solution was added. The mean value of the cell-count of the four big squares was multiplied with the chamber factor of 1×10^4 and the dilution factor resulting in the cell-count per milliliter of cell-suspension. The dead cells (stained blue with trypan blue) were counted separately and reported to the total number of cells counted.

2.2.4.5. Separation of PBMC subpopulations by magnetic bead isolation

For the immunomagnetic separation of leukocyte subpopulations based on the characteristic cell surface molecules, the Magnetic Activated Cell Separation (MACS) system was used (Miltenyi, Germany). The micro particles used by this system are super paramagnetic, so they manifest the magnetic effect only when they are in a magnetic field. These particles are directly coupled with monoclonal antibodies directed against the cell specific cluster designation molecules (CD). The mixture of magnetically labeled and unlabeled cells in suspension are passed through a column filled with paramagnetic material, situated in an intense magnetic field. The labeled cells will be hold back inside the column while the others will pass through. Upon removal of the column from the magnetic field, the separated cells are washed through with a powerful buffer-flow.

2.2.4.5.1. Magnetic isolation of peripheral blood B-cells, T-cells and monocytes by positive selection

MACS Buffer:	BSA	0.5%
	EDTA	2mM
	NaN ₃	0.02% (w/v)
	in PBS (-)	

The buffer is de-gassed over-night under vacuum conditions.

For the positive selection of subpopulations (B-cells, T-cells, monocytes) from PBMC, magnetically coupled monoclonal mouse antibodies specific for CD19 (B-cells), CD3 (T-cells) and CD14 (monocytes) were used. Separated PBMCs were centrifuged 10 min. at 400g at 4°C and resuspended in 80 μ l ice-cold MACS buffer per 10^7 cells. Per 80 μ l cell suspension 20 μ l from the

first magnetically labeled antibody were added and mixed shortly followed by 15 minutes incubation at 4°C. The cells were washed with 10-20 volumes MACS buffer and subsequently centrifuged for 10 minutes at 400g at 4°C. The washing was repeated and the cells were resuspended in 500µl MACS buffer per 10⁸ cells. A MiniMACS-column was placed in the MACS magnet unit and equilibrated with 500µl MACS buffer. 500µl MACS labeled cell suspension was carefully pipetted inside the upper column reservoir without creating air bubbles. After run-through, the column was washed four times with 500µl MACS buffer. Subsequently, the column was removed from the magnetic field, placed in a 15ml Falcon tube, and bound cells were eluted with 1ml MACS buffer. On the run-through cells the process was repeated with the other antibodies. The cell-count was determined and the purity of the selected cells was analyzed by Fluorescence Activated Cell Sorting (FACS).

2.2.4.6. Determination of the purity of separated subpopulations by FACS analysis

FACS buffer	BSA	0.1% (w/v)
	NaN3	3mM
	in PBS	
6% Paraformaldehyde solution	Paraformaldehyde	6%
	in PBS	
	pH	7.2

Paraformaldehyde (Merck, Germany) was solved in PBS at 70°C and the pH was adjusted after cooling. The solution was subsequently filtered through a membrane filter with 0.22µm pores and stored at 4°C in the dark.

Purified granulocytes, PBMC and subpopulations were analyzed in flow-through cytometry (FACS) according to their phenotype and specific membrane cell markers. The fluorescent labeling of purified leukocytes was performed on 1x10⁴ - 2x10⁵ cells at maximum. All buffers and solutions were kept ice-cold. Cells were pipetted in a FACS tube, centrifuged for 10 min. at 400g at 4°C and resuspended in 100 µl FACS buffer.

On the B-cells, T-cells and monocyte samples 20µl of mouse monoclonal antibody against CD19 (FITC labeled), CD 3 (FITC labeled) and CD14 (PE labeled) (Immunotech, Marseille, France) respectively was added. The cells were thoroughly re-suspended and incubated for 30 min. at 4°C in the dark. The granulocyte and PBMC samples were incubated only in FACS buffer. All cells were washed with 10 volumes of FACS buffer and centrifuged for 10 minutes at 1000rpm and 4°C.

The purity analysis of the cell populations was performed with FACS-Calibur equipment (BD, San Jose, USA). The readout was represented in a Dot Plot diagram using the Cell Quest software (BD, San Jose, USA). The PBMCs and granulocytes were characterized based on their size and granularity as given by the forward and side laser scatter. The B and T-cells were characterized by the intensity of FITC fluorescence and the monocytes by the intensity of PE fluorescence (Loken and Herzenber 1975).

2.2.5. Detection of virus specific DNA in peripheral blood cells by polymerase chain reaction (PCR)

The amplification of specific DNA fragments from cellular DNA was performed in a reaction volume of 50 μ l consisting of 1xPCR Buffer, 2.5 mM MgCl₂, 0.05% W-1 Buffer, 200 μ M from each upper and lower primer and 400 μ M from each dNTP in distilled water. After a 5 minutes denaturation step at 94°C, 10U Taq Polymerase (Invitrogen, Karlsruhe, Germany) was added in each reaction tube. Amplification was performed in a Peltier Thermal Cycler (MJ Research, Watertown, USA), for 40 cycles, each cycle consisting of a denaturation step (1min. at 94°C), an annealing step (at variable temperature and time, **Table M-1**) and an extension step (1min. at 72°C). All reactions were terminated with a final elongation step for 10min. at 72°C. The PCR products were characterized by agarose gel electrophoresis (method 2.2.3.5.) and by virus specific radioactive hybridization of the southern blots (methods 2.2.6.1 and 2.2.6.2.)

2.2.6. Specificity characterization of PCR amplified DNA fragments using hybridization techniques

2.2.6.1. Transfer of PCR amplified DNA fragments on nitrocellulose membrane for further analysis using Southern Blot

Denaturation Buffer	NaCl	1.5M
	NaOH	0.5M
Neutralization Buffer	NaCl	3M
	Tris	0.5M
	pH	5

Agarose gels containing electrophoretically separated DNA fragments were incubated 2 times 15 min. at room temperature in the denaturation buffer, washed shortly with distilled water, and then incubated 3 times 10 min. in neutralization buffer. Meanwhile, a Whatmann chromatography paper sheet (Whatmann, Maidstone, England) was placed on a glass plate over a 20xSSC buffer bath, with two ends diving in the buffer. After saturation the gel was placed on it avoiding air-bubble formation between the gel and the wet paper surface. Around the gel wide and thin (1mm) plastic spacers were placed covering the remaining surface of the Whatmann paper. The hybridization membrane (Hybond-N, Amersham Biosciences, Freiburg, Germany) was cut in the size of the gel adding 5mm on each side. The membrane was wetted shortly in distilled water and placed air-bubble free on the gel. Six Whatmann paper sheets were cut on the exact size of the gel, soaked in 20xSSC buffer and placed on top of the Hybond-N membrane. On top of this construct a 7cm thick absorbent paper layer was placed, and pressed together by 1kg weight. After 72 hours of DNA transfer, the ssDNA was fixed on the membrane by baking at 80°C for 2 hours and stored at 4°C.

2.2.6.2. Determining the specificity of the PCR amplified products using radioactive hybridization of Southern blots

2.2.6.2.1. Radioactive labeling of specific oligonucleotides as hybridization probes

Per 10 cm² DNA bound membrane 1pmol oligonucleotide to be labeled was mixed with 1U Terminal Transferase, 1xReaction Buffer and 1mM CoCl₂ (Terminal Deoxynucleotidyl Transferase (TdT) Kit, MBI Fermentas, Vilnius, Lithuania), 25μCi P³² labeled dATP (Amersham, UK) and brought to 25μl with distilled water. After mixing thoroughly, the reaction took place at 37°C for 90min. and was terminated by incubating the mixture at 70°C for 10 minutes. 75μl distilled water was added and the free P³² labeled dATP was eliminated by Sephadex G-50 chromatography (method 2.2.3.6).

Table M-1. Primer sequences and amplification conditions used JCV DNA detection in peripheral blood cells by PCR, nPCR and Southern blot

No.*	Function	DNA position **	Genomic region	Sequence	Amplification conditions	MgCl ₂ Conc.
169 ¹	5' primer	2126-2148	VP1	5' GGAGAAAATGTTCCCTCCAGTTC 3'	40 cycles: 1'94°C, 1'50°C, 1'72°C	2.5mM
204 ¹	3' primer	2458-2442	VP1	5' TGTTCCCTCAAAAACCTC 3'		
201 ²	5' primer	2136-2153	VP1	5' TTCCTCCAGTTCTTCATA 3'	40 cycles: 1'94°C, 1'50°C, 1'72°C	2.5mM
202 ²	3' primer	2331-2314	VP1	5' ACCCTCCTTTTTCTTAGC 3'		
149	Hybrid. primer	2277-2149	VP1	5' TGGGAACCAGATCTGTTAGTA 3'	Hybridization temperature: 50°C	
71 ¹	5' primer	4966-4993	CR	5' TAAATGCATAAGCTCCATGAATTCCTCC 3'	40cycles: 1'30''94°C, 1'30''60°C, 2'72°C	2.5mM
157 ¹	3' primer	540-518	CR	5' AAGTGCGGGATCCATGAACCTGA 3'		
53 ²	5' primer	5073-5103	CR	5' GCCTCCTAAAAAGCGTCGACGCCCTTACTAC 3'	40cycles: 1'30''94°C, 1'30''60°C, 2'72°C	2.5mM
61 ²	3' primer	410-385	CR	5' CTGTCTTCACCTGTGCAAAAAGTCCAGC 3'		
262	Hybrid. primer	142-180	CR	5' CTGCCAGCCAAGCATGAGTCTCATACCTAGGGAGCCAACCAG 3'	Hybridization temperature: 60°C	

* *Laboratory work number*

** *JCV strain MAD1 (Frisque, Bream et al. 1984)*

VP1 = viral protein 1

CR = transcriptional control region

¹ = *standard PCR primer*

² = *nested PCR primer*

Hybrid. = hybridization

2.2.6.2.2. Hybridization of membrane bound DNA with radioactive labeled oligonucleotide probes

Prehybridization Buffer	SSC	6x
	Denhardt solution	5x
	SDS	0.5%
	Denatured herring sperm DNA	100 ng/ml

The herring sperm DNA was denatured shortly before use by boiling for 10 min. at 100°C and shock cooled on wet ice.

Posthybridization Buffer	SSC	6x
	SDS	0.1%
Washing Buffer 1	SSC	2x
	SDS	0.1%
Washing Buffer 2	SSC	0.3x
	SDS	0.1%

All hybridization steps were performed inside a tightly sealed hybridization bag with 100 μ l buffer per cm² of membrane. The blot was incubated with prehybridization buffer for one hour at radioactively labeled oligonucleotide specific hybridization temperature (T_H) (**Table M-1**). After the prehybridization buffer was removed, the blot was hybridized for 24 hours at T_H with hybridization buffer containing 1pmol/ μ l radioactively labeled oligonucleotide probe (2.2.6.2.1.). After removal of the hybridization mixture, the blot was incubated with posthybridization buffer for 15 min. at T_H in a water-bath then washed 2 times 15min. with washing buffer 1 and 2 times 15min. with washing buffer 2. In the end, the blots were taken out from the hybridization bags, air-dried at 37°C and the signal was visualized by autoradiography on a RF500 Röntgen photographic film (Fujifilm, Japan). The time of exposure depended on the intensity of the signal and varied between 6 hours and 48 hours. The film was developed for 5 minutes in the developing solution (Agfa-Gevaert, Köln, Germany) washed shortly with water, fixed for 5 minutes in fixation solution (Agfa-Gevaert, Köln, Germany) and washed thoroughly with distilled water for 15-20min. and air-dried at 37°C.

2.2.6.3. Detection of virus DNA *in situ* using Fluorescence *in situ* Hybridization (FISH)

2.2.6.3.1. Fixation and permeabilization of cells on slides

1-2x10⁵ cells were spotted on slides, air-dried and fixed for 15 min. in a 4% paraformaldehyde solution (EMS, Munich, Germany) in PBS at 4°C. For permeabilizing the cellular membrane the cells were treated with a proteolytic mixture consisting of 1µg/µl Proteinase K, 0.5% pepsin and 0.2N HCl for 5min. at 37°C. The proteolytic reaction was blocked by washing the slides 3 times in a 0.2% glycine buffer and once for 5 minutes in PBS at RT. After air-drying the slides were immediately used in FISH. Permeabilization was controlled by Situs kit (Situs, Germany) FITC labeled marker (1:25 in PBS) for 10 minutes followed by Fluorescence microscopy.

2.2.6.3.2. Preparation of digoxigenin-labelled DNA probes for FISH

Double stranded DNA amplicons labelled with digoxigenin were prepared by PCR. All the primers used for amplification were generated with the software Oligo 6.0 (Cambio Ltd, Cambridge, UK) and analyzed in PCR reactions using plasmid target DNA. For the JCV probes 16 pairs of oligonucleotide primers were used to amplify 16 fragments of the JCV genome with a mean length of 200 bp and a cumulative length of 2811 bp, covering the three functional regions of the genome (**Table M-2**). As negative control for hybridization, an unrelated viral DNA probe was used, consisting of 11 feline immunodeficient virus (FIV) PCR DIG-labeled DNA fragments with a mean length of 177 bp and a cumulative length of 1955 bp (**Table M3**). As positive control for the nuclear membrane permeabilization, a mixture of 14 human genomic skeletal alpha actin (ACTA1) PCR DIG labeled DNA fragments was used, with a mean length of 160 bp and a total length of 2194bp, using the 14 primer pairs listed in **Table M-4**. The magnesium chloride concentrations and the annealing temperatures were optimized for each primer pair. Incorporation of digoxigenin-dUTP was done by PCR as described in the method 2.2.5.1., but no detergent (W1%) was used, and a fraction of 1: 3 dTTP:DIG-dUTP was used instead of dTTP alone. The unincorporated triphosphates including DIG-11-dUTP was eliminated from the product by

Table M-2. JCV specific primer pairs used for digoxigenin labeling of the JCV specific DNA hybridization probes

No.*	Function	DNA position **	Gen. reg.	Sequence	Amplification conditions
175	5'primer	4987-5012	CR	5' GAGGAATGCATGCAGATCTACAG 3'	35 cycles: 1'94°C, 1'51°C, 1'72°C
176	3'primer	10-5121	CR	5' TTAGGTGCCAACCTATGGAACAG 3'	35 cycles: 1'94°C, 1'51°C, 1'72°C
239	5'primer	234-251	CR	5' TGTTTTGCGAGCCAGAG 3'	40 cycles: 1'94°C, 1'52°C, 1'72°C
240	3'primer	405-385	CR	5' TTTTCCCGTCTACACTGTCT 3'	40 cycles: 1'94°C, 1'52°C, 1'72°C
227	5'primer	584-605	VP	5' CTGCCACAGGATTTTCAGTAG 3'	40 cycles: 1'94°C, 1'52°C, 1'72°C
228	3'primer	732-713	VP	5' CCGGAGCTCCAGTTATTACA 3'	40 cycles: 1'94°C, 1'52°C, 1'72°C
201	5'primer	668-686	VP	5' TTCCTCCAGTTCTTCATA 3'	40 cycles: 1'94°C, 1'50°C, 1'72°C
202	3'primer	846-829	VP	5' ACCCTCCTTTTCCTTAGC 3'	40 cycles: 1'94°C, 1'50°C, 1'72°C
203	5'primer	868-885	VP	5' AACCCCTACCCAATTTTC 3'	40 cycles: 1'94°C, 1'45°C, 1'72°C
204	3'primer	974-958	VP	5' TGTCCCCTCAAAAACACTC 3'	40 cycles: 1'94°C, 1'45°C, 1'72°C
171	5'primer	1286-1301	VP	5' CAGACAGCATTCAAGAAGAAGTTACCCA 3'	33 cycles: 1'94°C, 1'52°C, 1'72°C
121	3'primer	1444-1420	VP	5' TCACAGTCCCGTACAACCCTAAAAG 3'	33 cycles: 1'94°C, 1'52°C, 1'72°C
229	5'primer	1469-1484	VP	5' ATGGCCCCAACAAAAA 3'	40 cycles: 1'94°C, 1'55°C, 1'72°C
230	3'primer	1624-1604	VP	5' CTA AACCCCTAAGATGCTCA 3'	40 cycles: 1'94°C, 1'55°C, 1'72°C
231	5'primer	1632-1653	VP	5' TTAGGGGTTTTAGTAAGTCAA 3'	40 cycles: 1'94°C, 1'50°C, 1'72°C
232	3'primer	1792-1773	VP	5' CCCCTATAACCTCAGTTTTT 3'	40 cycles: 1'94°C, 1'50°C, 1'72°C
151	5'primer	1832-1854	VP	5' CACTCTAATGGGCAAGCAACTCA 3'	31 cycles: 1'94°C, 1'56°C, 1'72°C
152	3'primer	2037-2016	VP	5' AGGTACGCCTTGTGCTCTGTGT 3'	31 cycles: 1'94°C, 1'56°C, 1'72°C
173	5'primer	2796-2818	TAg	5' GGTCTCCCCATACCAACATTAG 3'	35 cycles: 1'94°C, 1'51°C, 1'72°C
174	3'primer	2946-2925	TAg	5' CTTTGCTTTTGCTTTTAATCTG 3'	35 cycles: 1'94°C, 1'51°C, 1'72°C
233	5'primer	3011-3032	TAg	5' GTAGGCCTTTGGTCTAAAATC 3'	40 cycles: 1'94°C, 1'52°C, 1'72°C
234	3'primer	3183-3166	TAg	5' TGGCATAAGCAACCTTGA 3'	40 cycles: 1'94°C, 1'52°C, 1'72°C
153	5'primer	3266-3287	TAg	5' CTGATCTATACCCACTCCTAA 3'	32 cycles: 1'94°C, 1'51°C, 1'72°C
170	3'primer	3435-3415	TAg	5' GCATTGTATTAACAATTCCA 3'	32 cycles: 1'94°C, 1'51°C, 1'72°C
115	5'primer	3901-3926	TAg	5' CATGCTCCTTAAGGCCCCCTGAAT 3'	35 cycles: 1'94°C, 1'51°C, 1'72°C
172	3'primer	4089-4061	TAg	5' TGTTTTTCTTAACACCACATAGACATAGA 3'	35 cycles: 1'94°C, 1'51°C, 1'72°C
57	5'primer	4228-4251	TAg	5' GAGGAATGCATGCAGATCTACAG 3'	40 cycles: 1'94°C, 1'52°C, 2' 72°C
154	3'primer	4430-4408	TAg	5' TTAGGTGCCAACCTATGGAACAG 3'	40 cycles: 1'94°C, 1'52°C, 2' 72°C
235	5'primer	4562-4583	TAg	5' GTTAAGTCACACCCAAACCAT 3'	40 cycles: 1'94°C, 1'52°C, 1'72°C
236	3'primer	4700-4681	TAg	5' CCTAACTGTGCCACTAATCC 3'	40 cycles: 1'94°C, 1'52°C, 1'72°C
237	5'primer	4698-4719	TAg	5' AAGGATTAGTGGCACAGTTAG 3'	40 cycles: 1'94°C, 1'52°C, 1'72°C
238	3'primer	4865-4850	TAg	5' AAGGTGGGGACGAAGA 3'	40 cycles: 1'94°C, 1'52°C, 1'72°C

* Laboratory work number

** JCV strain MAD1 (Frisque, Bream et al. 1984)

Gen reg.=functional region of the genome: CR=transcriptional control region, VP= viral capsid protein, TAg= large T antigen

Table M-3. FIV specific primer pairs used for digoxigenin labeling of the FIV DNA hybridization probe

No.*	Function	DNA Position **	Genomic region ^a	Sequence	Amplification conditions	MgCl ₂ Conc.
205	5'primer	637-653	GAG	5' GGACAGGGGCGAGATT 3'	35 cycles: 1'94°C, 1'50°C, 1'72°C	2.5mM
216	3'primer	803-783	GAG	5' CGCAAATAACCAACCTTAGTT 3'	35 cycles: 1'94°C, 1'50°C, 1'72°C	2.5mM
206	5'primer	1262-1283	GAG	5' CAGAATATGATCGCACACATC 3'	35 cycles: 1'94°C, 1'50°C, 1'72°C	2.5mM
217	3'primer	1415-1397	GAG	5' GCAGCCAATTTTCCTAATG 3'	35 cycles: 1'94°C, 1'50°C, 1'72°C	2.5mM
207	5'primer	4392-4413	POL	5' GTATTCTCCTCTTGGGTTGACG 3'	35 cycles: 1'94°C, 1'50°C, 1'72°C	2.0mM
218	3'primer	4564-4546	POL	5' ATACCAGGCCCTATTTTCA 3'	35 cycles: 1'94°C, 1'50°C, 1'72°C	2.0mM
208	5'primer	5243-5255	ORF1/2	5' AAGAAGATTGGCAGGTAAGTA 3'	35 cycles: 1'94°C, 1'50°C, 1'72°C	3.0mM
219	3'primer	5399-5381	ORF1/2	5' TCAGCTTCCGTAGTCTCT 3'	35 cycles: 1'94°C, 1'50°C, 1'72°C	3.0mM
209	5'primer	5527-5548	ORF1/2	5' AACCCACTATGGCATTCTCAG 3'	35 cycles: 1'94°C, 1'50°C, 1'72°C	2.5mM
220	3'primer	5661-5643	ORF1/2	5' CCCCATCCTGGTGAAACT 3'	35 cycles: 1'94°C, 1'50°C, 1'72°C	2.5mM
210	5'primer	5715-5734	ORF1/2	5' TTGTGGCGAAAGAAAGATT 3'	35 cycles: 1'94°C, 1'50°C, 1'72°C	2.5mM
221	3'primer	5892-5872	ORF1/2	5' GAAACAAAGCGTTGATTACAG 3'	35 cycles: 1'94°C, 1'50°C, 1'72°C	2.5mM
211	5'primer	6562-6583	ENV/ORF3	5' GGTCATGCGTTCATAGGATA 3'	35 cycles: 1'94°C, 1'50°C, 1'72°C	2.7mM
222	3'primer	6701-6681	ENV/ORF3	5' TAGGCAACATCGTCTACCATA 3'	35 cycles: 1'94°C, 1'50°C, 1'72°C	2.7mM
212	5'primer	6714-6733	ENV/ORF3	5' GTTGCCTAGGAACGGTGAC 3'	35 cycles: 1'94°C, 1'50°C, 1'72°C	2.5mM
223	3'primer	6884-6864	ENV/ORF3	5' TATCATTGCCCAAGAAAGTC 3'	35 cycles: 1'94°C, 1'50°C, 1'72°C	2.5mM
213	5'primer	7572-7593	ENV/ORF3	5' TAACGGGAGCTTGGATAGAGT 3'	35 cycles: 1'94°C, 1'50°C, 1'72°C	3.0mM
224	3'primer	7703-7685	ENV/ORF3	5' TCGCACCTGAAACTTTTTG 3'	35 cycles: 1'94°C, 1'50°C, 1'72°C	3.0mM
214	5'primer	7774-7795	ENV/ORF3	5' AAACGGGTTTACTATGAAGGT 3'	35 cycles: 1'94°C, 1'50°C, 1'72°C	2.5mM
225	3'primer	7941-7922	ENV/ORF3	5' GCTAGGACATGCCATTTTAG 3'	35 cycles: 1'94°C, 1'50°C, 1'72°C	2.5mM
215	5'primer	8621-8642	ENV/ORF3	5' GGACTATTGGGAGGTATCTTG 3'	35 cycles: 1'94°C, 1'50°C, 1'72°C	2.0mM
226	3'primer	8799-8782	ENV/ORF3	5' ACATGCCACATTGCCTAC 3'	35 cycles: 1'94°C, 1'50°C, 1'72°C	2.0mM

** *FIV/Petaluma (Olmsted, Barnes et al. 1989)*

* *Laboratory work number*

^a *GAG, POL, ENV, ORF 1, 2, 3 = viral proteins*

Table M-4. Human skeletal alpha actin gene specific primer pairs used for digoxigenin labeling of the ACTA1 hybridization probe

No.*	Function	DNA Position **	Genomic Region ^a	Sequence	Amplification conditions	MgCl ₂ Conc.
264	5'primer	256-273	ACTA1	5' ACCCGAAGAGGAGTTGA 3'	40 cycles: 1'94°C, 1'52°C, 1'72°C	3.0mM
265	3'primer	455-439	ACTA1	5' CTGACCCGACCCAGTTG 3'		
266	5'primer	527-543	ACTA1	5' CTCCTTCTTTGGTCAAC 3'	40 cycles: 1'94°C, 1'54°C, 1'72°C	2.5mM
267	3'primer	696-679	ACTA1	5' CTCTGCTCAGGTTTTAT 3'		
268	5'primer	759-775	ACTA1	5' GGGCCCGAGCCGAGAGT 3'	40 cycles: 1'94°C, 1'60°C, 1'72°C	3.0mM
269	3'primer	897-881	ACTA1	5' GGGCTGACCAGGTGAAC 3'		
270	5'primer	949-965	ACTA1	5' AAAGGAGGCAAGACAGT 3'	40 cycles: 1'94°C, 1'48°C, 1'72°C	3.0mM
271	3'primer	1063-1047	ACTA1	5' AGCAAAACCGTTTATCT 3'		
272	5'primer	1069-1085	ACTA1	5' TGTCGCCAAGGCAGTTC 3'	40 cycles: 1'94°C, 1'54°C, 1'72°C	3.0mM
273	3'primer	1217-1191	ACTA1	5' GAAGAGTGGCCTGTTAG 3'		
274	5'primer	1265-1281	ACTA1	5' CCAGCAAGCAGGCAGTG 3'	40 cycles: 1'94°C, 1'53°C, 1'72°C	3.0mM
275	3'primer	1374-1358	ACTA1	5' CTGCCTGACACCTGTTC 3'		
276	5'primer	1399-1415	ACTA1	5' ATGTTCCCCTGGCTATG 3'	40 cycles: 1'94°C, 1'52°C, 1'72°C	2.5mM
277	3'primer	1542-1526	ACTA1	5' GAGCCACTCAAATTCTG 3'		
278	5'primer	1605-1621	ACTA1	5' CCCCTGCCGTCGAGACT 3'	40 cycles: 1'94°C, 1'57°C, 1'72°C	2.5mM
279	3'primer	1789-1773	ACTA1	5' ACGATGGACGGGAACAC 3'		
280	5'primer	1895-1911	ACTA1	5' GTGGTGTCTCGGCTCTG 3'	40 cycles: 1'94°C, 1'50°C, 1'72°C	2.5mM
281	3'primer	1995-1979	ACTA1	5' CTCAGGGTCAGGATAC 3'		
282	5'primer	2049-2065	ACTA1	5' GCACCACACCTTCTACA 3'	40 cycles: 1'94°C, 1'52°C, 1'72°C	2.0mM
283	3'primer	2275-2259	ACTA1	5' GCGGGACGAGGGGACTG 3'		
284	5'primer	2326-2341	ACTA1	5' GCCTCGCCCCAGCCAC 3'	40 cycles: 1'94°C, 1'53°C, 1'72°C	2.5mM
285	3'primer	2525-2509	ACTA1	5' TGGTCACGAAGGAGTAG 3'		
286	5'primer	2779-2795	ACTA1	5' TCTTCCAGCCCTCCTTC 3'	40 cycles: 1'94°C, 1'57°C, 1'72°C	2.5mM
287	3'primer	2994-2978	ACTA1	5' GTGGTGCCCCCGACAT 3'		
288	5'primer	3266-3282	ACTA1	5' ATCGTCCACCGCAAATG 3'	40 cycles: 1'94°C, 1'53°C, 1'72°C	4.0mM
289	3'primer	3414-3397	ACTA1	5' TTTACGATGGCAGCAAC 3'		
290	5'primer	3543-3559	ACTA1	5' AAGTGGTCGTGTTTATT 3'	40 cycles: 1'94°C, 1'46°C, 1'72°C	3.0mM
291	3'primer	3644-3628	ACTA1	5' CATTCAATTGGGGTATC 3'		

* Laboratory work number

** ACTA1 (Taylor, Erba et al. 1988)

^a ACTA1 = human alpha actin gene

Sephadex G-50 chromatography (2.2.3.6.). Each amplicon was concentrated 10 times by ethanol precipitation (2.2.3.3.). The final concentration of each amplicon was determined with a GeneQuant photometer (Pharmacia, Uppsala, Sweden). All DNA products were subsequently diluted to 20ng/μl (An, Franklin et al. 1992). To create the mixed probe equal amounts of the amplicon solutions were mixed, aliquoted and stored in -20°C. The mean hybridization temperature of the mixed probe was mathematically calculated (table M-5).

2.2.6.3.3. Fluorescence *in situ* hybridization with chemical amplification of the signal

Prehybridization Buffer	Formamide	50%
	SSC	5x
	Denhardt solution	1x
	Denatured HSP DNA	200μg/ml
TN Buffer	Tris-HCl	100mM
	NaCl	150mM
	pH	7.5
TNB Buffer	Tris-HCl	100mM
	NaCl	150mM
	casein	0.5%
	pH	7.5
TNT Buffer	Tris-HCl	100mM
	NaCl	150mM
	Tween 20	0.05%
	pH	7.5
Denaturation Buffer	Formamide	95%
	0.1x SSC	5%
	freshly prepared before FISH	
Denatured probe mixture	Probe mixture (JCV, FIV or ACTA1)20ng/μl Denatured for 10min. at 100°C and shock cooled at 4°C. Stored at-20°C	

1-2x10⁵ cells, fixed and permeabilized on slides were rehydrated in 100, 70, 50, 30 % ethanol in PBS for 5min. each step. The cells were acetylated for 5min. in 0.1M Triethanolamine-HCl in PBS pH8.0, twice in 0.25% Acetanhydride in 0.1M Triethanolamine-HCl in PBS for 5min., washed 5min in 2xSSC buffer and dehydrated in reversed ethanol series. After air-drying for 15min. DNA was denaturated at 65°C in denaturation buffer for 20 minutes and shock cooled in ice-cold 0.1xSSC. The cells were incubated for one hour at 37°C in a wet chamber with 20µl/cm² prehybridization buffer per cell spot. The buffer was removed carefully using absorbant paper. The cells were subsequently hybridized for 70 hours at 37°C in a wet chamber with 20µl/cm² prehybridization buffer per spot containing 1µl denatured probe mixture. After hybridization the slides were washed 2 times 15min. in 2xSSC and 5 min. in PBS at room temperature. To inhibit endogenous peroxidase activity the cells were incubated one hour in 3% H₂O₂ in methanol at 4°C then washed 10min. in 1xTN solution.

Unspecific binding sites were blocked for 30min. at 37°C with 20µl/cm² TNB buffer (NEN Life Science Products Inc., Boston, MA, USA) per spot. The hybridization product was detected with 20µl/cm² monoclonal mouse anti-Digoxigenin antibody (Roche Diagnostics, Mannheim, Germany) per spot, diluted 1:100 in 5% normal goat sera in TNB over night at 4°C in a wet chamber. After washing the slides 2 times 5min. in TNT buffer, the endogenous biotin was blocked with 20µl/cm² TNB buffer per spot containing 0.05% Tyramide-OHCl. After absorbing the buffer, the cells were incubated with 20µl/cm² goat anti-mouse HRP conjugated antibody per spot (Dako Diagnostika GmbH, Hamburg, Germany) diluted 1:100 in 5% normal goat sera in PBS over night at 4°C. To enhance the peroxidase signal a biotinylated tyramide amplification system (TSA) was used (NEN Life Science Products Inc., Boston, MA, USA). Prior to application the biotinylated-tyramide solution (BT) was diluted 1:50 with the Amplification Dilutant (NEN Life Science Products Inc., Boston, MA, USA). The cells were incubated with 35µl/cm² BT solution per spot for 5min. at RT then washed 3 times 5min. in TNT buffer. The signal was developed for 30min at 37°C with 25µl/cm² Streptavidin-Texas Red (Molecular Probes Inc., Eugene, OR, USA) per spot, diluted 1:800 in TNB. After washing 3 times 5min. with TNT the nuclei were stained with DAPI, 7-AAD (Sigma-Aldrich, Germany), Bo-Pro-1 or To-Pro-1 (Molecular Probes, Leiden, The Netherlands) according to manufacturers protocols then mounted with a drop of Vectashield (Vector Laboratories, Germany). The cells were then observed at the fluorescence or confocal microscope. On each blood sample two experiments were performed and from each 10⁵ cells were counted. The number of positive cells was reported to 1000.

2.2.6.3.4. Fluorescence *in situ* Hybridization without chemical amplification

The method is identical with the FISH with chemical amplification except that the secondary antibody used is a goat anti mouse polyclonal antibody directly labeled with a fluorophore, either Texas-Red (Dianova, Germany) or Alexa 594 (Molecular Probes, Leiden, The Netherlands). After washing the slides 3times 5min. with TNT the nuclei were stained with Bo-Pro-1 or To-Pro-1 at a concentration of 100 μ M then mounted with a drop of Vectashield (Vector). The cells were then observed at the confocal microscope. From each sample 10⁵ cells were counted and the number of positive cells was reported to 1000.

2.2.6.4. Estimation of digoxigenin labeled DNA probe specificity by Dot-blot hybridization

Probe as well as genomic DNA was denatured at 100°C for 10min. and shock-cooled on ice. From the target DNA a decimal dilution series was prepared in the range from 100ng to 100fg/ μ l and from a heterologous DNA ranging from 10 μ g to 10ng/ μ l. After denaturation, from each DNA dilution step, 1 μ l was spotted on a membrane stripe (Nytran, Schleicher & Schuell, Dassel, Germany), and incubated for 2 hours at 80°C. For hybridization the membrane was moisturized in 5xSSC and blocked in 350 μ l buffer/cm² prehybridization buffer for one hour at 37°C in a sealed hybridization bag. Without washing the membrane was transferred in a new bag and hybridized over-night at 37°C with 70 μ l/cm² hybridization buffer containing 20ng denatured digoxigenin labeled probe per blot. After hybridization the membrane was washed 5 min. in 2xSSC with 0.02%SDS and two times 5 min. in 0.1xSSC with 0.02%SDS. The hybridization product was detected by immunostaining.

2.2.6.4.1. Immunostaining detection of dot-blot hybridization products

Buffer 1	Maleic acid	0.1 M
	NaCl	0.15 M
	pH	7.5
	in H ₂ O	
Buffer 2	1% Blocking reagent (Boehringer, Mannheim, Germany) solved under heat in Buffer 1, cooled, sterile filtered	

Buffer 3	Tris-HCl	0.1 M
	NaCl	0.1M
	MgCl ₂	50mM
	pH	9.5
	in H ₂ O	

The membrane was always air bubble free in the buffer.

To determine the sensitivity of the digoxigenin probe, a decimal dilution row ranging from 20ng to 2fg of the probe was prepared in parallel with the dot-blot hybridization and pipetted on a membrane stripe (Nytran, Schleicher & Schuell, Dassel, Germany). After incubating the membrane for 2 hours at 80°C, the bound labeled DNA was detected by immunohistochemistry. The membrane was equilibrated 1 to 5 minutes in buffer 1 then incubated for 30 minutes in buffer 2 and, without washing, incubated for 60 minutes with 150µl/cm² mouse anti-digoxigenin monoclonal antibody (Roche Diagnostics, Mannheim, Germany) diluted 1:1000 with buffer 2 with 5% normal goat serum. After washing two times 15 minutes in buffer1 with 0.3% Tween 20 the membrane was incubated exactly 60 minutes at RT with goat anti-mouse -HRP (Dako, Denmark) diluted 1:1000 with buffer 2 with 5% normal goat serum. After washing two times 15 min. in buffer 1 with 0.3% Tween 20, the membrane was equilibrated for 5 minutes with buffer 3 then incubated with 1.5ml TMB substrate until maximal color was observed. After washing 3 times 5 min. with distilled water the membrane was dried and scanned (SnapScan, Agfa-Gevaert, Köln, Germany).

2.2.8. Visualization of *in situ* fluorescent signals using microscopy

2.2.8.1. Assessing the FISH results using classical fluorescence microscopy

The classic visualization of fluorescent signals obtained after FISH was performed using an Aristoplan microscope (Leica, Wetzlar, Germany) provided with an Osram Short arc Mercury HBO lamp, emitting in both UV and visible spectrum. The fluorochrome excitation and emission are insured by a series of filter-blocks. DAPI was visualized using the UV filter A (ex. 340-380nm/em. 425nm), FITC using blue light filter I3 (ex. 450-490nm/em. 515nm) and Texas Red using the red light filter TX2 (ex. 560-540nm/em. 645-675nm). A special filter, used for the simultaneous visualization of both FITC and Texas red was the filter G/R for excitation in blue (490-420nm) and green (575-530nm) and emission in green (525-520nm) and red (635-640nm).

The fluorescent signals were captured with a DC300F digital camera controlled by the QFluoro v.1.2.0 software (Leica Microsystems Imaging solutions Ltd, Germany), and further processed with the Photoshop® graphics program (Adobe Systems Incorporated, USA).

2.2.8.2. Visualization and localization of fluorescent signals using Laser Scanning Microscopy (LSM)

For intracellular visualization and localization of the positive fluorescent signals, a LSM Meta 510 laser scanning microscope (Carl Zeiss GmbH, Jena, Germany) was used. Comparative with the classical fluorescence microscopy, LSM can effectuate section pictures through the cell, making the localization of positive signals to subcellular levels possible. The sum of images generated in different focal plane through the cell generates a 3-dimensional image of a single cell. The LSM Meta 510 from Zeiss is equipped with three lasers, an Argon (Ar) laser of 30mW, which provides excitation waves at 458, 477, 488 and 514nm, and two Helium/Neon (He/Ne) lasers for 543 respectively 633nm excitation. The separation of 10 different wavelength signals, even close together, was possible due to dichroic beamsplitters, which reflect all wavelengths shorter and transmit all wavelengths longer then the threshold. Especially due to the META detector the separation of two overlapping emission spectra was performed based on emission fingerprinting. The microscope's optical and mechanical functions are controlled by a Digital Signal Processor (DSP), administrated by the LSM Image Browser program (Carl Zeiss GmbH, Jena, Germany). The digital pictures were further processed with Huygens Essential deconvolution software (SVI, Netherlands), Adobe® Photoshop® graphics program, QuickTime™ Player v.6.4. (Apple Computer Inc., USA) and Graphic Converter X v.4.9 (Lemke Software, USA).

3. Results

3.1. Aim of the study

One of the most important questions in the analysis of mechanisms associated with JCV pathogenesis is the characterization of the type of virus interaction with peripheral blood cells during persistent infection. Recently, JCV DNA was detected in individual peripheral blood subpopulations by PCR analyses (Dorries, Sbiera et al. 2003). However, the PCR technique is not able to differentiate between unspecific association of the virus with the cells due to membrane association or phagocytosis and JCV infection with presence of viral DNA within the nucleus of the affected cells. Therefore, our aim was to differentiate between unspecific types of association and infection. For the localization of JCV within the affected blood cells, a JCV specific fluorescence *in situ* hybridization (FISH) method for the detection and quantification of JCV DNA was established (Fig. R-1).

3.2. Study groups for analysis of JCV infection in peripheral blood cells

The first study group consisted of 60 blood samples from healthy individuals. This group was constituted of 15 professional blood donors where the health state of the donor was controlled by the blood transfusion authorities and 45 samples from healthy laboratory workers.

To establish a possible role of the JCV infection in peripheral blood cells for the pathogenesis of PML the second group consisted of 8 HIV-1 immune-impaired donors for different periods of time under HAART treatment and a group of 7 patients with PML, as proven by stereotactic diagnostic biopsy of the CNS.

The third study group was formed by three donors who received influenza immunization with inactivated influenza virus in order to detect possible modulation of the virus status in the host related to modulation of the immune system. As it is known that the peak of immune activation in response to the virus antigen is one week after inoculation and relapses again after another week the time points of blood collection were set one day before vaccination as a reference and 6, 13 and between 140 and 228 days post vaccination.

3.3. Material collection strategy

3.3.1. Isolation of peripheral blood cell populations

3.3.1.1. Isolation of PBMCs and granulocytes by density gradient centrifugation

Blood from human donors was subjected to cell separation less than 8 hrs after collection to reduce influences by external stimuli on cell functions to a minimum. Peripheral blood mononuclear cells (PBMCs) are known to be recovered at a density of 1.077g/ml (Zipursky, Bow et al. 1976) and granulocytes at a density of 1.090g/ml (Mergenthaler, Staber et al. 1982) by density gradient centrifugation (**Fig. R-1**). Therefore the two cell populations were separated on a Ficoll cushion at a density of 1.077g/ml (Ferrante and Thong 1982). Under these conditions PBMCs accumulated at the interface between the Ficoll solution and the plasma. Granulocytes were found together with erythrocytes as a pellet. To recover the granulocyte population the suspension was treated with a hypotonic, buffered solution of ammonium chloride (155mM) (Eggleton, Gargan et al. 1989). Due to the high number of contaminating erythrocytes, the hypotonic treatment had to be repeated between two and four times for a granulocyte population of high purity. Under these conditions viability of the cells was between 72% and 80% and recovery was 36 to 58 % of input cell number. In addition to the low rate of cells recovered, prolonged preparation time was reported to lead to functional changes of the resulting cells (Malm-Erjefalt, Stevens et al. 2004).

In the attempt to reduce the influence of prolonged purification time and to increase the cell yield, a two-step Percoll density gradient, originally used for animal cells (Weiss, Kraemer et al. 1989), was adapted for separation of human blood cells (Info R.Dörries). The blood was layered on top of Percoll solutions with a density of 1.077g/ml and 1.090g/ml, respectively. In the resulting gradient PBMCs were located at the interface between plasma and the layer of lower density. Granulocytes accumulated at the interface between the two layers and erythrocytes were found in the pellet. Residual erythrocytes in the granulocyte population could be removed by a single hypotonic treatment. With this method the rate of granulocyte recovery improved to 83% and the viability of the cells to 90 - 95%.

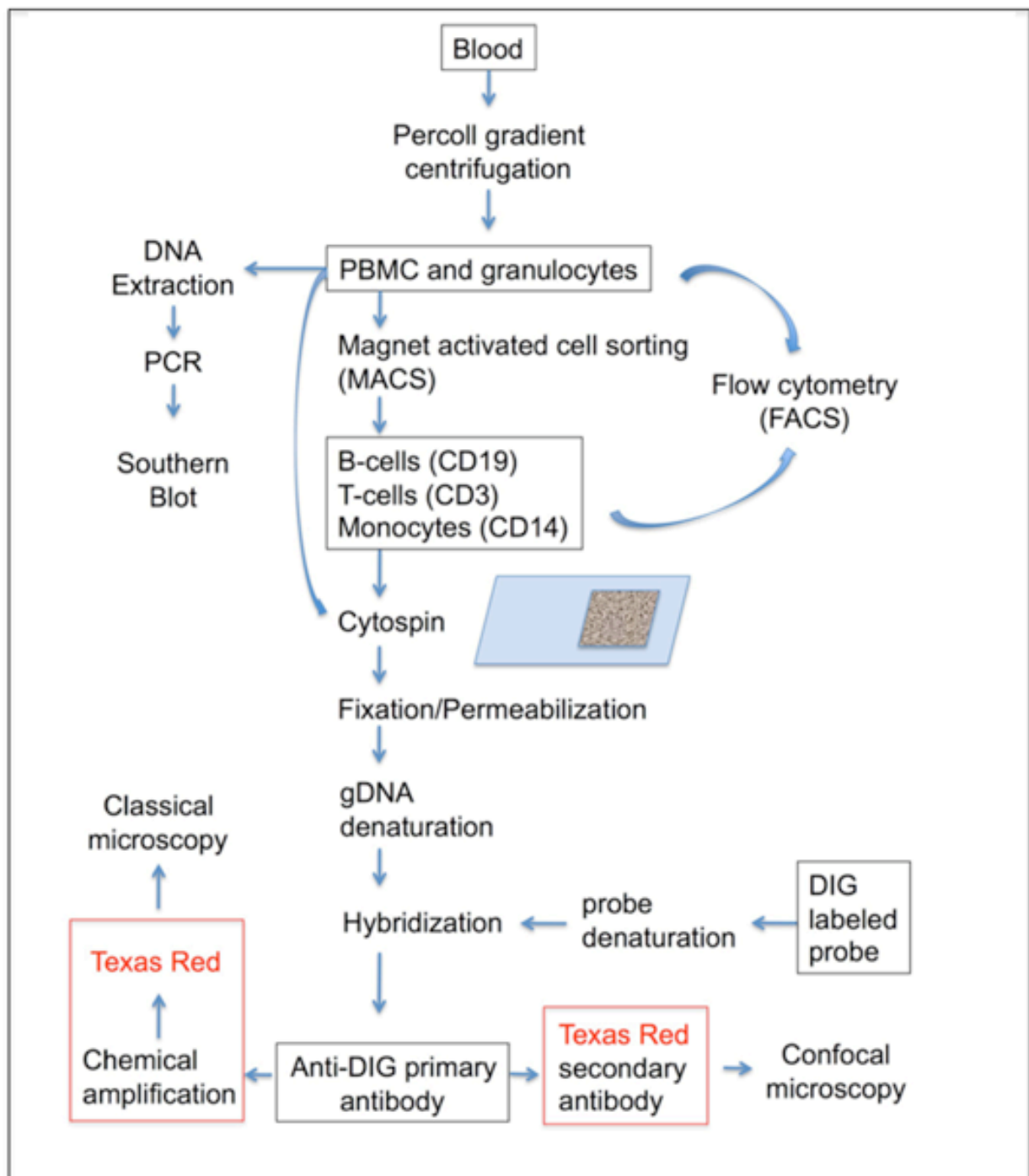


Fig. R-1. Flow chart of experimental procedures. Materials are presented framed and methods unframed. The blood analyzed was taken from healthy blood donors and laboratory personnel, patients with human immunodeficiency virus (HIV) infections with and without established progressive multifocal leukoencefalopathy (PML).

PBMC=peripheral blood mononuclear cells; PCR=polymerase chain reaction; FACS=fluorescence activated cell sorting; CD19, CD3, CD14= clusters of differentiation specific for B-cells, T-cells and monocytes, respectively; gDNA= genomic DNA, DIG= digoxigenin.

3.3.1.2. Enrichment of PBMC subpopulations by magnetic cell separation system

PBMCs are a heterogeneous cell population regularly consisting of 4-6% B-cells, 60-80% T-cells and 2-5% monocytes, each of which was reported to be affected by JC virus (Goldmann, Petry et al. 1999; Koralnik, Schmitz et al. 1999; Wei, Liu et al. 2000; Dorries, Sbiera et al. 2003). To clarify the type of JCV-cell interaction with each subpopulation, B-cells, T-cells and monocytes were separated by magnetic bead isolation (MACS, Miltenyi Biotech, Bergisch Gladbach, Germany). The beads were covered with mouse monoclonal antibodies directed against the respective cell surface marker, for B-cells CD19, for T-cells CD3 and for monocytes CD14. In a first step a maximum of 10^9 density-purified PBMCs was incubated with mouse anti CD19 coupled beads and the cells were positively separated on a mini MACS column by magnetic forces. The flow-through contained CD19 negative cells (T-cells and monocytes). After removing the magnetic field, bound cells (CD19+ Bcells) were recovered. The same procedure was performed with the cells in the flow through. Using MACS mouse anti CD14 antibody the monocytes were separated and finally the T-cells were recovered from the last flow-through using MACS mouse anti CD3 antibody.

The cells obtained after each separation were counted. Starting with 10^9 initial PBMCs, between 4 and 5×10^7 cells were obtained after CD19 selection, between 2 and 3×10^7 after CD14 selection and 9 to 9.4×10^8 after CD3 positive selection.

3.3.1.3. Purity of hematopoietic cell subpopulations

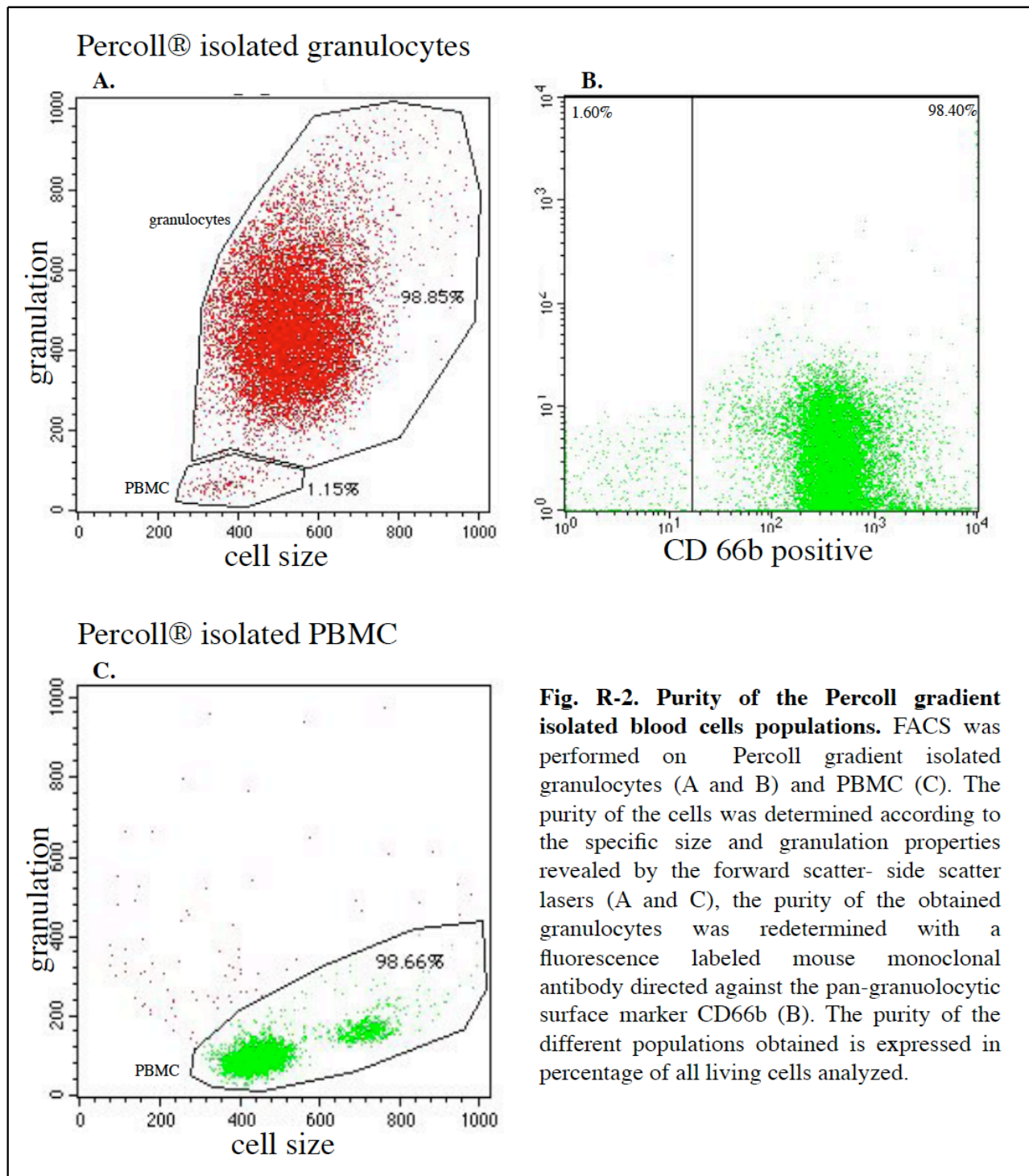
3.3.1.3.1. Purity of density gradient purified PBMCs and granulocytes

The purity of freshly isolated PBMCs and granulocytes was determined by fluorescence activated cell sorting (FACS) analysis based on the size and granulation properties as visualized by the forward and side scatter lasers, respectively. Composition of populations was plotted linearly on the X-axis according to size and on the Y-axis according to granulation using CellQuest software (BD Biosciences, San Jose, USA). Due to larger size and higher granulation granulocytes were located in the upper-right region of the detection window (**Fig. R-2A**). Lymphocytes (B- and T-cells), as small, un-granulated cells, were found in the lower-left of the window (**Fig R-2C**, lower population). Monocytes, which are bigger and more granulated than lymphocytes, were plotted at the upper-right side of the lymphocytes (**Fig. R-2C**, upper population). The two cell populations were gated as described (Pattanapanyasat, Kyle et al. 1994) and the purity of PBMCs and

granulocytes obtained after Percoll gradient centrifugation was determined to be between 97.5 and 99.8% (**Fig. R-2A, B and C**).

3.3.1.3.2. Purity of MACS isolated leukocyte subpopulations determined by FACS analysis

To determine the purity of viable MACS isolated cells, FACS analysis was performed using fluorescence labelled monoclonal mouse antibodies against CD3, CD19 and CD14 cell markers. The subpopulations resulting from the MACS separation were incubated with fluorescent labelled monoclonal antibodies. The CD19 positively selected cells were labelled with fluorescein isothiocyanate (FITC) labelled mouse anti CD19 antibody (B-cells), the CD14+ isolated cells with phycoerythrin (PE) labelled mouse anti CD 14 antibody (monocytes) and the CD3+ selected cells with FITC labelled mouse anti CD3 antibody (T-cells), respectively. The results were plotted on a fluorescence logarithmic scale, where the negative cells appear under the 10^1 both on X or Y axis and the positive cells for the respective marker appear over the 10^1 on the X axis for the FITC labelled cells and on the Y axis for the PE labelled cells. The cells in each fluorescence gate were counted using the CellQuest software (BD Biosciences, San Jose, USA) and reported as percentage from the total number of cells counted (Tollerud, Clark et al. 1989; Paz, Fiszer et al. 1999). After this analysis the B-cells purity was found to be between 92 and 97% (**Fig. R-3a-B**), T-cells between 72 and 80 % (**Fig. R-3b-B**) and monocytes between 80 and 86% (**Fig. R-3c-B**). Most of the positive cells ranged over 10^2 on the fluorescent axis. However, it was repeatedly reported that magnetic separation yields regularly purities of 90 -99 % (Manyonda, Soltys et al. 1992; Jacobs, Moutschen et al. 1993). The low percentage of cell purity in case of T-cells and monocytes suggested a possible interference of antibody binding. Since magnetic cell separation and FACS analysis were based on the same CD markers, it was assumed that the monoclonal antibodies used in FACS analysis competed for the same surface markers that were also targeted by the magnetic beads. This was confirmed by the appearance of 0 to 7% positive B-cells (**Fig. R-3a-B**), 3 to 8% T cells (**Fig. R-3b-B**, blue square gated cells) and 9 to 13% monocytes (**Fig. R-3c-B**, blue square gated cells) of intermediate antibody binding, meaning between 10^1 and 10^2 fluorescent molecules bound per cell. This indicated that residual MACS mouse mABs and antibodies used in FACS analysis compete for the same surface markers (Miltenyi Biotech, personal communication). To demonstrate residual MACS mouse anti CD antibodies, the cells were incubated after MACS separation with FITC labeled antibodies directed against mouse immunoglobulins. FACS analysis of these cells demonstrated the presence of 2 to 3% of B-cells (**Fig. R-3a-C**), 27 to 34% of T-cells (**Fig. R-3b-C**) and 17 to 20% of monocytes (**Fig. R-3c-C**) still carrying MACS mouse antibodies.



The interference between FACS and MACS antibody binding for the same epitope of the CD cell markers indicated that the purity of cell populations after MACS separation was determined by additional measurements of the residual MACS binding frequency. Summing the percentage of cells still carrying MACS antibodies to the percentage of cells positive for the CD markers the purity of the cells resulting after MACS separation was obtained. This was found to be between 92 and 97% for the B-cell, 95 to 99% for the T-cell and 90 to 94% for the monocyte populations.

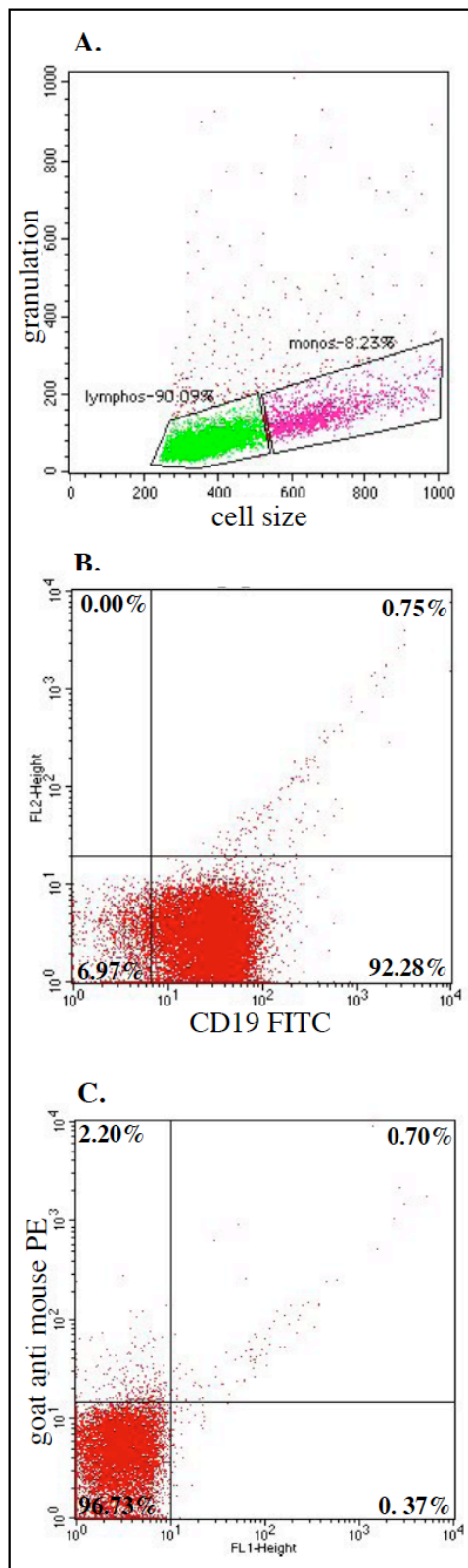


Fig. R-3 a. Purity of MACS isolated B-cell sub-population. FACS was performed on MACS CD-19 (B-cell marker) positively selected cells from a healthy blood donor (NL47).

A. The size and granulation properties of the separated cells was analyzed using the forward scatter-side scatter lasers. The purity of the different populations obtained is expressed in percentage of all the living cells analyzed.

B. The specific surface markers were detected with FITC (fluorescein isothiocyanate) labeled mouse monoclonal antibodies against CD19 (B-cells).

C. The persistence of the MACS monoclonal mouse antibodies attached to the CD-19 molecules which are competing with the antibodies used in the FACS detection was determined using PE (phycoerythrin) labeled goat anti mouse antibodies.

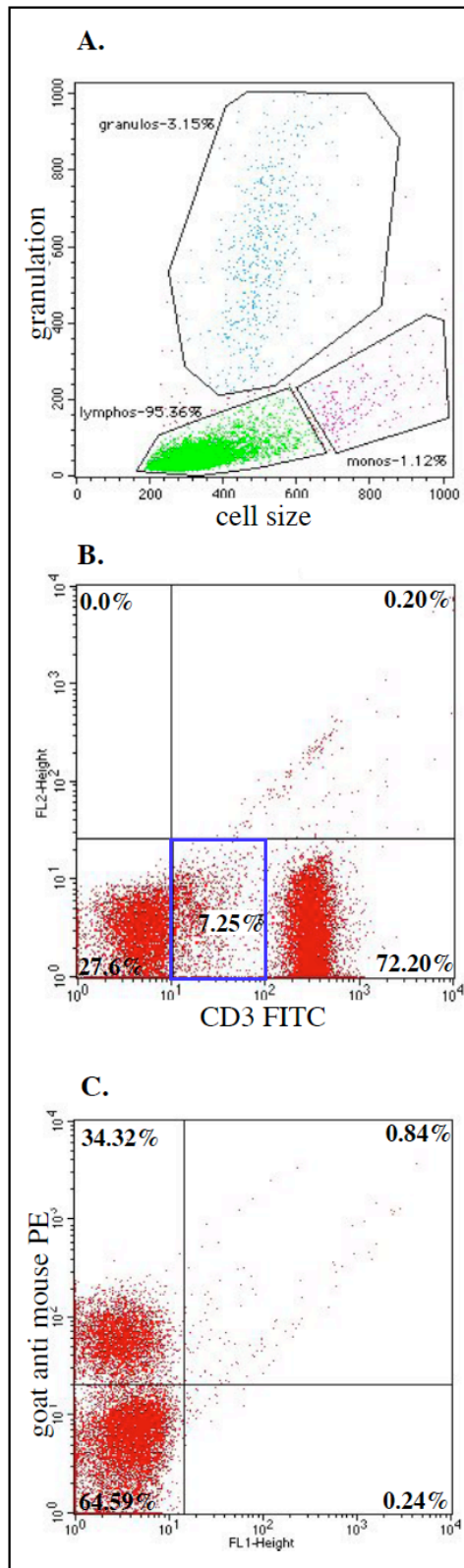
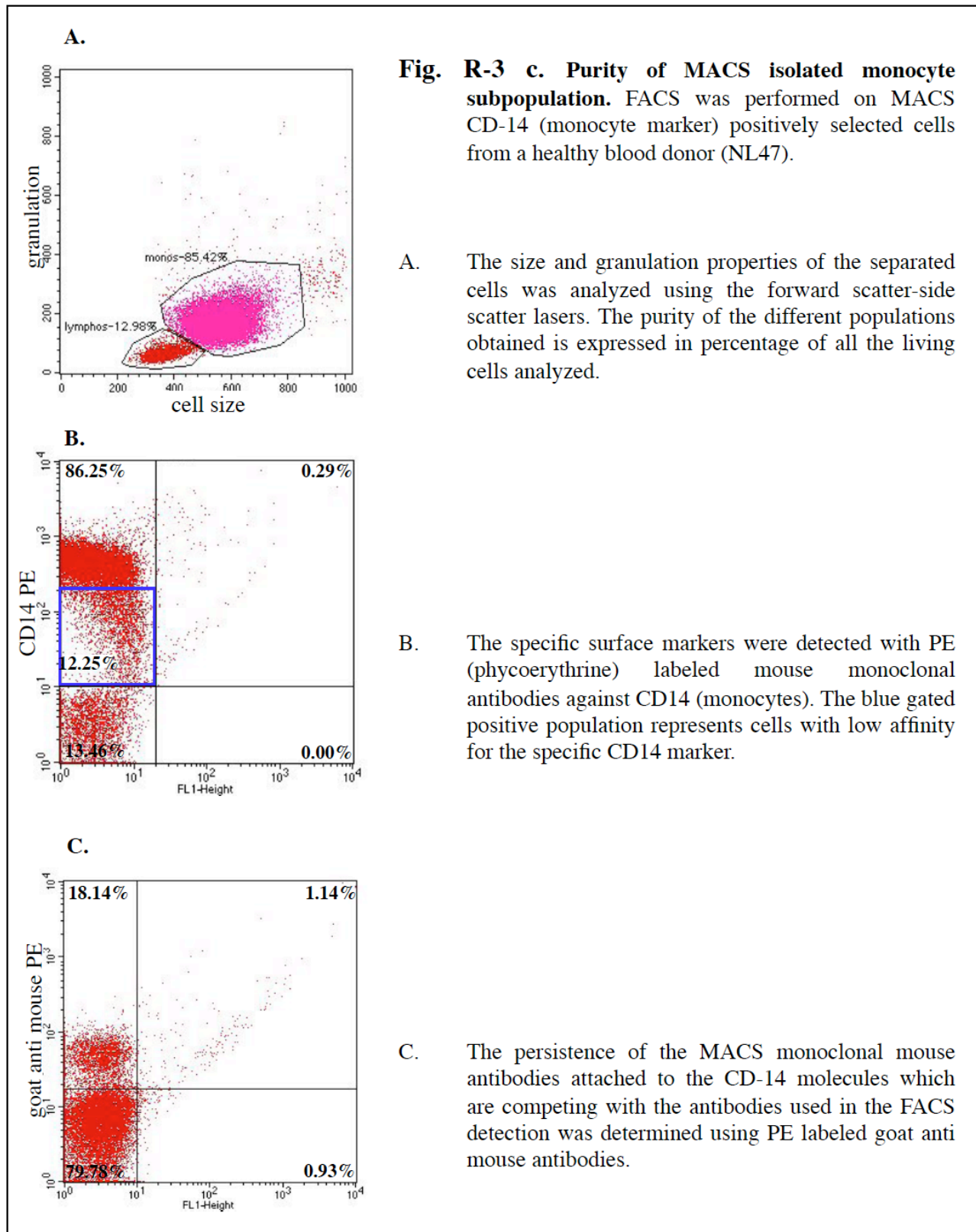


Fig. R-3 b. Purity of MACS isolated T-cells sub-population. FACS was performed on MACS CD-3 (T-cell marker) positively selected cells from a healthy blood donor (NL47).

A. The size and granulation properties of the separated cells was analyzed using the forward scatter-side scatter lasers. The purity of the different populations obtained is expressed in percentage of all the living cells analyzed.

B. The specific surface markers were detected with FITC (fluorescein isothiocyanate) labeled mouse monoclonal antibodies against CD3 (T-cells). The blue gated positive population represents cells with low affinity for the specific markers.

C. The persistence of the MACS monoclonal mouse antibodies attached to the CD-3 molecules which are competing with the antibodies used in the FACS detection was determined using PE (phycoerythrin) labeled goat anti mouse antibodies.



3.4. Detection of JCV DNA in peripheral blood cells

3.4.1. Sensitivity and specificity of the polymerase chain reaction (PCR) for the detection of JCV DNA in peripheral blood cells

The first step in establishing a possible interaction of JCV with peripheral blood cells was the demonstration of viral DNA in the respective cell population. The most sensitive method for DNA detection at present is the polymerase chain reaction (PCR). The DNA sequence of interest was amplified exponentially using oligonucleotides specific for the target DNA as primers. Analyses of JCV DNA in different organs have shown (Monaco, Atwood et al. 1996; Monaco, Jensen et al. 1998; Bofill-Mas, Formiga-Cruz et al. 2001; Schmid, Nitschko et al. 2005) that in persistent infection the JCV DNA load regularly is low (Dorries, Sbiera et al. 2003; Randhawa, Shapiro et al. 2005).

JCV specific primer pairs selected on the sequence of the two published JCV genomic prototypes, JCV Mad-1 and JCV GS/B (Howley, Rentier-Delrue et al. 1980; Loeber and Dorries 1988) by the Oligo 6.0 software (**Table R-1**) were used. In addition, due to the genomic heterogeneity among JCV isolates, primer pairs for different regions of the genome, the non-coding, transcriptional control region (CR) (71-157), and the late region coding for the virus capsid protein (VP1) (169-204) were included in the system. In all the three regions of the genome targeted, a second, nested amplification with internal primer pairs (CR, pair 53-61, VP1, pair 201-202) was performed to further increase the detection sensitivity and JCV specificity.

The primer pair for the control region amplifies a fragment of 703bp in the standard PCR and of 305bp in length in the nested reaction. For the late region the product length for the standard and nested primer pair was 476 bp and 196 bp, respectively. The sensitivity of the primer pairs was determined by amplification of cloned JCV GS/B target DNA in dilutions from 100fg to 0.1fg. The sensitivity of the first primer pair for the control region was 0.1fg or 12 genome equivalents (GE). For determining the amplification sensitivity, the internal primer pair was used in a standard PCR reaction exhibiting a sensitivity of detection of 1fg or 120 GE, respectively. The sensitivity on the late region primer pairs was found to be 0.1 fg or 12 GE, respectively.

Table R-1. Sensitivity and specificity of the JCV primer pairs used for JCV DNA amplification from peripheral blood cells extracted DNA.

No*	Function	Individual sensitivity		Specificity	
		JCV VE DNA	GE	BKV VE DNA	GE
169-204	external primer pair VP	0.1 fg	12	10ng	12x10 ⁷
201-202	nested primer pair VP	0.1 fg	12	1ng	12x10 ⁶
71-157	external primer pair CR	0.1fg	12	1ng	12x10 ⁶
53-61	nested primer pair CR	1fg	120	1ng	12x10 ⁶

* *primer internal number*

GE= genomic equivalents, VE= vector, JCV=JC polyomavirus, BKV=BK polyomavirus, VP=viral capsid protein, CR= control region

Due to 70% genomic homology between the two human polyomaviruses JCV and BKV (Frisque 1983; Schatzl, Sieger et al. 1994) the cross reactivity of each primer pair selected on the JCV DNA sequence was determined by PCR on BKV DNA under the conditions used for JCV PCR. A 10 fold dilution series of pBKV DNA from 0.1fg to 10ng was subjected to PCR and analyzed by electrophoresis. Whereas the external JCV late region primer pair (149/204) amplified the homologous target DNA at a sensitivity of 12 GE, the heterologous BKV target DNA amplified a product at a concentration of 10ng. This represents a detection limit of 120 x 10⁶ GE BKV DNA. The nested VP primer pair as well as the two pairs for the control region detected 1ng DNA or 12 x 10⁶ of BKV GE (**Table R-1**). This means that the sensitivity of JCV primer pairs was between 10⁵ to 10⁷ times higher for detecting the homologous JCV DNA than the related heterologous BKV DNA, which shows the high specificity of our primer pairs for detecting the JCV DNA in peripheral blood cells.

3.4.2. Presence of JCV DNA in peripheral blood cell preparations

3.4.2.1. Detection of JCV DNA in peripheral blood cells of healthy blood donors

To establish the presence of JCV DNA in PBMCs and granulocytes of healthy blood donors, DNA was extracted using standard phenol-chloroform extraction from PBMCs and granulocytes after isolation by Percoll density gradient centrifugation. 500 ng cellular DNA were used as a template for PCR amplification. From the amplified products 1µl was subjected to nested PCR and the amplified products from both standard and nested PCR were characterized in Southern blot analysis.

- JCV late region (VP1) DNA amplification in PBMCs and granulocytes of healthy blood donors

PCR followed by Southern blot was performed on DNA from 11 PBMC and 14 granulocyte matched samples from 14 professional blood donors (BD) and 24/24 PBMC and granulocyte samples from 24 laboratory workers (LP) using the JCV specific primers for the late (VP1) region of the genome (internal numbers 169-204). As a positive reaction control JCV vector DNA and as a contamination control sterile H₂O were used as template (**Fig. R-4**). The JCV vector DNA showed always a positive specific product while the negative control was negative during the entire procedure. In comparison, the number of blood DNA probes detected as positive varied depending on the sensitivity of the detection method, with sensitivity increasing from gel analysis of standard PCR (sPCR) products to Southern blot hybridization followed by nested PCR (nPCR). For example, in **figure R-4**, after sPCR most of the samples had unspecific amplification products at other lengths, only in 2/7 granulocyte samples the JCV specific 333bp band was clearly visible (64-g and 65-g). The JCV specificity of these products was confirmed by the strong hybridization with the JCV specific radioactive labeled probe in Southern Blot analyses. One other granulocyte (62-g) and two PBMC samples (62-m and 63-m) were also positive after Southern Blot hybridization despite being negative in the gels of sPCR products. This suggested that too low amounts of JCV products were amplified as to be visible in the gel electrophoresis but were detectable in the more sensitive Southern blot analyses. In the nPCR in all samples the 196bp JCV specific product was detectable, the same was valid for the Southern blotting, suggesting that the PBMC samples of patients 61, 64 and 67 and the granulocyte samples of patients 61, 63, 66 and 67 carried very low amounts of JCV DNA, which could be detected only by repeated amplification and hybridization. Analyzing the results from all the samples studied, JCV VP1 sequences were detected in 1/11 (9%) of PBMC samples and 3/14 (21%) of granulocyte samples of the BDs and in 14/24 (58%) of the PBMCs and 17/24 (70%) of the granulocytes samples of the LPs after electrophoretic visualization of the standard PCR products. However, the detection sensitivity increased after both nested PCR and Southern blot analysis. The Southern blot analysis of the PCR products with standard primer pairs revealed 6/11 (55%) of the PBMC samples of the BDs and 19/24 (79%) of the LPs and 8/14 (57%) of the granulocytes samples of the BDs and 19/24 (79%) of the LPs to be positive. This percentage increased even further to 100% of all the PBMC and granulocyte samples from both the professional blood donors and the laboratory personnel in both the electrophoretic and the Southern blot analysis of the PCR products using the nested primer pairs (**Table R-2 and R-3**).

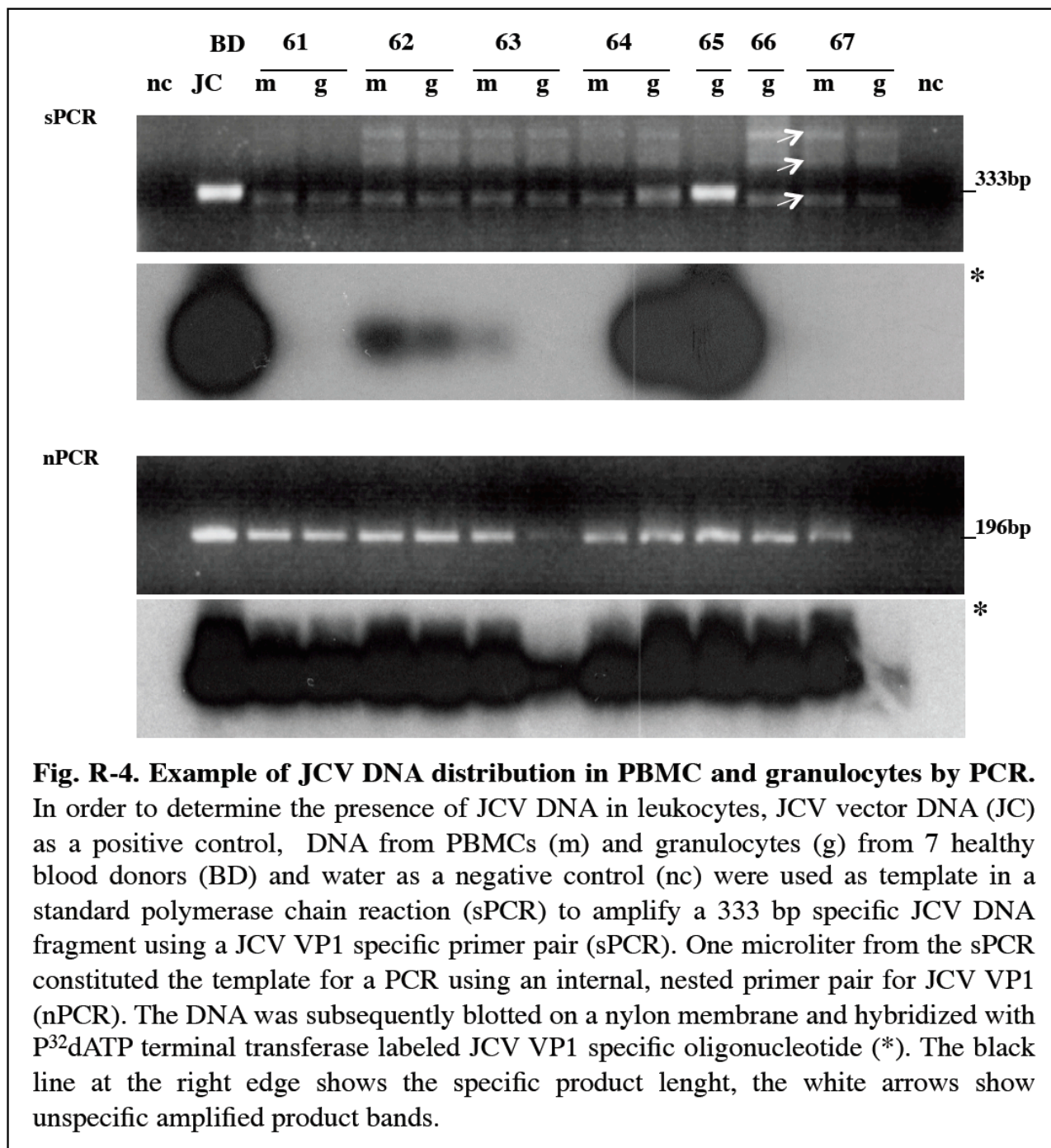


Table R-2. JCV late region (VP1) PCR on peripheral blood mononuclear cells (PBMC) and granulocytes of professional blood donors (BD)

Donor	PBMC				granulocytes			
	sPCR	*sPCR	nPCR	*nPCR	sPCR	*sPCR	nPCR	*nPCR
BD 48	-	+	+	+	-	-	+	+
BD 50	-	+	+	+	+	+	+	+
BD 51	+	+	+	+	-	+	+	+
BD 52	-	+	+	+	-	+	+	+
BD 53	-	-	+	+	-	+	+	+
BD 54	-	-	+	+	-	-	+	+
BD 55	-	-	+	+	-	+	+	+
BD 59	na	na	na	na	-	-	+	+
BD 62	-	+	+	+	-	+	+	+
BD 63	-	+	+	+	-	-	+	+
BD 64	-	-	+	+	+	+	+	+
BD 65	na	na	na	na	+	+	+	+
BD 66	na	na	na	na	-	-	+	+
BD 67	-	-	+	+	-	-	+	+
Σ (14)	1/11(9%)	6/11(55%)	11/11(100%)	11/11(100%)	3/14(21%)	8/14(57%)	14/14(100%)	14/14(100%)

*Standard PCR (sPCR) was performed on DNA extracted from PBMCs and granulocytes of professional blood donors (BD) using human polyomavirus JC (JCV) late region (VP1) specific primer pairs followed by internal, nested PCR (nPCR). PCR products were analyzed by gel electrophoresis and subsequently by Southern Blot hybridization (*sPCR and *nPCR) with a JCV VP1 specific radioactively labeled oligonucleotide. The results are represented by the number of positive samples and by percentage of positive samples in the total number of evaluable samples and the final result is highlighted in red.*

na = sample not available

Table R-3. JCV late region (VP1) PCR on peripheral blood mononuclear cells (PBMC) and granulocytes of laboratory personnel (LP)

Donor	PBMC				granulocytes			
	sPCR	*sPCR	nPCR	*nPCR	sPCR	*sPCR	nPCR	*nPCR
LP 56	-	+	+	+	-	+	+	+
LP 57	-	+	+	+	-	-	+	+
LP 58	-	+	+	+	-	-	+	+
LP 61	-	-	+	+	-	-	+	+
LP 89	-	-	+	+	+	+	+	+
LP 86	+	+	+	+	-	-	+	+
LP 75	+	+	+	+	+	+	+	+
LP 200	+	+	+	+	+	+	+	+
LP 201	-	-	+	+	+	+	+	+
LP 202	+	+	+	+	+	+	+	+
LP 203	+	+	+	+	+	+	+	+
LP 204	-	+	+	+	+	+	+	+
LP 205	+	+	+	+	+	+	+	+
LP 206	+	+	+	+	+	+	+	+
LP 207	+	+	+	+	+	+	+	+
LP 208	+	+	+	+	+	+	+	+
LP 209	+	+	+	+	+	+	+	+
LP 210	+	+	+	+	+	+	+	+
LP 211	-	-	+	+	+	+	+	+
LP 212	+	+	+	+	+	+	+	+
LP 213	-	-	+	+	+	+	+	+
LP 214	+	+	+	+	-	+	+	+
LP 215	-	+	+	+	-	-	+	+
LP 216	+	+	+	+	+	+	+	+
Σ (24)	14/24(58%)	19/24(79%)	24/24(100%)	24/24(100%)	17/24(70%)	19/24(79%)	24/24(100%)	24/24(100%)

Standard PCR (sPCR) was performed on DNA extracted from PBMCs and granulocytes of laboratory personnel (LP) using human polyomavirus JC (JCV) late region (VP1) specific primer pairs followed by internal, nested PCR (nPCR). PCR products were analyzed by gel electrophoresis and subsequently by Southern Blot hybridization (*sPCR and *nPCR) with a JCV VP1 specific radioactively labeled oligonucleotide. The results are represented by the number of positive samples and by percentage of positive samples in the total number of evaluable samples and the final result is highlighted in red.

- JCV control region (CR) DNA amplification in PBMCs and granulocytes of healthy blood donors

PCR for the JCV control region followed by Southern blot hybridization was performed on DNA from 12 PBMC and 15 granulocyte matched samples from 15 professional blood donors (BD) and 7 PBMC and granulocyte samples from 7 laboratory workers (LP) using the JCV specific primers for the noncoding control region (CR) (internal numbers 71-157 and 53-61 for the nPCR). In contrast to the late region amplification results, the level of JCV CR detection was much lower, varying from 0/12 and 0/15 (0%) in the PBMC and granulocyte samples of BDs and 0/7 (0%) in the LP samples after electrophoretic visualization of the standard PCR to 8/15 (67%) of the PBMC and 11/15 (73%) of the granulocyte samples of the BDs and 3/7 (43%) of both, the PBMC and granulocyte samples of the LPs, after the Southern Blot analysis of the nested PCR (**Table R-4 and R-5**).

3.4.2.2. Detection of JCV DNA in peripheral blood cells of immune impaired patients

Similar to previous analyses, 15 matched PBMC and granulocyte samples from HIV-1 positive donors were analyzed for the presence of JCV specific DNA by amplification with JCV specific primer pairs for the late (VP1) region of the genome followed by Southern blot analysis. Electrophoretic visualization of the standard PCR results revealed that 5/15 (33%) of the PBMC and 10/15 (66%) of the PBMC samples amplified the JCV VP1 sequence. The percentage of positive samples increased after nested PCR and Southern blot analysis to 13/15 (87%) of the PBMC and 15/15 (100%) of the granulocyte samples (**Table R-6**).

The low rate of JCV DNA detection after sPCR in the samples of all the groups studied confirmed that the level of viral DNA was generally very low. However, detection of JCV DNA in all individuals after Southern blot analyses of the nPCR amplicons suggested that JCV DNA is regularly associated with peripheral blood cells of adult individuals.

Table R-4. JCV control region (CR) PCR on peripheral blood mononuclear cells (PBMC) and granulocytes of professional blood donors (BD)

Donor	group	PBMC				granulocytes			
		sPCR	*sPCR	nPCR	*nPCR	sPCR	*sPCR	nPCR	*nPCR
BD 48	BD	-	-	+	+	-	-	-	-
BD 49	BD	-	-	-	-	-	-	+	+
BD 50	BD	-	-	+	+	-	-	+	+
BD 51	BD	-	-	+	+	-	-	+	+
BD 52	BD	-	-	-	-	-	-	+	+
BD 53	BD	-	-	+	+	-	-	-	-
BD 54	BD	-	-	+	+	-	-	+	+
BD 55	BD	-	-	+	+	-	-	+	+
BD 59	BD	na	na	na	na	-	-	-	-
BD 62	BD	-	-	-	-	-	-	+	+
BD 63	BD	-	-	+	+	-	-	+	+
BD 64	BD	-	-	+	+	-	-	+	+
BD 65	BD	na	na	na	na	-	-	+	+
BD 66	BD	na	na	na	na	-	-	-	-
BD 67	BD	-	-	-	-	-	-	+	+
Σ (15)	NL	0/12(0%)	0/12(0%)	8/12(67%)	8/12(67%)	0/15(0%)	0/15(0%)	11/15(73%)	11/15(73%)

*Standard PCR (sPCR) was performed on DNA extracted from PBMCs and granulocytes of professional blood donors (BD) using JCV control region (CR) specific primer pairs followed by internal, nested PCR (nPCR). PCR products were analyzed by gel electrophoresis and subsequently by Southern Blot hybridization (*sPCR and *nPCR) with a radioactively labeled oligonucleotide. The results are represented by the number of positive samples and by percentage of positive samples in the total number of evaluable samples and the final result is highlighted in red.*

na = sample not available

Table R-5. JCV control region (CR) PCR on peripheral blood mononuclear cells (PBMC) and granulocytes of laboratory personnel (LP)

Donor	PBMC				granulocytes			
	sPCR	*sPCR	nPCR	*nPCR	sPCR	*sPCR	nPCR	*nPCR
LP56	-	-	+	+	-	-	-	-
LP 57	-	-	+	+	-	-	+	+
LP 58	-	-	+	+	-	-	+	+
LP 61	-	-	-	-	-	-	+	+
LP 75	-	-	-	-	-	-	-	-
LP 86	-	-	-	-	-	-	-	-
LP 89	-	-	-	-	-	-	-	-
Σ (7)	0/7(0%)	0/7(0%)	3/7(43%)	3/7(43%)	0/7(0%)	0/7(0%)	3/7(43%)	3/7(43%)

*Standard PCR (sPCR) was performed on DNA extracted from PBMCs and granulocytes of laboratory personnel (LP) using JCV control region (CR) specific primer pairs followed by internal, nested PCR (nPCR). PCR products were analyzed by gel electrophoresis and subsequently by Southern Blot hybridization (*sPCR and *nPCR) with a radioactively labeled oligonucleotide. The results are represented by the number of positive samples and by percentage of positive samples in the total number of evaluable samples and the final result is highlighted in red.*

Table R-6. JCV late region (VP1) PCR on peripheral blood mononuclear cells (PBMC) and granulocytes of HIV-1 and HIV-1/PML patients

Donor	PBMC				granulocytes			
	sPCR	*sPCR	nPCR	*nPCR	sPCR	*sPCR	nPCR	*nPCR
HIV-1 pat 1	-	+	+	+	+	+	+	+
HIV-1 pat 2	+	+	+	+	-	-	-	+
HIV-1 pat 3	-	-	-	-	+	+	+	+
HIV-1 pat 4	-	-	-	+	-	-	+	+
HIV-1 pat 5	-	+	+	+	+	+	+	+
HIV-1 pat 6	-	-	-	+	+	+	+	+
HIV-1 pat 7	-	-	+	+	+	+	+	+
HIV-1 pat 8	-	-	+	+	+	+	+	+
HIV-1 pat 19	-	-	-	+	-	-	+	+
HIV-1 pat 20	-	-	-	-	-	-	-	+
HIV-1 pat 21	-	-	-	+	-	-	-	+
HIV-1 pat 26	+	+	+	+	+	+	+	+
HIV-1 pat 27	+	+	+	+	+	+	+	+
HIV-1 pat 28	+	+	+	+	+	+	+	+
HIV-1 pat 29	+	+	+	+	+	+	+	+
Σ (15)	5/15(33%)	7/15(47%)	9/15(60%)	13/15(87%)	10/15(67%)	10/15(67%)	12/15(80%)	15/15(100%)

*Standard PCR (sPCR) was performed on DNA extracted from PBMCs and granulocytes of human deficiency virus (HIV-1) infection patients using JCV late region (VP1) specific primer pairs followed by internal, nested PCR (nPCR). PCR products were analyzed by gel electrophoresis and subsequently by Southern Blot hybridization (*sPCR and *nPCR) with a radioactively labeled oligonucleotide. The results are represented by the number of positive samples and by percentage of positive samples in the total number of evaluable samples and the final result is highlighted in red.*

3.5. Characterization of JCV-peripheral blood cells association

Cell types found positive for JCV DNA by PCR included both lymphocytes and granulocytes. However, the concentration of JCV DNA appeared to be more prominent in the granulocytes. Since these cells are professional phagocytes, it appeared possible that JCV uptake might be mediated by phagocytosis of circulating virus as JCV is regularly reported in cell free serum and plasma samples (Koralnik, Boden et al. 1999). In contrast to this hypothesis, polyomavirus infection is characterized by nuclear localization of viral DNA. Therefore, intracellular localization of JCV DNA by fluorescence *in situ* hybridization (FISH) was used to differentiate viral infection from phagocytosis of circulating virus.

3.5.1. Establishment of the fluorescence *in situ* hybridization technique for sub-cellular localization of JCV DNA in peripheral blood cells

A highly sensitive and specific method for the detection of viral genomes in single cells is the DNA hybridization *in situ* (Lawrence, Marselle et al. 1990). Therefore a fluorescent JCV DNA *in situ* hybridization technique (FISH) was developed (Nath and Johnson 1998) (Raap 1998). Fluorescence *in situ* hybridization includes a series of experimental steps allowing subcellular localization of DNA hybrids by indirect fluorescence labeling (McNeil, Johnson et al. 1991).

After separation of PBC populations, cells were counted, cytopinned on slides, air-dried and fixed. Prior to *in situ* hybridization the cells were re-hydrated and permeabilized for the introduction of labeled DNA probes and detection antibodies. The hybridization procedure included temperature denaturation in formamide and hybridization of the DNA probe consisting of digoxigenin PCR-labeled DNA fragments. This was followed by detection of the hybridized digoxigenin-labeled probe by indirect immune detection with an enzyme labeled anti digoxigenin monoclonal antibody and a secondary anti mouse antibody coupled directly with Texas-red. Alternatively, for the amplification of the JCV specific hybridization signal, the secondary antibody was coupled with peroxidase and the signal was enhanced by precipitating tyramid coupled with biotin. Biotin was then detected with streptavidin coupled with Texas-Red. The fluorescent signal was visualized using classical fluorescence microscopy, confocal microscopy and postmicroscopic signal processing. For the development of a JCV specific *in situ* detection system that is able to target JCV DNA in all primary blood cell types at low copy number, each technical step was specifically adapted to high detection sensitivity.

3.5.1.1. Fixation of primary peripheral blood cells for FISH

The fixation procedure of primary blood cells was the first important step for following *in situ* detection. It has not only to insure adhesion to the glassware and stability of cell structures during the experimental procedures, but insure also sufficient cytoplasmic and nuclear membrane permeabilization to enable the viral DNA probe to reach subcellular compartments.

Three major fixative solutions were previously used to support *in situ* hybridization techniques in various cell types in culture and sectioned tissue. This included methanol-acetic acid (3:1) (Krejci, Kleinwachter et al. 1976), acetone 100% (Suthipintawong, Leong et al. 1996) and paraformaldehyde 4% (Eldred, Zucker et al. 1983; Shibuya, Miwa et al. 1992). The temperature and duration for fixation varied from 4°C to 23°C and 5 to 30 min. In all methods a post fixation proteolytic treatment with 1µg/ml proteinase K for 10 min was included (Nuovo 1995). All these techniques were analyzed on positive cells for JCV FISH. Permeabilization of the cells was controlled by fixation of the JCV transformed glial cell line HJC-15, and on PCR positive granulocyte populations followed by hybridization of the JCV specific probe and fluorescent detection techniques. None of these fixation protocols proved to be sufficient for hybridization.

A. Determining the basic fixative

A series of fixation procedures for *in situ* detection techniques (Looi and Cheah 1992) was analyzed to improve the permeabilization of the cells. (**Table R-7**) Most important variables were the concentration of fixative, diluting buffers and their pH, temperature, time of fixation and the post-fixation treatment of the cells. All these factors have been analyzed independently. Fixation analyses were performed on transformed cell line HJC-15, PBMC and granulocyte samples. The degree of cytoplasmic and nuclear permeabilization was controlled with a FITC labeled marker (Situs control kit, Situs, Germany) originally developed for the controlled proteolytic digestion of pores in cellular membranes of cell-lines without losing cellular integrity, but strong enough for the penetration of DNA probes at a length of 200bp and detection antibodies in FISH. By addition of the diluted FITC marker (1:25 in PBS) during fixation of cells, nuclear transfer of the marker could be followed by fluorescence microscopy. In addition to the chemicals used, the time necessary for the permeabilization of the nuclear membrane structures for each individual cell type was determined by permanent monitoring.

Methanol/Acetic Acid

Primary PBMCs and granulocytes were transferred on glass slides and fixed with methanol-acetic acid 3:1 at -20°C , 4°C or room temperature (RT, 23°C) for 10 or 20 minutes. After fixation the cells were treated with $1\mu\text{g/ml}$ proteinase K / 4% Sitis marker for 1, 3, 5, 10 or 15 minutes and analyzed by microscopy. Under all fixation temperatures the fluorescent marker was discriminated exclusively in the cytoplasm after 10 minutes fixation time. The cytoplasmic localization was also observed in cells fixed for 20 min. at 4°C and RT. However, perinuclear concentration of the signal was observed in cells fixed for 20 minutes at -20°C and treated for 1 minute with $1\mu\text{g/ml}$ proteinase K. Under all conditions, proteolytic treatment longer than one minute destroyed irreversibly the cellular structures. In addition, after methanol/acetic acid fixation, almost half of the cells dissociated from the slides.

These results demonstrated that fixation with methanol/acetic acid followed by $1\mu\text{g/ml}$ proteinase K treatment did not permeabilize the nuclear membrane of the PBCs for influx of a digoxigenin labeled DNA probe and the indirect immune detection system.

Acetone

The same procedure was followed using acetone as fixative. Primary PBMCs and granulocytes on glass slides were fixed with 100% acetone at -20 or 4°C and RT for 10, 15 or 20 minutes. The post fixation procedure was identical to that of methanol/acetic acid fixation. At 20 minutes fixation time -20°C as well as 4°C temperature achieved a better permeabilization of the cytoplasmic membrane than at RT leading to perinuclear concentration of the fluorescent signals, however, the nuclear membrane was not trespassed by the marker molecules.

Acetone and postfixation with Methanol/acetic acid

It was reported (Pichon, Monsigny et al. 1999) that post-fixation with Methanol/acetic acid (M/AA) improves acetone permeabilization of the nuclear membrane. Therefore cells were fixed for 20, 30, 40, 50 or 60 minutes with acetone 100% at -20°C followed by a second fixation step for 20 or 30 minutes in M/AA 3:1 at -20°C . Acetone fixation at times longer than 30 minutes resulted in complete impermeabilization of the cells with the fluorescent signal co-localizing only with the cytoplasmic membrane. At 20 min. fixation in acetone followed by 20 min fixation in M/AA showed a perinuclear concentration of the signal but without nuclear penetration. Acetone solutions with up to 20% H_2O were reported to improve the permeabilization effect compared to that of

Table R-7. Experiments performed in order to assess cell treatment conditions to achieve complete nucleus permeabilization without loss of cellular structures.

Fixative	Concentration	Temperature (°C)	Time (min)	Secondary treatment	Concentration	Temperature (°C)	Time (min)	Proteolytic treatment * at 37°C	Concentration	Time (min)
A. Determining the basic fixative										
Methanol:Acetic acid	3:1	-20, 4, 23 (RT)	10, 20	-	-	-	-	Proteinase K	1µg/ml	1, 3, 5, 10, 15
Acetone	100%	-20, 4, 23 (RT)	10, 15, 20	-	-	-	-	Proteinase K	1µg/ml	1
	100%	-20	20, 30, 40, 50, 60	Methanol:Acetic acid	3:1	-20	20, 30	Proteinase K	1µg/ml	1
	99.75, 99.5, 99.25, 99, 98, 95, 90, 85, 80%	4	10	Methanol:Acetic acid	3:1	-20	20	Proteinase K	1µg/ml	1
PFA in PBS (+)	4%	4, 23(RT)	5, 10, 15, 20	-	-	-	-	Proteinase K	1µg/ml	1
B. Optimization of paraformaldehyde fixation										
PFA in PBS (+)	4%	4	15	-	-	-	-	Proteinase K	1µg/ml	1
PFA in PBS (-)	4%	4	15	-	-	-	-	Proteinase K	1µg/ml	1
				Triton-X 100	0.2, 0.3, 0.5, 0.6%	23 (RT)	15, 30, 60	Proteinase K	1µg/ml	10
				Saponin	0.2, 0.3, 0.5, 0.7%	23(RT)	15, 30, 60 24h, 48h, 72h	Proteinase K	1µg/ml	10
				-	-	-	-	Proteinase K	1µg, 1mg, 10mg/ml	5, 10, 15, 30
				-	-	-	-	Pepsin	0.1, 0.25, 0.5%	5, 10, 15, 30
				-	-	-	-	Proteinase K : pepsin	1mg/ml : 0.25%	5

*= all proteolytic treatment solutions contained 4% Situs Control for fluorescence microscopy visualization of the cellular permeabilization

PFA= paraformaldehyde

PBS (+)= Phosphate Buffer Saline containing calcium and magnesium ions

PBS (-)= Phosphate Buffer Saline without calcium and magnesium ions

100% acetone (Glasova, Konikova et al. 1995). A fixation row of 99.75, 99.5, 99.25, 99, 98, 95, 90, 85 or 80% acetone for 10 min. at 4°C followed by post-fixation with M/AA for 20 minutes at –20°C did not improve the permeabilization of the cells. Although cytoplasmic signals were detected, no intranuclear signal could be observed. Obviously, acetone even with M/AA post-fixation was not suitable for permeabilization of primary PBCs.

Paraformaldehyde

Paraformaldehyde (PFA) with its ability to stabilize protein structures by cross-linking was recently described to be not only a highly valuable fixative for immune histochemical methods but also for *in situ* hybridization techniques (Holland, Mackenzie et al. 1996). Nucleic acid hybridization of PFA fixed material strongly depends on time of treatment. Therefore the cells were fixed with 4% PFA in PBS for 5, 10, 15 or 20 minutes either at 4°C or RT, followed by the same proteolytic treatment as in the case of acetone or M/AA fixation. Fixation at room temperature had a clogging effect on the cell structures after any time course. The best results were obtained with 4% paraformaldehyde for 15 min at 4°C. The cells exhibited a clear cytoplasmic localization of the fluorescent marker with limited nuclear penetration. Shorter or longer exposure to the fixative resulted in lower intensity of the signal.

Overall, methanol/acetic acid fixation exhibited a better permeabilization than acetone and paraformaldehyde. However, cell adhesion to the glassware was severely reduced, the cells being easily removed from the slides by experimental procedures. Acetone proved to be a strong fixative, at long treatment times and higher temperatures. Even lowering the percentage of acetone and re-fixing the cells with methanol-acetic acid did not improve the drastic fixation of acetone. The cells fixed with a 4% PFA solution showed a better permeabilization than the acetone fixed cells and in the same time were much more resistant than the methanol-acetic acid treated cells. Therefore 4 % PFA was chosen as a basic fixative and further criteria analyzed to improve permeabilisation of the nuclear membrane.

B. Optimization of paraformaldehyde fixation

Influence of metal ions on paraformaldehyde fixation

As metal ions are important for the activity of the fixative (Pollard, Lunny et al. 1987), the function of Calcium (Ca^{++}) and Magnesium (Mg^{++}) in the dilution buffer solutions (PBS with (+) and without (-))were analyzed. The cells were fixed for 15 minutes in 4% PFA diluted in PBS with and without Ca^{++} and Mg^{++} at 4°C for 15 min. followed by proteolytic treatment for 1 min. In

contrast to buffer solutions with ions, cells treated with buffer without ions showed a clearer fluorescent signal. Therefore PBS without calcium and magnesium was introduced as a standard. However, localization of the marker molecules remained unchanged.

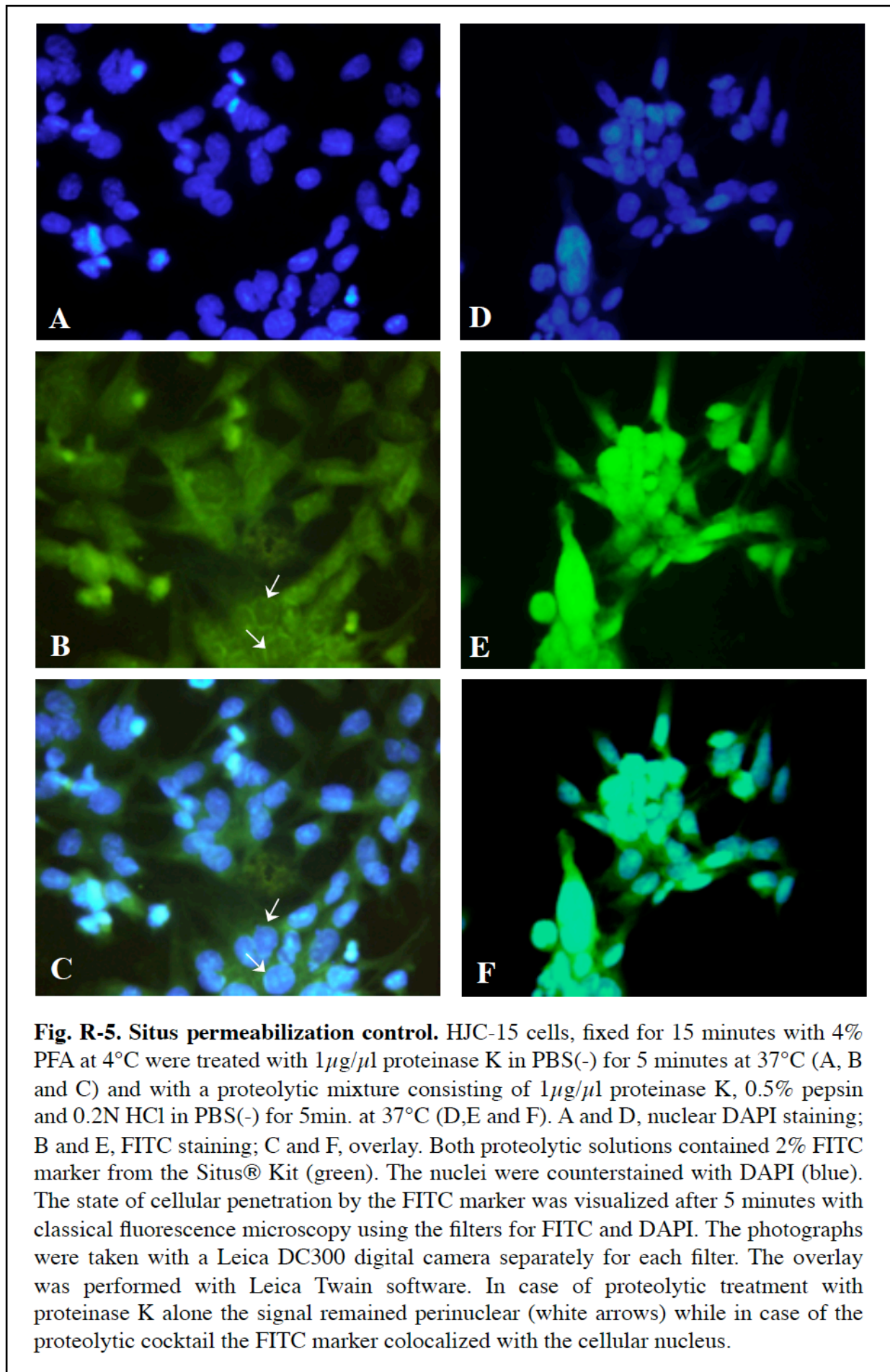
Influence of surfactants on paraformaldehyde fixation

Cytoplasmic localization of fluorescent signals with a light perinuclear concentration suggested that stronger treatment of the membranes might be needed to open up the nuclear membrane. Therefore Triton X-100 and saponine, both surfactants known to enhance the penetration of macromolecules through cell membranes (Dourmashkin, Dougherty et al. 1962; Wikstrom, Bakke et al. 1987; To and Bernard 1992), were introduced at different concentrations and for different periods of times at RT. The cells were fixed with 4% PFA in PBS(-) at 4°C for 15 min and then treated with Triton X-100 0.2, 0.3, 0.5 or 0.6% for 15, 30 or 60 minutes (Wikstrom, Bakke et al. 1987) or with saponin 0.2, 0.3, 0.5 or 0.7% for 15, 30 or 60 min. or 24, 48 or 72 hours (To and Bernard 1992). In addition, the cells were treated with proteinase K 1µg/ml containing 4% Sitis marker for 10 minutes. The results were assayed in Fluorescence microscopy. Triton X-100 combined with paraformaldehyde fixation led to the disintegration of the cell structures after prolonged treatment (60 min.) and to no visible effects after short treatment (15 min.). Overall, the best result was obtained with 0.5 % saponine treatment for 60 minutes. The integrity of the cell structures was kept and the nucleus was permeabilized. The disadvantage was that the buffers in all steps of experiments have to contain saponine for an effective permeabilization due to the time reversibility of the saponine effect (Francis, Kerem et al. 2002). However, saponine inhibits the DNA-DNA binding of hybridization probes therefore it is not compatible with the *in situ* hybridization technique (Simons, Morrissey et al. 2006).

Thus, the overall effect of surfactants on paraformaldehyde fixed primary PBCs had either a negative effect upon cell integrity (Triton X-100) or the treatment was incompatible with the hybridization technique (saponin).

Influence of enzymatic treatment on paraformaldehyde fixation

In contrast to surfactant treatment, which acts unspecific on the membrane lipid double layer, proteases are known to act specifically on different classes of proteins (Hedstrom 2002) and insure membrane permeability upon short treatment without structural loss. Therefore, the effect of proteolytic treatment with different concentrations of proteinase K and pepsine (Ebeling, Hennrich et al. 1974; Macville, Van Dorp et al. 1995) was studied.



One important factor for the enzymatic activity is the pH (Farinas, Bulter et al. 2001), therefore different concentrations of HCl or acetic acid were analyzed concomitant with different proteases. The cells were prefixed for 15 minutes with PFA 4% and then treated at 37°C for 5, 10, 15 or 30 minutes either with 1µg/ml, 1mg/ml or 10 mg/ml proteinase K or with 0.1, 0.25 or 0.5% pepsin, both proteases diluted in H₂O containing 0.1, 0.2 or 0.5N HCl or acetic acid. In general, it was found that low pH was positively influencing cell permeabilization when used in combination with proteolytic treatment. The cells treated for 5minutes with 1µg/ml or 1mg/ml proteinase K or 0.25 or 0.5% pepsin containing 0.2N of HCl or acetic acid showed a higher amount of cytoplasmic FITC staining then those containing only 0.1N acid, and the signal was mostly concentrated in the perinuclear region. However, at too low pH (0.5N HCl or acetic acid) this effect was reversed for both proteases at any concentration and the cell uptake of the FITC marker was lower. Longer treatment (10, 15, 30 minutes) with any of the proteases or higher concentration of Proteinase K (10mg/ml) for any amount of time did not improve the nuclear permeabilization, the signal remaining perinuclear. The best result was obtained with 0.2N HCl and 1mg/ml proteinase K for 5 minutes (**Fig.R-5 A, B and C**).

This demonstrated that, used separately, both enzymes, proteinase K and pepsine, did not lead to sufficient permeabilization of fixed cells. Therefore a combination treatment of the two proteases at 37°C and low pH was used (1mg/ml proteinase K and 0.5% pepsin in 0.2N HCl) and as seen from nuclear localization of the fluorescent marker, the two proteases insured after a 5 minute treatment complete cellular and nuclear permeabilization (**Fig R-5 D, E and F**).

Combining all factors responsible for improving individual fixation steps, a procedure was established for the fixation and permeabilization of human PBLs that is suitable for FISH. It combined a 15 minutes fixation step at 4°C with 4% paraformaldehyde diluted in PBS without calcium and magnesium ions followed by a 5 minutes proteolytic treatment at 37°C with a mixture consisting of 1mg/ml proteinase K and 0.5% pepsin diluted in H₂O containing 0.5N HCl. The double proteolytic reaction in combination with low pH after PFA fixation insured both the stability of cell structures and permeability of the nuclear membrane required by JCV specific hybridization probe and the fluorescence detection system.

3.5.1.2. Development of a highly sensitive JCV specific fluorescence probe for *in situ* hybridization

The hybridizing system consists of a labeled DNA probe annealing to the target DNA at variable concentrations in single cells and a read out system detecting labeled DNA hybrids. The reliability of DNA hybridization techniques strongly depends on the specificity of the probe for the targeted nucleic acid as well as the specificity and the sensitivity of the detection system. Each individual component was analyzed to ensure maximum specificity as well as sensitivity of the respective reaction.

A. Synthesis of the digoxigenin labeled JCV specific hybridization probe

The non-radioactive digoxigenin system (Roche Diagnostics, Germany) is based on the labeling of the DNA probe using deoxy Uracil triphosphate (dUTP) coupled with a digoxigenin molecule. Digoxigenin is a highly thermo-stable molecule keeping its tertiary structure even at 100°C. As it does not have a correspondent in the animal world, cross-reactivity of the detection system with human proteins was excluded. The labeling rate of digoxigenin is one Digoxigenin-coupled dUTP per each 15 base pairs (Chevalier, Yi et al. 1997). This insures a high specific activity of the labeled probe. Labeling of the DNA was controlled by electrophoretic mobility difference due to digoxigenin incorporation between the labeled and non-labeled DNA products (**Fig.R-6B, R-8B and R-9B**).

Previous experiments had shown that oligonucleotides end-labeled by digoxigenin-coupled triphosphates as signalling molecule by terminal transferase with digoxigenin coupled triphosphates are not able to detect JCV genomic DNA by FISH. This was probably due to the low concentration of signal molecules bound per probe (Doerries, personal communication). In the attempt to generate a JCV specific probe with a higher concentration of labeled molecules, PCR amplified JCV DNA fragments were synthesized by replacing the deoxy- Thymidine-triphosphate (dTTP) in standard PCR reactions by Digoxigenin- coupled dUTP. Primer pairs used for PCR amplification of JCV DNA were selected by the software Oligo 6.0, and analyzed for performance under standard PCR conditions on 1 fg JCV DNA as a template. The yield of PCR product was evaluated by band density after gel electrophoresis of the products.

To detect JCV target DNA at high sensitivity a hybridization probe was designed consisting of 16 individual virus specific DNA fragments covering about 55% of the JCV genome (2811 bp). The PCR fragments were located in early and late as well as in the noncoding region of the genome

(**Fig. R-6A**). To ensure specificity of binding to JCV DNA and reduce cross-reactivity with related polyomaviruses each fragment had a length of around 200 bp (147 to 256bp), which is the optimal size for a FISH probe in terms of cell penetration, specific activity and detection sensitivity (Muhlegger, Huber et al. 1990).

B. Detection sensitivity of the JCV hybridization probe

To assess the labeling efficiency and the detection equality of each individual probe the sensitivity of each JCV digoxigenin labeled DNA probe was analyzed by dot-blot (An, Franklin et al. 1992). Each amplicon was diluted to a concentration of 20ng/ μ l. Additionally, a probe mix was created by combining the individual probes in equal quantities with a final concentration of 20ng/ μ l. Subsequently, from each individual probe and from the combined probe 10 fold dilution series from 20ng to 2fg/ μ l were prepared and from each dilution 1 μ l was spotted on a nylon membrane. The digoxigenin labeled triphosphates were subsequently detected with a mouse monoclonal antibody directed against digoxigenin and a goat anti mouse antibody coupled with horseradish peroxidase (HRP). After developing the peroxidase signal for 5min with TMB substrate (see Materials and Methods 2.2.6.4.1) the blots were air-dried and scanned. The detection sensitivity of the individual digoxigenin probes in the dot-blot system was determined to be in a similar range between 200fg and 200pg cloned JCV DNA. The detection sensitivity of the mixed JCV probe was 200fg (**Fig R-7**).

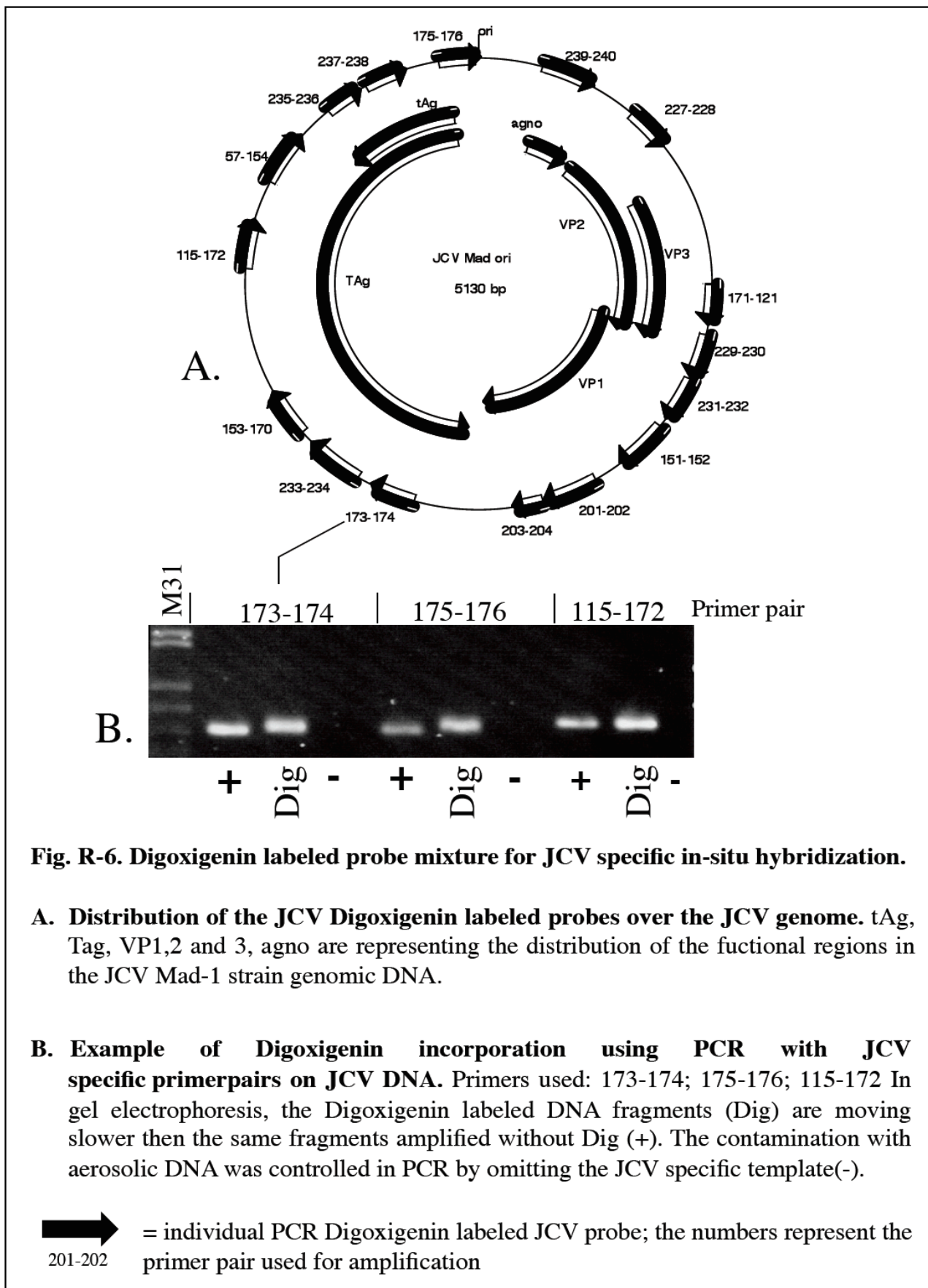
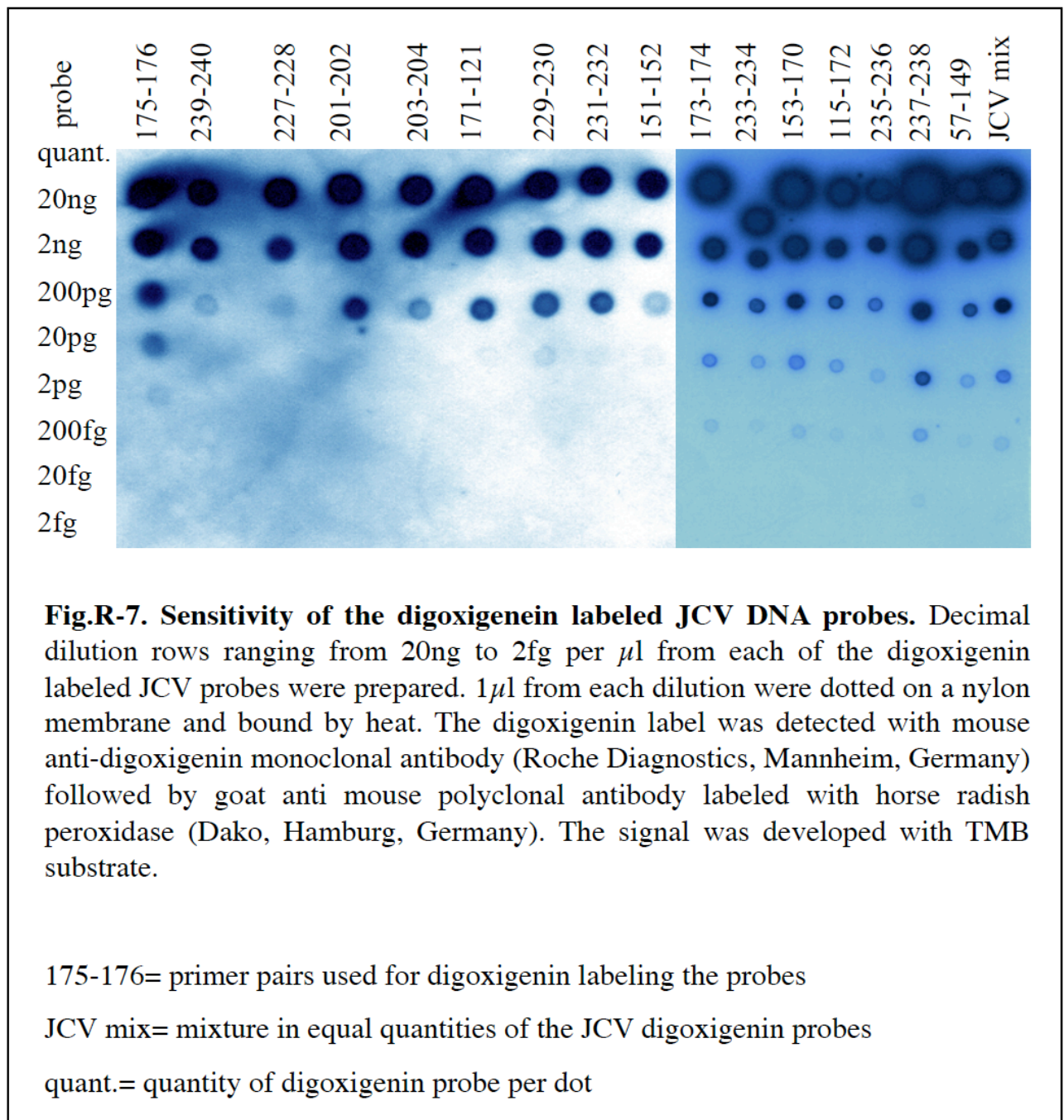


Fig. R-6. Digoxigenin labeled probe mixture for JCV specific in-situ hybridization.

A. Distribution of the JCV Digoxigenin labeled probes over the JCV genome. tAg, Tag, VP1,2 and 3, agno are representing the distribution of the functional regions in the JCV Mad-1 strain genomic DNA.

B. Example of Digoxigenin incorporation using PCR with JCV specific primerpairs on JCV DNA. Primers used: 173-174; 175-176; 115-172 In gel electrophoresis, the Digoxigenin labeled DNA fragments (Dig) are moving slower than the same fragments amplified without Dig (+). The contamination with aerosolic DNA was controlled in PCR by omitting the JCV specific template(-).

= individual PCR Digoxigenin labeled JCV probe; the numbers represent the primer pair used for amplification



C. Specificity of hybridization

- Conditions for hybridization of Digoxigenin labeled probes in FISH

Beside the DNA probe properties, the specificity of the hybridization is not only dependent on the probe itself but also on the temperature of reaction. The hybridization temperature for FISH had to meet two conditions: first, to ensure a specific hybridization reaction. Therefore the stringency was set at -20°C below melting temperature at a salt concentration of 5xSSC (Fisher, Gusella et al. 1984; Durm, Sorokine-Durm et al. 1998). Second, physiological temperature

conditions to minimize denaturation of cellular proteins and loss of cellular structures. This was achieved by the addition of formamide (50%) to the buffer that decreases the melting temperature of the nucleic acids by 0.7 °C per 1% of formamide and thus the final hybridization temperature (Durm, Haar et al. 1996). Due to the application of a combined probe for JCV *in situ* hybridization a common hybridization temperature had to be chosen. While the mean melting temperature of the 16 individual probes was 72.8°C it was determined to be 92.5°C under 5xSSC conditions and decreased to 72.5°C considering the -20°C stringent hybridization rule described before. The final hybridization temperature of all 16 probes was calculated for the 50% formamid buffer and was set to 37 °C (Table R-8).

Table. R-8. Calculation of the common hybridization temperature for the JCV combined probe for FISH.

A	B	C	D	E
PCR amplified probe	melting temp. %GC based	melting temp. at 5xSSC	-20°C = stringent hybr. temp.	-35°C= 50%formamid
175-176	73.6°C	93.5 °C	73.5°C	38.5 °C
239-240	73.7°C	93.6 °C	73.6°C	38.6 °C
227-228	74.9°C	95 °C	75°C	40 °C
201-202	74.7°C	94.5 °C	74.5°C	39.5 °C
203-204	72.7°C	92.5 °C	72.5°C	37.5 °C
171-121	72.2°C	92 °C	72°C	37 °C
229-230	73.3°C	93 °C	73°C	38 °C
231-232	72.8°C	92.5 °C	72.5°C	37.5 °C
151-152	75.3°C	95.5 °C	75.5°C	40.5 °C
173-174	72°C	91.5 °C	71.5°C	36.5 °C
233-234	71.5°C	91 °C	71°C	36 °C
153-170	70.9°C	90 °C	70°C	35 °C
115-172	71°C	90 °C	70°C	35 °C
235-236	72°C	91.5 °C	71.5°C	36.5 °C
237-238	71.7°C	91 °C	71°C	36 °C
mean value	72.8 °C	92.5 °C	72.5 °C	37 °C

The recommended melting temperatures (B) of the 16 JCV DNA probes (A) were obtained with the software Oligo 6.0 (Cambio Ltd, Cambridge, UK). The hybridization temperatures were calculated for a salt concentration of 5xSSC (C) at high stringency (20°C below the melting temperature (D) (Fisher, Gusella et al. 1984)). Final hybridization temperatures at 50% formamide were calculated for each probe. Mean values were determined for each of the 16 probes (E) and the final hybridization temperature for the JCV probe mixture was calculated (in red).

- JCV unrelated viral and cellular probes

After developing the JCV specific probe a house-keeping gene probe was necessary as an internal control to demonstrate the sensitivity of the hybridization system *in situ*. As we wanted to detect JCV DNA in human leukocytes, a human skeletal alpha actin gene (ACTA1) was chosen. This gene had the advantage that it is present in human genome as a single gene (2 alleles), but it is not expressed in PBCs (Vandekerckhove and Weber 1978; Khaitlina 2001). This eliminates the possibility of the genomic probe hybridizing the messenger RNA (mRNA) sequences as would be the case when using a house-keeping gene that is expressed in the PBCs. Therefore the expected sensitivity of the ACTA1 probe would be that of 1 allele or 1 hybridization signal per cell. The conditions for the production of the ACTA1 cellular DNA probe were identical to that of the JCV specific probe. A combined ACTA1 probe was amplified by PCR from genomic DNA extracted from PBCs. The probe consisted of 14 ACTA1 PCR digoxigenin labeled DNA fragments, with a mean length of 160 bp and a total length of 2194bp and was analyzed just as the JCV specific probe (**Fig. R-8A**).

The specificity of the digoxigenin-labeled probes for their homologous target was analyzed with an unrelated probe. The feline immunodeficiency virus (FIV) genome is not present in the human system (Gardner and Luciw 1989), therefore it was selected as target sequence. As a non-human specific probe the FIV probe was expected to give information about potential unspecific binding of the DIG labeled probes if any signal would have developed in the human PBCs. 11 PCR primer pairs were selected on the FIV genome (9474bp in length) and their products used to combine a FIV PCR DIG-labeled DNA probe. Amplification of digoxigenin labeled products was analyzed in gel electrophoresis. The individual FIV probes had a mean length of 177 bp and the combined probe covered 1955 bp of the FIV genome. The distribution of the different probe fragments covered all genomic regions, GAG, POL and ENV (**Fig. R-9A**). Assessment of the functionality of the ACTA1 and FIV probes was performed directly in FISH.

3.5.1.3. Detection conditions for digoxigenin-labeled hybridization probes in primary blood cells

The hybridization conditions *in situ* differ from the hybridization on extracted DNA due to the complexity of the cellular environment. Therefore the function of the JCV digoxigenin labeled PCR products as hybridization probe was analyzed on human leukocytes (**Table R-9**).

Table R-9. Post hybridization improvements of FISH detection

Cells*	Post JCV hybridization procedure								Result
Direct anti-digoxigenin detection									
PBMC and granulocyte samples (BD 48,49,50,51,52)	-	-	-	-	-	-	PBS (-)	ms- α -DIG TXR labeled	3/10 samples with low positive signal
Tyramide amplification									
5 PBMC and 5 granulocyte samples(BD 48,49,50,51,52)	-	-	-	-	PBS(-)	ms- α -DIG-HRP	Biotinylated tyramide substrate	Streptavidin-TXR	9/10 samples with positive signal + high background
Granulocytes BD 48	-	-	-	PBS(-)	Tyramide OHCl	ms- α -DIG-HRP	Biotinylated tyramide substrate	Streptavidin-TXR	1/1 samples positive +background
Granulocytes BD 48	-	-	PBS(-)	Tyramide OHCl	3%H ₂ O ₂	ms- α -DIG-HRP	Biotinylated tyramide substrate	Streptavidin-TXR	1/1 samples positive +low background
DNA acetylation									
VERO cells	-	0.1M triethanolamine 5min, RT	PBS(-)	Tyramide OHCl	3%H ₂ O ₂	ms- α -DIG-HRP	Biotinylated tyramide substrate	Streptavidin-TXR	low background
VERO cells	-	0.1M triethanolamine+ 0.25%acetanhydride 5min, RT	PBS(-)	Tyramide OHCl	3%H ₂ O ₂	ms- α -DIG-HRP	Biotinylated tyramide substrate	Streptavidin-TXR	negative
Unspecific antibody binding									
HJC-15	0.1M triethanolamine+ 0.25%acetanhydride 5min, RT	0.5% casein	PBS(-) +0.05% tween-20	Tyramide OHCl	3%H ₂ O ₂	-	Biotinylated tyramide substrate	Streptavidin-TXR	negative
HJC-15	0.1M triethanolamine+ 0.25%acetanhydride 5min, RT	5% normal mouse serum	PBS(-) +0.05% tween-20	Tyramide OHCl	3%H ₂ O ₂	-	Biotinylated tyramide substrate	Streptavidin-TXR	negative

JCV= human polyomavirus JC, PBMC= peripheral blood mononuclear cells, BD48=blood donor number, VERO = african green-monkey epithelial cells (JCV negative),

HJC-15= JCV transformed hamster glial cell line, ms- α -DIG=mouse anti digoxigenin antibody, TXR= Texas red, HRP=horseradish peroxidase

-direct anti-digoxigenin detection

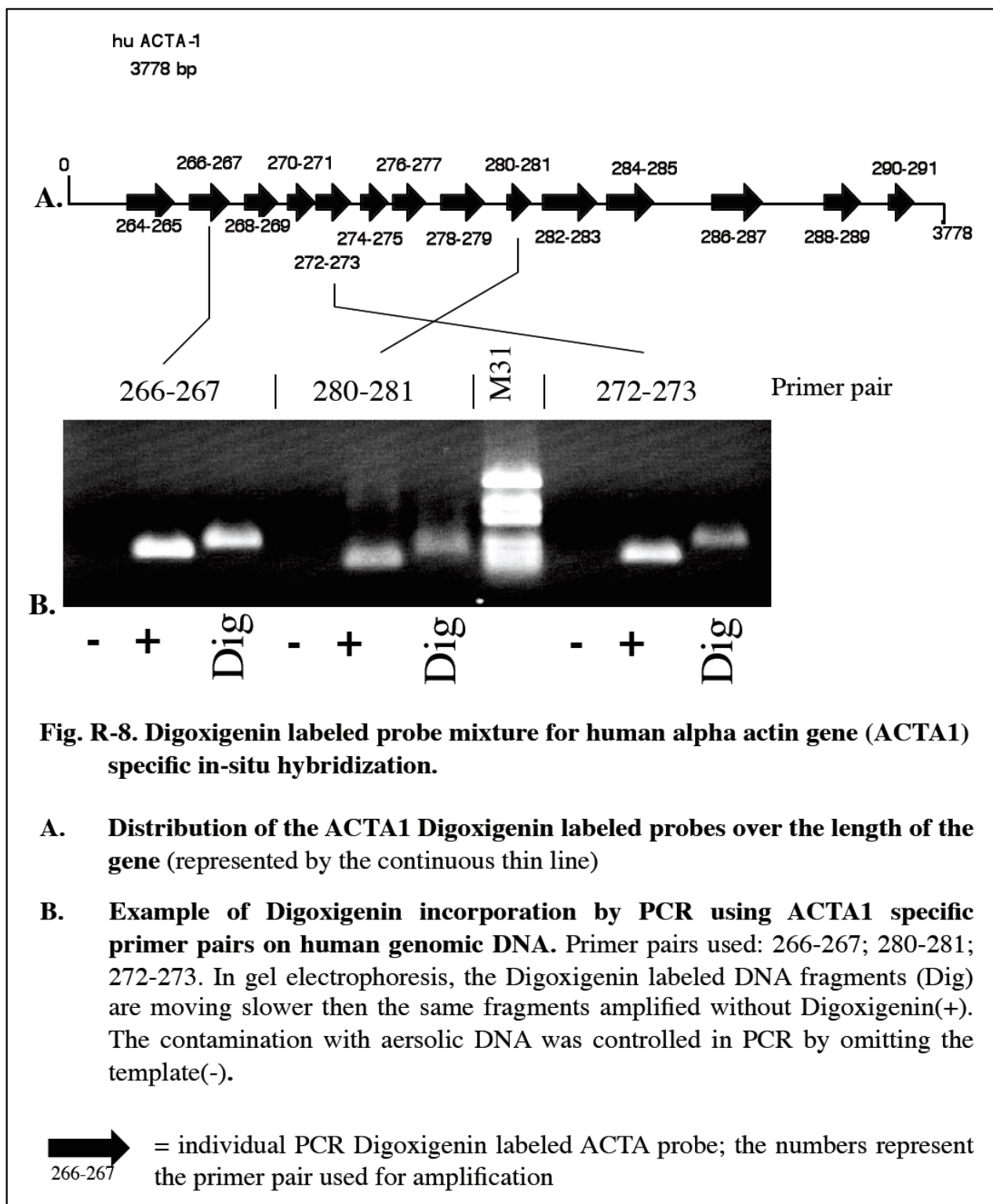
JCV specific *in situ* hybridization with the combined Dig-labeled probe was applied on PBMCs and granulocytes from 5 healthy blood donors (BD48, 49, 50, 51 and 52) previously found positive for JCV DNA by PCR. After fixation and permeabilization of the cells as described, the cellular DNA was denatured and hybridized with denatured JCV specific digoxigenin probe for 72 hours. After washing with PBS, the labeled DNA was detected directly with a monoclonal mouse anti Digoxigenin antibody followed by goat anti mouse antibody labeled with Texas Red. The nuclei were counterstained with DAPI. The hybridization signal was visualized with classical fluorescence microscopy (FM). Although these cell samples amplified JCV DNA by PCR on cellular DNA of 10^6 cells, digoxigenin signals were detected only occasionally, in 3 out of 10 samples. This result suggested that the sensitivity of the hybridization system was too low to detect virus DNA in PBCs.

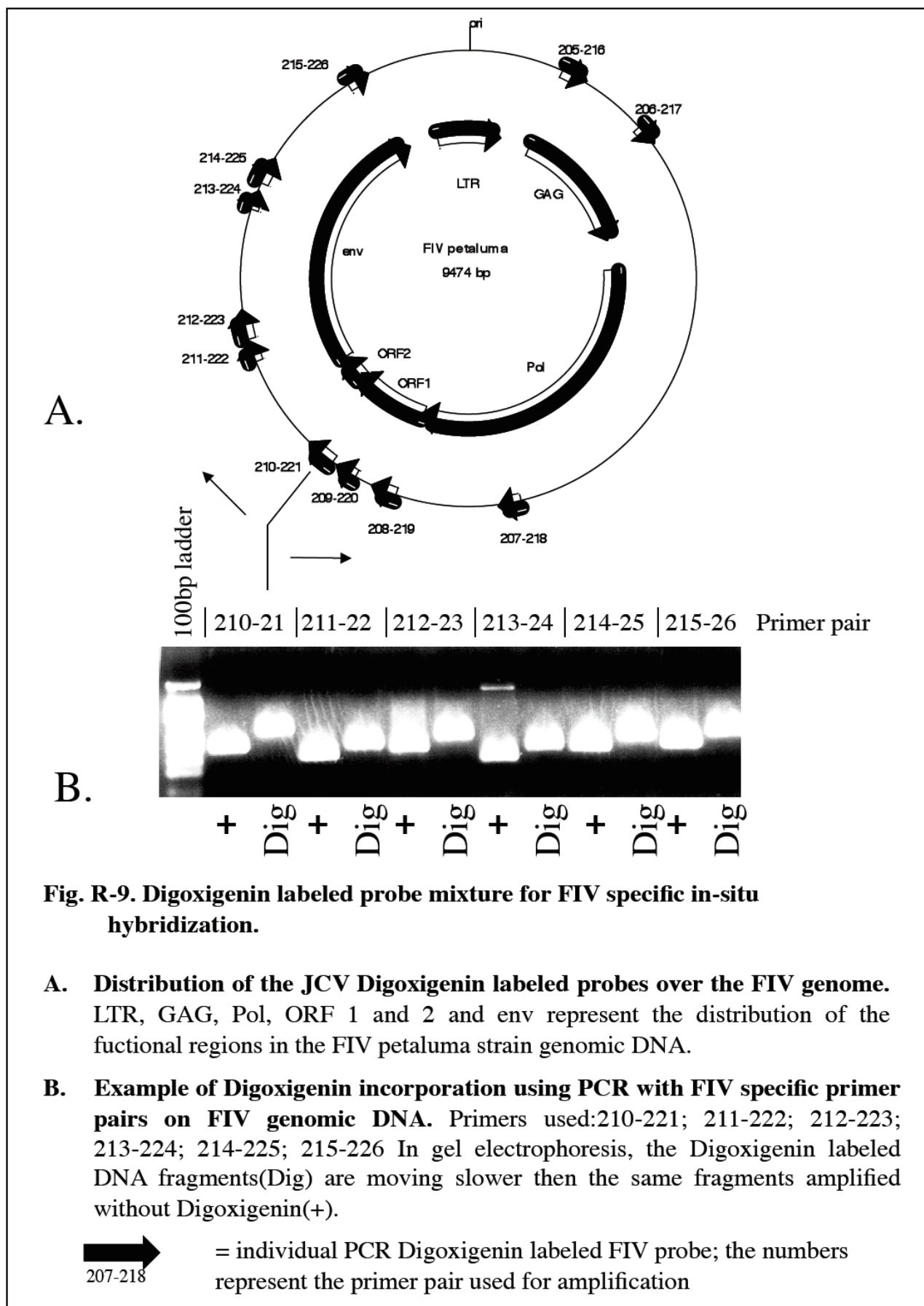
-tyramide amplification of the signal

Attempting to improve the detection sensitivity of the hybridization signal a post-hybridization chemical enhancement step with biotinylated tyramide (Truong, Boenders et al. 1997; Sano, Hikino et al. 1998; Murakami, Hagiwara et al. 2001) was introduced. In contrast to the classical detection, the secondary antibody was coupled with HRP that enzymatically cleaved a biotinylated tyramide substrate the precipitate of which depositing around the enzymatic spot. The substrate was then detected by development of the biotin signal with Texas-Red labeled streptavidin. The enhancement reaction on the same samples allowed detection of JCV DNA in single cells of PBC populations in 9 out of 10 cases thus demonstrating the increased sensitivity of detection of JCV DNA in single cells. Chemical amplification of the signal was therefore applied to detect JCV DNA *in situ* combined with FM.

However, the addition of chemical amplification often increased the background signals from endogenous peroxidase or biotin, found especially in the granulocytes. In order to increase the JCV specificity by reducing the background, the endogenous molecules had to be inactivated. To control the protocol for inactivation (Hasui, Takatsuka et al. 2002), two slides with 2×10^5 granulocytes were incubated with non-labeled tyramide-OHCl that saturates endogenous biotin (Evans, Aliesky et al. 2003). On the first slide, the cells were treated with 3% H_2O_2 in methanol for one hour to inhibit the endogenous peroxidase activity (Kohler, Lauritzen et al. 2000) and on the second slide the cells remained untreated. The cells were then incubated with biotinylated tyramide

and developed with streptavidin Texas-Red. The results were compared in FM. The cells without treatment of H₂O₂ had visible background levels compared to the treated cells that remained negative in FM (Table R-9).





-blocking unspecific DNA binding for background reduction

However, it remained unclear whether an increase in specific detection sensitivity may also increase unspecific detection. Factors known to be responsible for unspecific bindings in *in situ* hybridization techniques include electrostatic DNA-DNA attraction force and unspecific antibody binding (Min and Swansbury 2003).

Although undenatured double stranded DNA does not hybridize to single- or double-stranded DNA, due to free OH⁻ residues, electrostatic forces can develop between two DNA molecules, leading to unspecific signaling in FISH. This can be reduced by acetylation (Stuckenholz, Kageyama et al. 1999). The effect of acetylation on background levels was analyzed on the JCV negative African Green Monkey kidney cell-line Vero. Prior to hybridization fixed and permeabilized Vero cells were either incubated with 0.25% acetanhydride in 0.1M triethanolamine in PBS for 5 minutes or with triethanolamine buffer alone. Both types of treated cells were then hybridized with the JCV specific probe, followed by antibody detection, HRP/biotin inhibition and chemical amplification. The acetylated JCV negative Vero cells showed no JCV hybridization signals while in the unacetylated cells sparse unspecific fluorescent signals could be observed demonstrating that inhibition of electrostatic DNA-DNA attraction forces by acetylation is essential for a highly specific FISH (Table R-9).

-blocking unspecific antibody binding for background reduction

In contrast to unspecific binding forces of the probe, the antibody detection system may also lead to background either due to antibody binding to fragment crystallizable (Fc) receptors present on the surface of the cells or due to low affinity binding to intracellular unspecific molecules. The Fc receptors are expressed on the surface of many types of immune cells including phagocytes. Their physiological role is to bind antibodies that are attached to microbes or infected cells at their unspecific, Fc region (or tail), thus insuring opsonisation. Thereby they may interfere with molecular methods *in situ* by creating false signals through unspecific low-affinity binding of those antibodies to the cell surface that are used in these methods. Possible interference reactions were reduced by standard measures as diluting the antibodies in buffers containing 0.5% casein (Kenna, Major et al. 1985) and 5% normal serum (Lalli, Gibellini et al. 1992). To detach low affinity bound antibodies from the cells, 0.05% Tween-20 detergent (Xu, Huang et al. 1998) was added to all the washing buffers. On this basis, unspecific antibody binding was analyzed by hybridization of JCV transformed cell-line HJC-15 with JCV specific probe and omitting either the primary or the

secondary antibody from the posthybridization detection system. The cells hybridized and processed in this manner showed no background signals thus demonstrating that while using the improved incubation and washing buffers the antibodies did not generate unspecific reactions (**Table R-9**).

The optimized FISH procedure included fixation with 4% paraformaldehyde in PBS, postfixation proteolytic treatment with Proteinase K and pepsine at low pH. After acetylation of the cells, DNA was denatured in 95% formamide at 72°C. Hybridization was performed at 37 °C in 50% formamide and the digoxigenin signal was detected with mouse anti digoxigenin monoclonal antibody with 0.5% casein and 5% normal goat serum. After washing the cells in 0.2% Tween20 buffer the endogenous peroxidase was quenched with H₂O₂ and the endogenous biotin with tyramide buffer. The cells were then incubated with HRP labeled goat anti mouse polyclonal antibody. The peroxidase signal was amplified with biotinylated tyramide, and the precipitated biotin was detected with streptavidin Texas-Red. The nuclei were counterstained with DAPI and the result was visualized in classical fluorescence microscopy.

3.5.1.4. JCV specificity of the FISH hybridization in single cells

JCV shares 75% similarity with the other ubiquitous human polyomavirus, BKV. As these two viruses have been reported of co-infecting some other organs (Degener, Pietropaolo et al. 1997; Pietropaolo, Fioriti et al. 2003; Doerries 2006), and as there are no conclusive studies regarding the association of BKV with cells of the immune system, the specificity of the DNA hybridization had to be assayed in order to exclude the possibility of cross-reactivity. Therefore the specificity of the digoxigenin labeled probes was analyzed by *in situ* hybridization under the newly established conditions.

Firstly, the JCV-DIG probe detection capacity for its specific sequence was analyzed by FISH on the JCV transformed hamster glioma cell line HJC-15, carrying multiple JCV DNA integration sites in the cellular genome (Wold, Green et al. 1980). HJC-15 cells were fixed and underwent post fixation treatment and JCV specific hybridization as established. The JCV-DIG probe hybridized and developed fluorescent signals covering the cytoplasm and nuclei of each cell (**Fig. R-10A**).

Secondly, the specificity of DIG labeled probe molecules in general for their target DNA was established by hybridization of an unrelated FIV probe with JCV transformed cells. On HJC-15 cells, which carry no FIV DNA, a FIV specific hybridization was performed under hybridization conditions used for the JCV probe. The FIV probe did not hybridize in any of the cells

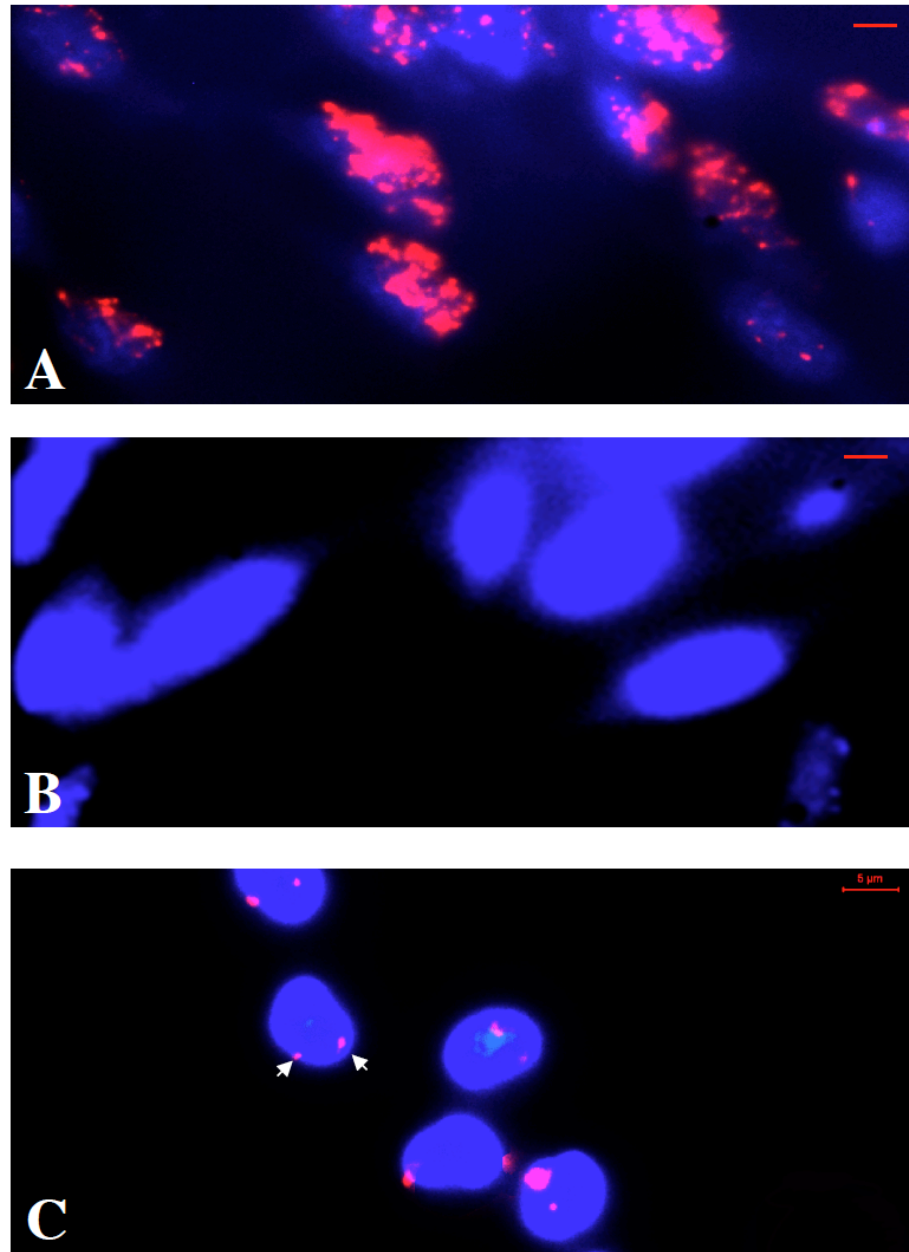


Fig. R-10. Analysis of the specificity and sensitivity of the digoxigenin labeled DNA probes by FISH and classical fluorescence microscopy. HJC-15 cells (A,B) and human peripheral granulocytes (C) were hybridized for three days with denatured digoxigenin labeled JCV (A), FIV (B) and ACTA-1 (C) probes. The signal was detected with two antibody system and developed with Texas-Red (red). The nuclei were counterstained with DAPI (blue). In the JCV transformed HJC cells the JCV probe hybridized in all the cells (A) while the unspecific FIV probe gave a negative result (B). The human alpha actin probe was able to detect each of the two alleles of the gene in all the human granulocytes (C, white arrows).

The scale=5 μ m (red line in the upper right corner)

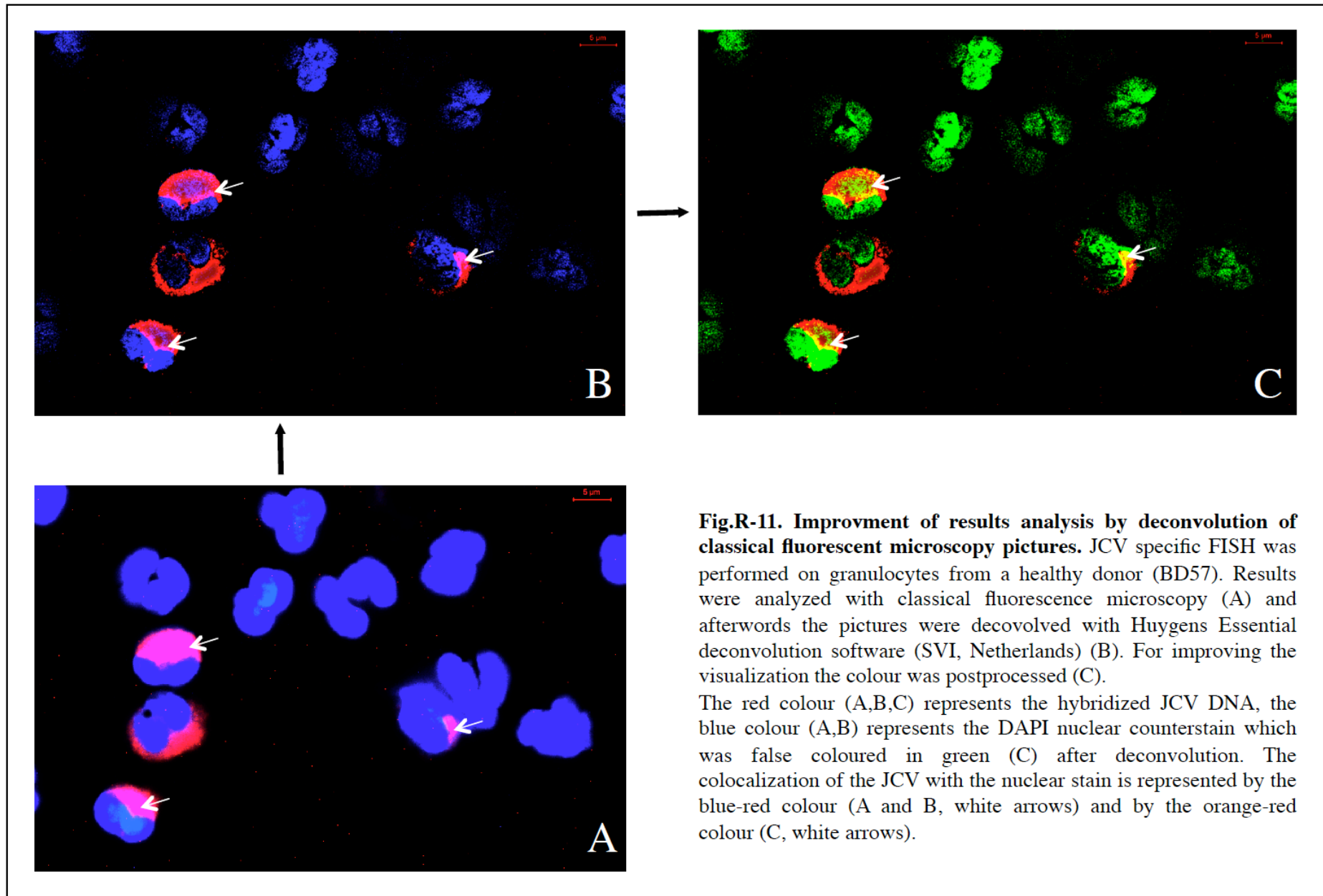
(**Fig. R-10B**). This proved that the digoxigenin probes do not bind unspecifically to unrelated DNA or cellular structures.

3.5.2.1. Improvement of the in-situ visualization by deconvolution software

Although it became clear that digoxigenin labeled probes did not bind to unrelated DNA unspecifically, the JCV specific hybridized signals were, at high concentrations of JCV DNA, highly intensive and appeared diffuse (**Fig. R-10A**). This was probably due to the chemical amplification that gives high signal intensity combined with classic fluorescence microscopy, the picture of which generated a perspective of the entire cell. So even if the visualization of the hybridized virus DNA *in situ* brought an important advantage compared to molecular methods as PCR on bulk cell DNA, the interpretation of the results remained difficult because of the imprecise localization of the JCV signal at sub-cellular levels.

Therefore we used deconvolution software post-processing of the classic fluorescent microscopy pictures (Manz, Arp et al. 2000). Based on nearest neighbour algorithms, this program (Huygens Essential, SVI, Netherlands) is able to eliminate the artificial glow of the fluorochromes, revealing exclusively the source of the signal.

JCV specific FISH followed by chemical amplification was performed on granulocytes of a healthy donor (NL85) (**Fig. R-11A**). The JCV specific signal was developed using streptavidin-Texas Red (red) and the nuclei were counterstained with DAPI (blue). The result was visualized by classical fluorescence microscopy and documented using a DC300F digital camera controlled by the QFluoro v.1.2.0 software (Leica Microsystems Imaging solutions Ltd, Germany). The colocalization of the two signals before deconvolution was difficult to estimate, as the DAPI signal was much stronger than that of the Texas-Red specific signal and additionally stretched out of the nuclear limits (**Fig. R-11A**). By the use of the deconvolution software the exact nuclear structures in the studied granulocytes were outlined. However, as compared to the primary picture of the DAPI stained nuclei, the colocalization of the viral and nuclear signal still remained difficult. Specifically, in regions of the overlay of red (Texas-Red) and blue (DAPI) color an over-nuclear situation could not be differentiated from an intra-nuclear situation (**Fig. R-11B**). Therefore we used the implemented possibility of artificially changing the fluorophore color. In the interest of a better differentiation, the color of the nuclei was changed from blue to green. Using this method the areas of JCV-nuclei co-localization became more defined as the combination of green nuclear staining and red viral signal changed from blue-red to orange (**Fig. R-11C**).



In conclusion, under the classical fluorescence microscopy conditions, the problematic of co-localization of two different fluorophore signals could be solved using a deconvolution software which eliminates the fluorescence glow and facilitates the clear visualization and evaluation of the *in situ* results. But due to the sensitivity limitations of the digital camera the weak signal emitted by single JCV DNA molecules hybridized could be detected only after extensive exposition, increasing the bleaching process of the fluorophores and increasing the background risk. On the other hand, the compensation of signal intensity by chemical amplification eliminated the quantification possibility.

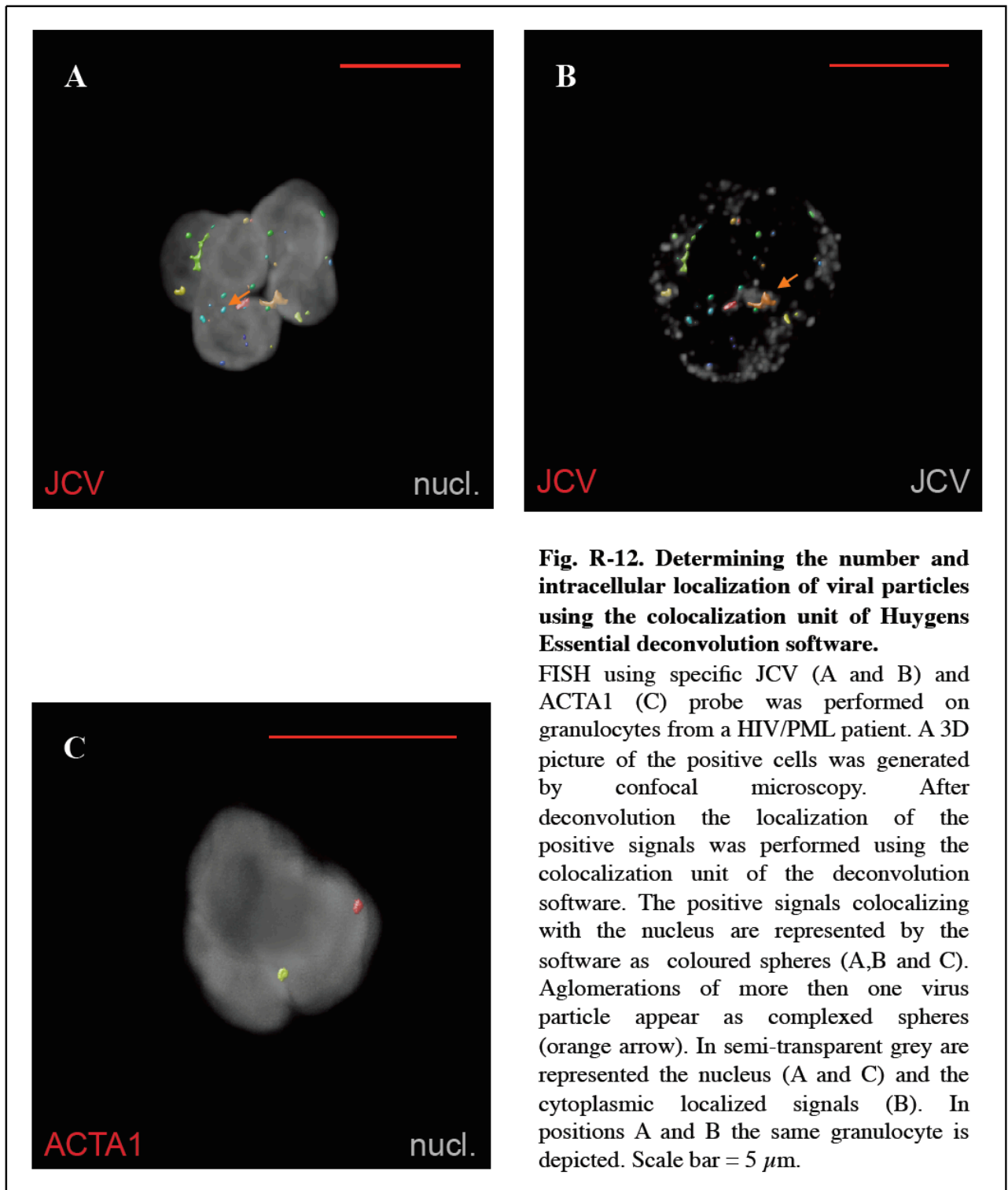
3.5.2.2. JCV localization at single cell level by confocal microscopy

In classical fluorescence microscopy, cells are excited with light having the specific excitation wavelength of one of the fluorophores, which upon excitation emits light of a different wavelength that is filtered by the microscope and caught by the terminal digital camera. Only one fluorophore at a time can be excited and the overlay of different emissions is software processed and not always exact. Another problem of the classical fluorescence microscopy is that the emission signal comes from the whole volume of the cells without making a depth distinction. Therefore the overlapping of two signals of different wavelength can mean co-localization but there are also chances of a simple overlapping of the signals.

However, for the detection as well as the results interpretation of cell associated viral genome copies, an exact intracellular localization is required. Compared with the classical fluorescence microscopy, confocal microscopy uses simultaneous laser beams of different wavelengths for the excitation of the cells. Therefore different fluorophores can be used simultaneously, the filtration of the emitted light taking place in several successive optical steps. Another advantage is that the excitation and the emission can be concentrated at successive depth levels of the cell, permitting a three-dimensional visualization of the fluorescent signals in the studied cells at consecutive levels of 20nm. It also allows the concentration on a single cell by optical means. This feature combined with the high sensitivity of detection due to the increased intensity of the signal enabled the JCV DNA localization and quantification at single cell level.

3.5.2.3. Software based localization of JCV signals at subcellular level

Generally, visual appreciation of colocalization signals tends to be inexact due to personal interpretation. Therefore a newly developed iso-colocalization unit of the Huygens Essential



deconvolution software was used in order to assess the exact localization of the FISH positive signals within the cells.

This unit uses a Nyquist algorithm which mathematically calculates the rate of signal overlapping from two different wave-length signals in a confocal three-dimensional picture. In the same time the software creates a 3D false image of the intranuclear signals and estimates its volume in voxels (1 voxel=1 3D pixel). FISH using specific JCV (**Fig.12 A and B**) and ACTA1 (**Fig.12 C**)

probe was performed on granulocytes from a PML patient (PML 3) and a 3D picture of the positive cells was acquired by confocal microscopy. After deconvolution the iso-colocalization unit was used to generate colocalization areas between the FISH positive signals and the nuclear counterstain and represented them as colored volumes (**Fig. 12 A, B and C**). The nuclear counterstain (**Fig. 12 A and C**) and the extranuclear signals (**Fig. 12 B**) are represented in semitransparent grey tones in order to permit visualization of the intranuclear signals. To estimate the number of virus copies contained in the colocalization surface the volume in voxels of each surface is divided by the smallest volume found in the cell. If the value is smaller than 3 then the surface represents one virus copy. Over 3, the result of the division gives the number of copies.

3.5.3.1. JCV localization in peripheral blood cells

JCV specific FISH was performed on matched PBMC and granulocyte samples from 37 individuals (22 from healthy donors and 15 from HIV-1 infected patients, from which 7 with established PML). In parallel, ACTA1 and FIV FISH were performed as a positive and negative hybridization control, respectively. The localization of the positive signals within the cells was analyzed with fluorescence and confocal microscopy. Only samples where the ACTA1 staining was positive and FIV staining negative were further evaluated for the presence of JC virus.

Three types of virus localization in the cellular compartments were found, cytoplasmic, cytoplasmic/nuclear and nuclear. The cytoplasmic signal was variably distributed, some signals were concentrated at the outer rim of the cell, not reaching the nucleus, probably associated with the cellular membrane (**Fig. R 13** und **Fig. R 14**, white arrows (1)). In the other case, the JCV positive signals evenly filled the cellular cytoplasm, without any preferential concentration towards the cellular membrane or the nucleus (**Fig. R 13** und **Fig. R 14**, white arrows (2)). In contrast, the cytoplasmic/nuclear signal distribution was concentrated in the perinuclear region, associated with the nuclear membrane (**Fig. R 13** und **Fig. R 14**, white arrows (3)) and the nuclear signal was identified by the colocalization of the JCV fluorescent signal with the nuclear counterstain (**Fig. R 13** und **Fig. R 14**, white arrows (4)). These types of localization were not exclusive, many of the cells presenting combinations of these distribution types, for example cytoplasmic/perinuclear/nuclear.

While all these types of localization were present in both PBMCs and granulocytes, the rate of representation according to the number of samples differed between the two cell types. In case of the PBMCs, the intracellular localization of the JCV DNA was mainly cytoplasmic in almost all the donors studied (34 of 35 evaluable donors (97%)) or cytoplasmic/nuclear (15 of 35 evaluable

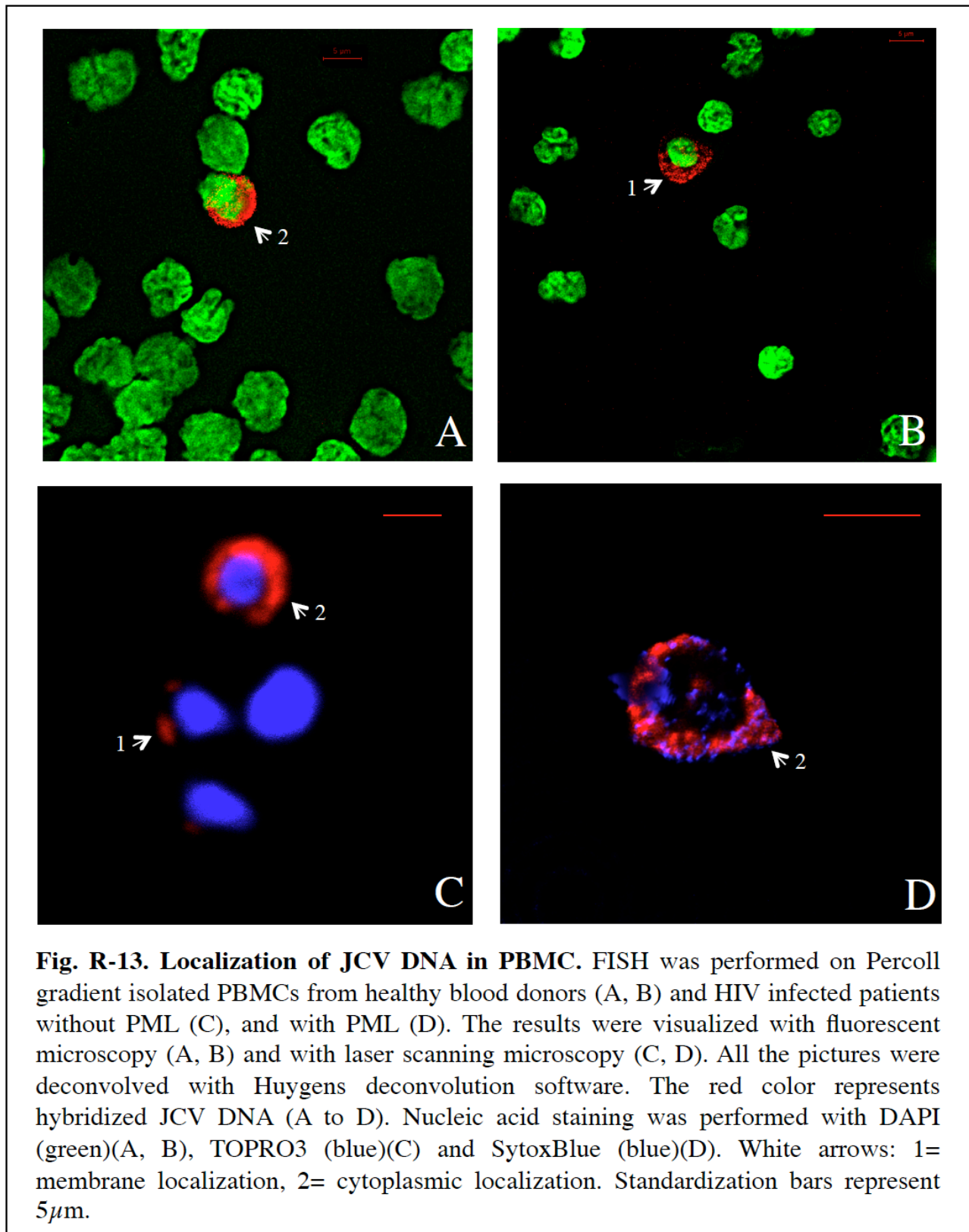
donors (43%). Rare intranuclear localization was found only in 1 of 35 evaluable donors (3%) and that one was of an HIV-1 infected patient (without PML)(**Fig. R 13, A, B, C and D; Table R-10 and R-11**).

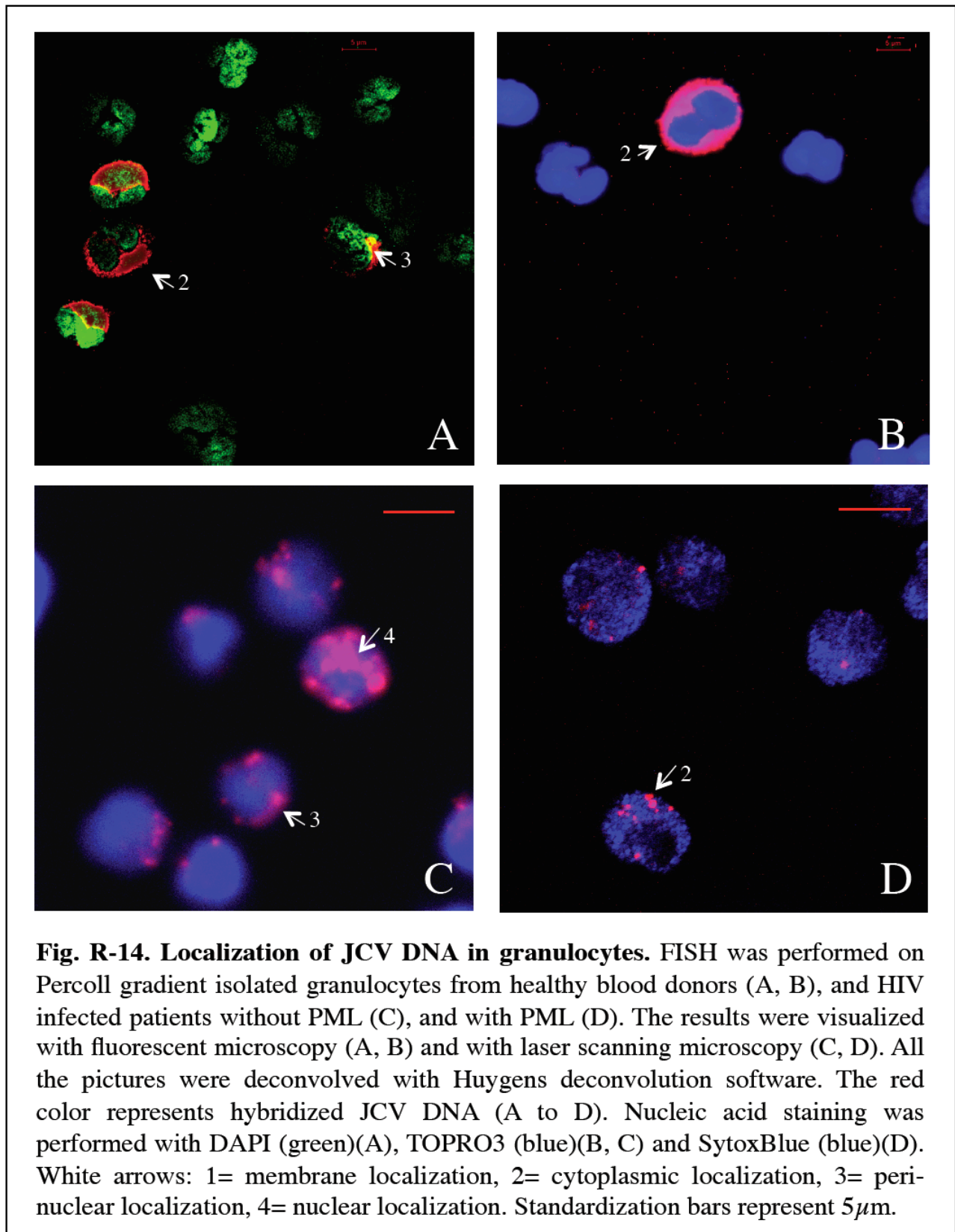
Compared with the PBMCs, the distribution of the JCV DNA in the granulocytes gave a more complex picture (**Fig. R 14.A, B, C and D**). While all the donors, as in the case of the PBMC, presented granulocytes with exclusive cytoplasmic localization of JCV (37 of 37 donors (100%)) the percentage of donors with cytoplasmic/nuclear localization increased (27 of 37 donors (73%)) compared with the number of donors carrying PBMC with cytoplasmic/nuclear JCV (43%). The same was the case with the donors with granulocytes carrying exclusive nuclear JCV (18 of 37 donors (49%)). Especially in the case of the HIV-1 infected patients this gain was obvious, as 15 of 15 (100%) immunodeficient donors had granulocytes carrying exclusive nuclear JCV compared to 3 of the 22 (14%) healthy blood donors. However, there was no difference between the HIV-1 infected patients with and without established PML as all (15 of 15 (100%)) of these patients' granulocytes presented all the types of JCV signal localization in FISH (**Table R-10 and R-11**).

3.5.3.2. Rate of peripheral blood cells associated with the JCV DNA

The localization of the JCV DNA in the PBCs revealed significant differences of JCV intracellular localization especially regarding the granulocyte population, where all 15 immuneimpaired donors carried granulocytes with nuclear presence of JCV. In contrast, only 3 of 22 immunocompetent donors revealed nuclear localization of the signals. However, the extent of the JCV-PBC association is also based on the number of cells affected in different individuals. Therefore, in addition to determining the intracellular localization, the number of JCV affected cells was analyzed in the 22 healthy donors and the group of 15 HIV-1 infected patients. For every patient sample, both PBMC and granulocyte, a total of 5×10^4 cells were counted using fluorescence and confocal microscopy and the number of JCV positive cells among these were reported to 1000 counted cells.

In both sample groups the number of PBMCs affected was comparable ranging from 0 to 20 per 1000 cells counted, even though slightly higher in the immune impaired individuals (14.5 ± 0.9 (SEM) positive PBMC per 1000 cells counted) than in the healthy donors (2.5 ± 0.4 (SEM) positive PBMC per 1000 cells counted) (**Table R-10 and R-11**). However, in case of the granulocyte population, the difference between the cell numbers affected was considerable among





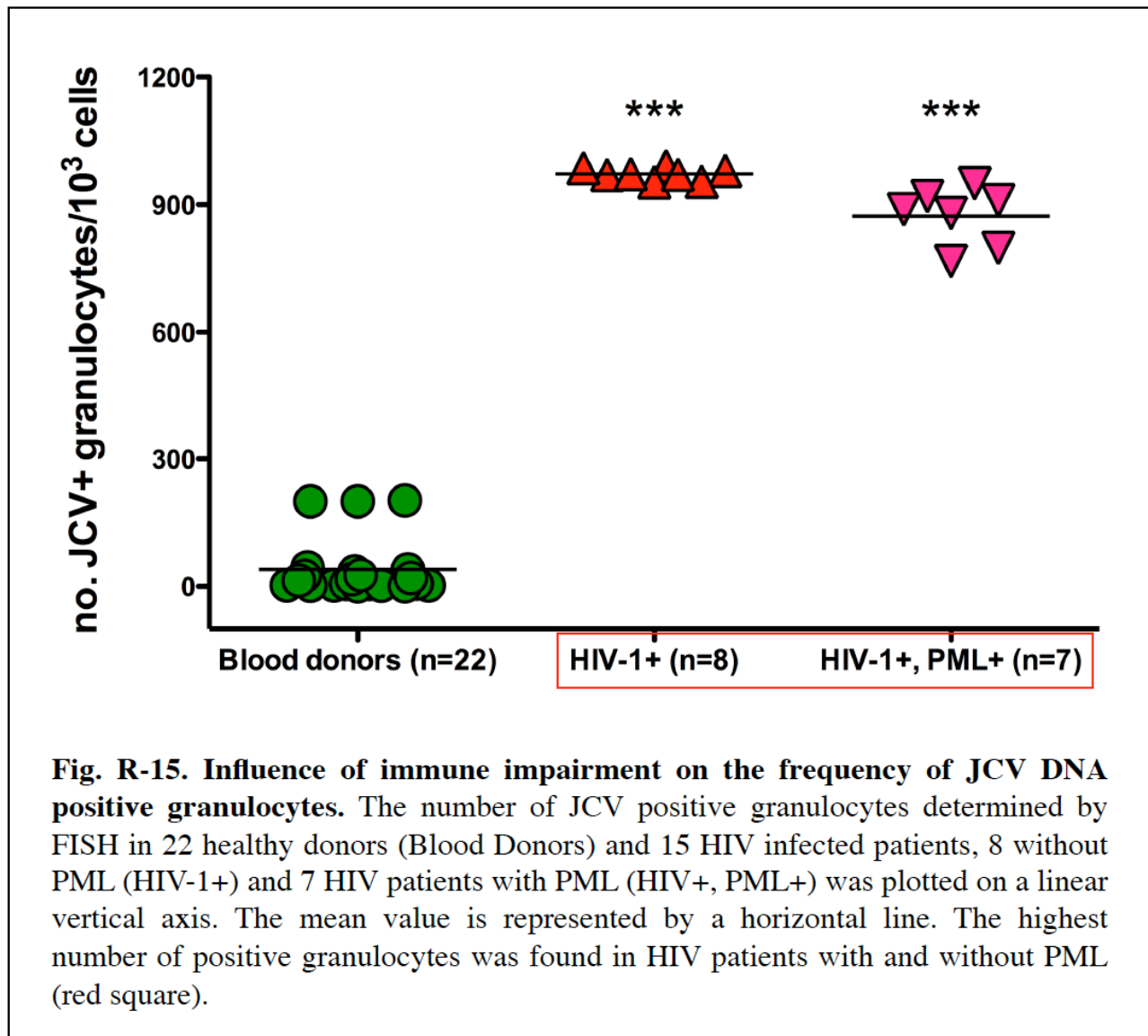


Fig. R-15. Influence of immune impairment on the frequency of JCV DNA positive granulocytes. The number of JCV positive granulocytes determined by FISH in 22 healthy donors (Blood Donors) and 15 HIV infected patients, 8 without PML (HIV-1+) and 7 HIV patients with PML (HIV+, PML+) was plotted on a linear vertical axis. The mean value is represented by a horizontal line. The highest number of positive granulocytes was found in HIV patients with and without PML (red square).

the immunocompetent and the immunodeficient individuals. Whereas in case of healthy donors it ranged from 1 to 202 cells per 1000 (40 ± 14 (SEM)) (Table R-10), it varied between 767 and 991 positive cells per 1000 in the immune impaired patients (926 ± 17.5 (SEM)) (ANOVA, $p < 0.0001$). Remarkably there was no significant difference among PML (873 ± 25 (SEM)) and the non-PML patients (972 ± 5 (SEM)) (ANOVA, $p > 0.05$) (Table R-11)(Fig. R-15).

If correlated with the intracellular localization, described in chapter 3.5.3.1, an increase in number of positive cells was associated with an increase of combined cytoplasmic and nuclear localization. This was the case in both the PBMC (Fig. R-16A, $r^2 = 0.93$, $p < 0.0001$) and the granulocytes (Fig. R-16B, $r^2 = 0.84$, $p < 0.0001$). Interestingly, in the granulocytes from the 15 HIV-1 infected patients, where the rate of affected cells was almost 100% (926 ± 17.5 (SEM) out of 1000 counted cells), the rate of the cells carrying nuclear associated JCV DNA reached a peak at 30% of

the total amount of granulocytes (307 ± 25 (SEM) out of 1000 counted cells) (Fig. R-16B , Table R-11).

Table R-10. Presence of JCV DNA in PBMC and granulocytes of professional blood donors (BD) and laboratory personnel (LP) as determined by FISH

Donor	granulocytes				PBMC			
	no. gran affected /1000				no. PBMC affected /1000			
	total	cyto	cyto/nuc	nucl	total	cyto	cyto/nuc	nucl
BD 48	15	14	1	0	1	1	0	0
BD 49	6	6	0	0	4	4	0	0
BD 50	3	3	0	0	5	5	0	0
BD 51	3	3	0	0	2	2	0	0
BD 52	2	2	0	0	2	2	0	0
BD 53	7	7	0	0	4	4	0	0
BD 54	40	36	4	0	6	6	0	0
BD 55	6	6	0	0	4	4	0	0
LP 56	1	1	0	0	0	0	0	0
LP 57	35	26	9	0	1	1	0	0
LP 58	17	15	2	0	1	1	0	0
LP 61	200	130	65	15	1	1	0	0
BD 62	2	2	0	0	1	1	0	0
BD 63	1	1	0	0	3	3	0	0
BD 64	20	14	6	0	5	5	0	0
BD 65	45	34	11	0	na	na	na	na
BD 66	25	19	6	0	na	na	na	na
BD 67	3	3	0	0	3	3	0	0
BD 68	14	12	2	0	3	3	0	0
LP 69	202	122	83	17	2	2	0	0
LP 70	200	120	74	11	1	1	0	0
LP 73	27	22	5	0	2	2	0	0

FISH with JCV specific probe and chemical amplification was performed on PBMC and granulocytes of healthy blood donors (BD) and laboratory personnel (LP). The hybridized virus was visualized by classical fluorescence microscopy and documented using QFluoro software (Leica, Wetzlar, Germany). 5×10^4 cells were counted and the number of JCV positive cells as was reported to 1000 cells counted. After deconvolution (Huygens Essential deconvolution software, SVI, The Netherlands) the intracellular localization of the virus was assayed and the number of cells carrying exclusively cytoplasmic (cyto), cytoplasmic and nuclear (cyto/nucl.) and exclusively nuclear (nucl.) JCV signals were reported to 1000 total counted cells. The number of virus particles in the cell was not possible to assay due to the chemical amplification of the signal.

na= not available; NL= normal leukocytes sample number

Table R-11. JCV FISH results on PBMC and granulocytes of HIV-1 and HIV-1/PML patients

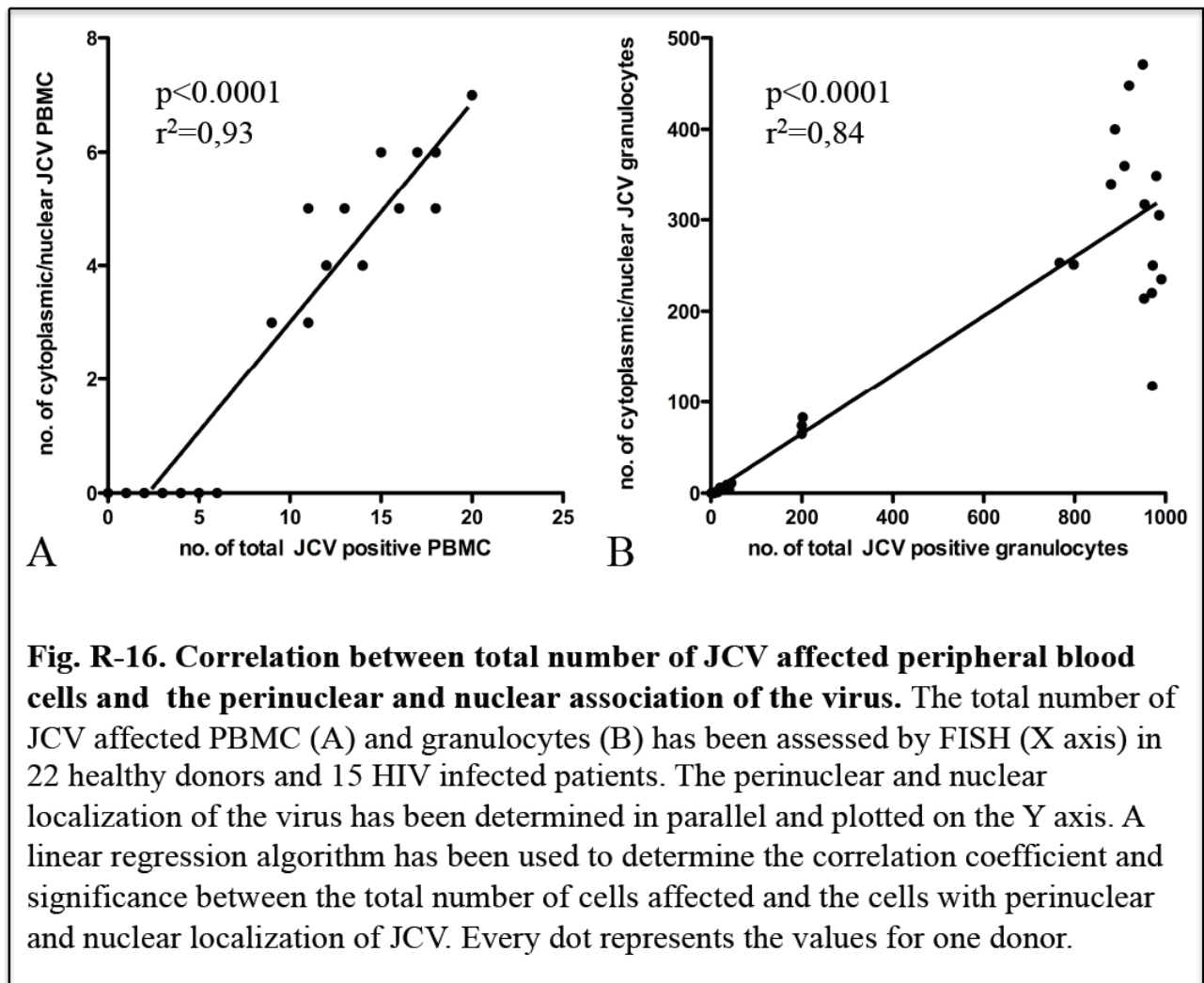
Donor	granulocytes							PBMCs						
	no. gran affected /1000				no. of virus copies/cell			no. PBMCs affected /1000				no. of virus copies/cell		
	total	cyto	cyto/ nucl	nucl	cyto	nucl	total	total	cyto	cyto/ nucl	nucl	cyto	nucl	total
HIV-1 patients														
HIV-1 pat. 1	991	751	235	5	11	3	14	12	8	4	0	3	2	5
HIV-1 pat. 2	980	625	349	6	10	2	12	14	10	4	0	4	2	6
HIV-1 pat. 3	970	747	220	3	14	6	20	16	11	5	0	2	3	5
HIV-1 pat. 4	954	623	317	5	11	4	15	9	6	3	0	5	1	6
HIV-1 pat. 5	986	676	305	7	11	1	12	11	8	3	0	3	2	5
HIV-1 pat. 6	953	733	214	6	10	2	12	12	7	4	1	5	3	8
HIV-1 pat. 7	971	851	118	2	9	0	9	18	13	5	0	4	1	5
HIV-1 pat. 8	972	716	250	6	10	1	11	12	8	4	0	4	3	7
HIV-1/PML patients														
PML pat. 1	880	534	340	6	9	7	16	13	8	5	0	3	2	5
PML pat. 2	920	464	448	7	12	9	21	11	6	5	0	2	4	6
PML pat. 3	798	542	251	5	8	4	12	20	13	7	0	5	3	8
PML pat. 4	889	482	400	7	13	6	19	15	9	6	0	4	2	6
PML pat. 5	910	543	360	7	20	11	31	17	11	6	0	4	1	5
PML pat. 6	767	510	253	4	11	6	17	20	13	7	0	6	5	11
PML pat. 7	950	472	471	7	14	12	26	18	12	6	0	3	2	5

FISH with JCV specific probe was performed on PBMC and granulocytes of HIV-1 and HIV-1/PML patients. The hybridized virus was visualized in confocal laser scanning microscopy and documented using LSM 510 Meta acquisition software (Karl Zeiss GmbH, Jena, Germany). 5×10^4 cells were counted and the number of JCV positive cells as was reported to 1000 cells counted. After deconvolution (Huygens Essential deconvolution software, SVI, The Netherlands) the intracellular localization of the virus was assayed and the number of cells carrying exclusively cytoplasmic (cyto), cytoplasmic and nuclear (cyto/nucl.) and exclusively nuclear (nucl.) JCV signals were reported to 1000 total counted cells. The number of virus particles in the cell was counted in maximum 100 JCV positive cells and the mean value of total amount of virus copies per cell as well as the average cytoplasmic and nuclear JCV copies was reported.

HIV-1 pat. = HIV-1 patient number

PML pat. = PML patient number

1 = PBMC sample with exclusive nuclear localization of JCV



3.5.3.3. Intracellular quantification of viral genomes in PBCs

From the assessment of JCV DNA localization and the number of affected peripheral blood cells as described in 3.5.3.1 and 2, it became clear that the JCV DNA was mostly present in the cytoplasm of these cells, and that nuclear association was strongly dependent on the number of cells affected in individual donors. Especially the granulocytes of the HIV-1 infected patients seemed to be affected, raising the supposition that these professional phagocytes may be taking up free circulating virus particles. However, the presence in the granulocytes of the same patients of nuclear associated JCV raised also the question of persistent infection. During active JC virus infection, for example in PML, the virus genomes are replicated by order of thousands in the nucleus of the infected cells. In persistent infection the levels of viral replication was not yet determined even at the DNA level. Assuming that the JCV association with the peripheral blood cells represents a persistent infection, we were interested to determine the viral load in the respective cells, and especially the number of the nuclear JCV genomes. In order to determine the

JC virus load in the cells of the peripheral blood we assessed the number of viral copies in both the cytoplasm and nucleus of PBMC and granulocytes using FISH.

To be able to address the viral load at single cell level, the sensitivity of the FISH detection has to reach single virus genome level. This cannot be achieved using the FISH with chemical amplification and classical fluorescence microscopy method applied for the detection of rare virus cell associations in the healthy blood donors as with this method no individual signals can be detected due to signal amplification. As peripheral blood cells of HIV-1 infected patients were shown to be more affected by the JCV than those of healthy blood donors we analyzed the JC viral load in the group of 15 immune deficient patients (8 HIV-1 infected patients without PML and 7 with PML). To allow genomic quantification *in situ* FISH without chemical amplification was used combined with confocal microscopy. Thus allowing the analysis of successive layers of an individual cell. This method permitted the determination of an approximate JCV genomes load at different subcellular levels and in the entire cell. To determine the sensitivity of detection, human alpha actin gene (ACTA1) without chemical amplification was performed in parallel in peripheral blood cells.

FISH method without chemical amplification permitted detection of one gene exemplified by the two alleles of the human skeletal alpha actin gene, which was used further as reference for the determination of the number of JCV genomes in the affected PBCs (**Fig. R-17, A and C**). As the size and configuration of the JCV signals obtained after specific FISH on granulocytes of HIV-1 patients was similar to that obtained after ACTA1 specific FISH on the same cells, the number of individually delimited fluorescent signals detected in one cell was taken as equivalent with the number of viral DNA copies existent in the respective cell. (**Fig. R 17, B and D**). The differentiation between nuclear and cytoplasmic localization of the specific signals was done by staining the nuclei with a nuclear counterstain (**Fig. R-17, A,B,C and D**). Putting together all the 24 stacks resulting from the dimensional analysis of a single cell, a picture of the three dimensional distribution and extent of the virus DNA presence in the respective cells was formed. Both the nuclear and the cytoplasmic JCV signals were counted for 50 cells per peripheral blood population per patient and the result was reported as mean value \pm SEM. Even in the case of the HIV-1 and HIV-1/PML patients, where the number of positive granulocytes was very high (873 ± 25 cells per 1000 for the patients with PML and 972 ± 5 per 1000 for those without PML), the total number of viral genomic copies was quite low, the granulocytes of PML patients carrying an average of 20.3 ± 2.4 JC virus copies and of HIV-1 infected patients without PML only 13.1 ± 1.1 viral copies (**Table 10 and 11**). From these signals only 7.8 ± 1.1 (38%) were localized in the nucleus for the PML patients and 2.3 ± 0.7 (18%) for the non-PML patients. In the PBMCs of the same patients, the

number of viral copies per cell was much lower, varying from 6.6 ± 0.8 for the PML patients and 5.8 ± 0.4 for the patients without PML and the nuclear copies number was 2.7 ± 0.5 (40% of the total virus copies per cell) and 2.1 ± 0.3 (36%) respectively (**Table 10 and 11**).

In conclusion, the fluorescence *in situ* hybridization (FISH) results confirmed the PCR results that the most affected peripheral blood cell population by JCV is the granulocyte population both in healthy blood donors and HIV-1 infected patients. However, in the HIV-1 infected patients the rate of positive granulocytes was much higher (926 ± 67 positive cells per 1000) than in the healthy donors (40 ± 14 positive cells per 1000). This increase in the number of cells affected correlated also with an increase in the rate of nuclear associated virus genomes (coefficient of correlation $r^2=0.84$, $p<0.0001$). This predominant association of JCV with granulocytes of HIV-1 infected patients seemed to be associated with the immunological status of these patients rather than with the JCV infection status as there was no significant difference between the patients with active JCV infection in the CNS and those without. The rate of JCV affected granulocytes in the HIV-1 infected patients with PML was even slightly lower (873 ± 25 per 1000) than in those without PML (972 ± 5 per 1000). However, the number of JCV genomic copies per granulocytes in these patients was quite low (16.5 ± 1.5 genomes) with no significant differences based on the PML status even though the granulocytes of PML patients carried in average a slightly higher number of JCV DNA copies (20.3 ± 2.4) than those without (13.1 ± 1.1).

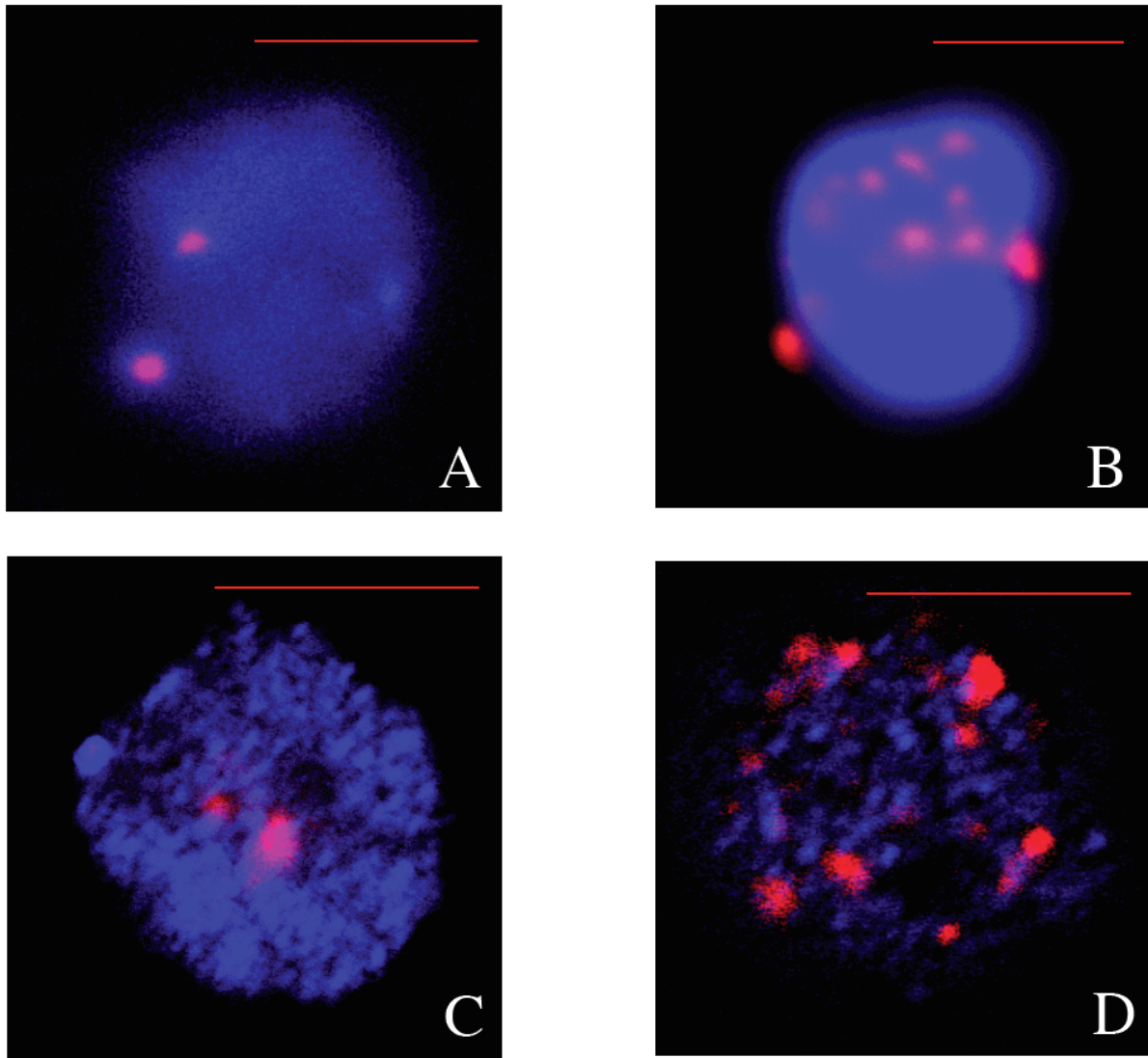
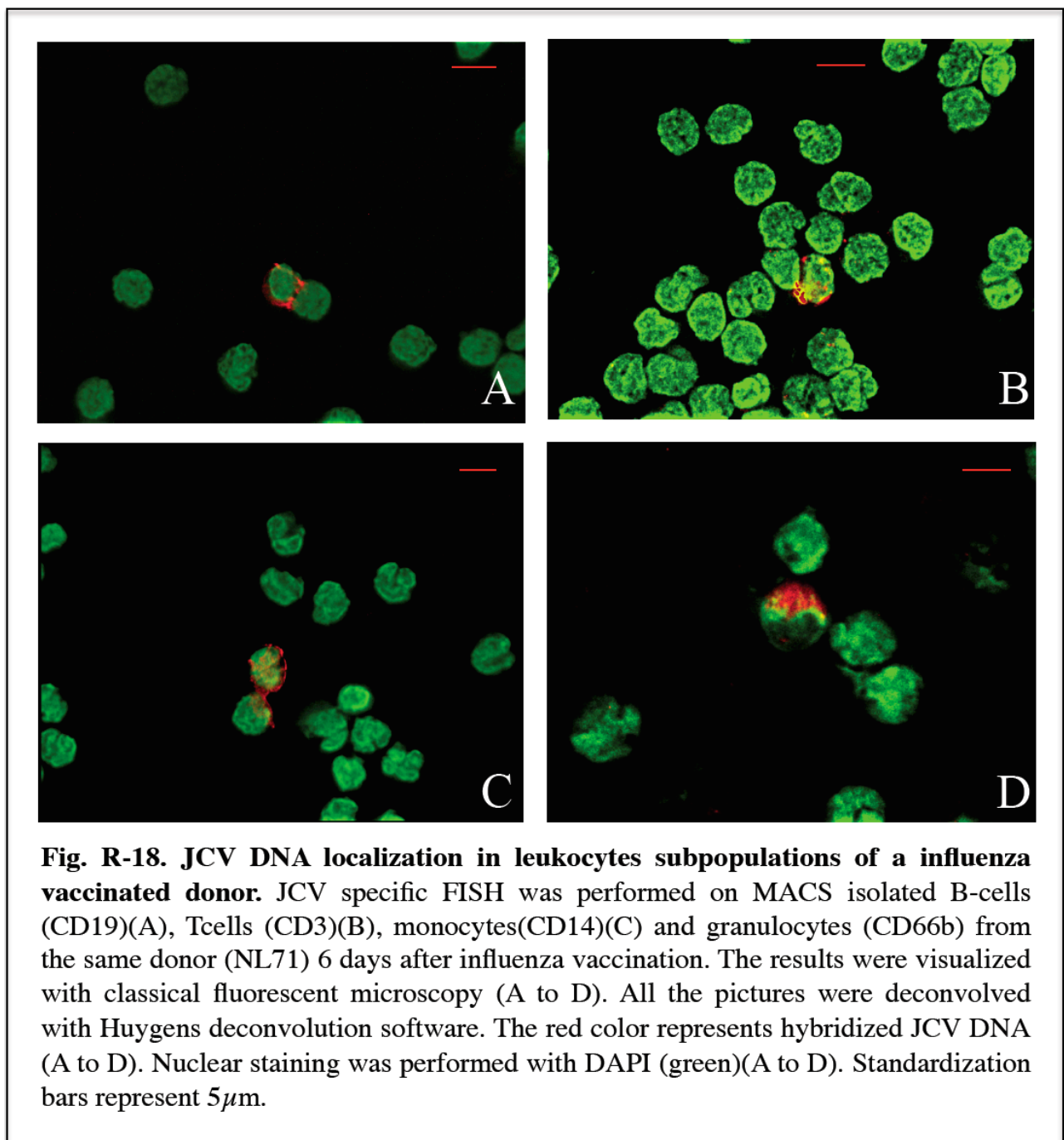


Fig. R-17. Estimation of JCV DNA number of copies per cell in the granulocytes of HIV patients. FISH without chemical amplification was performed on Percoll gradient purified granulocytes from HIV patients without PML (A,B), and with PML (C,D). As a hybridization control, the human alpha actin gene (ACTA1) probe mixture was used (A,C). The JCV DNA was detected by hybridization with a JCV specific probe (B,D). The results were visualized with confocal microscopy (A to D). The red color represents hybridized DNA (A to D). The nucleic acid counterstain used was DAPI (blue)(A,B) and SytoxBlue(blue) (C,D). All the pictures were deconvolved with Huygens deconvolution software. Standardization bars represent $5\mu\text{m}$.

The pictures represent the 12th section of a stack of 24 pictures through the cells.

3.5.3.4. Influence of short time immune system activation on JCV association with peripheral blood cells

As described in the previous chapters, from the JCV FISH experiments on peripheral blood cells of healthy blood donors and HIV-1 infected patients it became clear that modulation of the immune system appeared to play an important role in the increase of JCV association with PBCs. HIV-1 infection represents a major disruption in the immunity of the patient which made the HIV-1 infected patients the group with the highest incidence of PML infections before the arrival of the

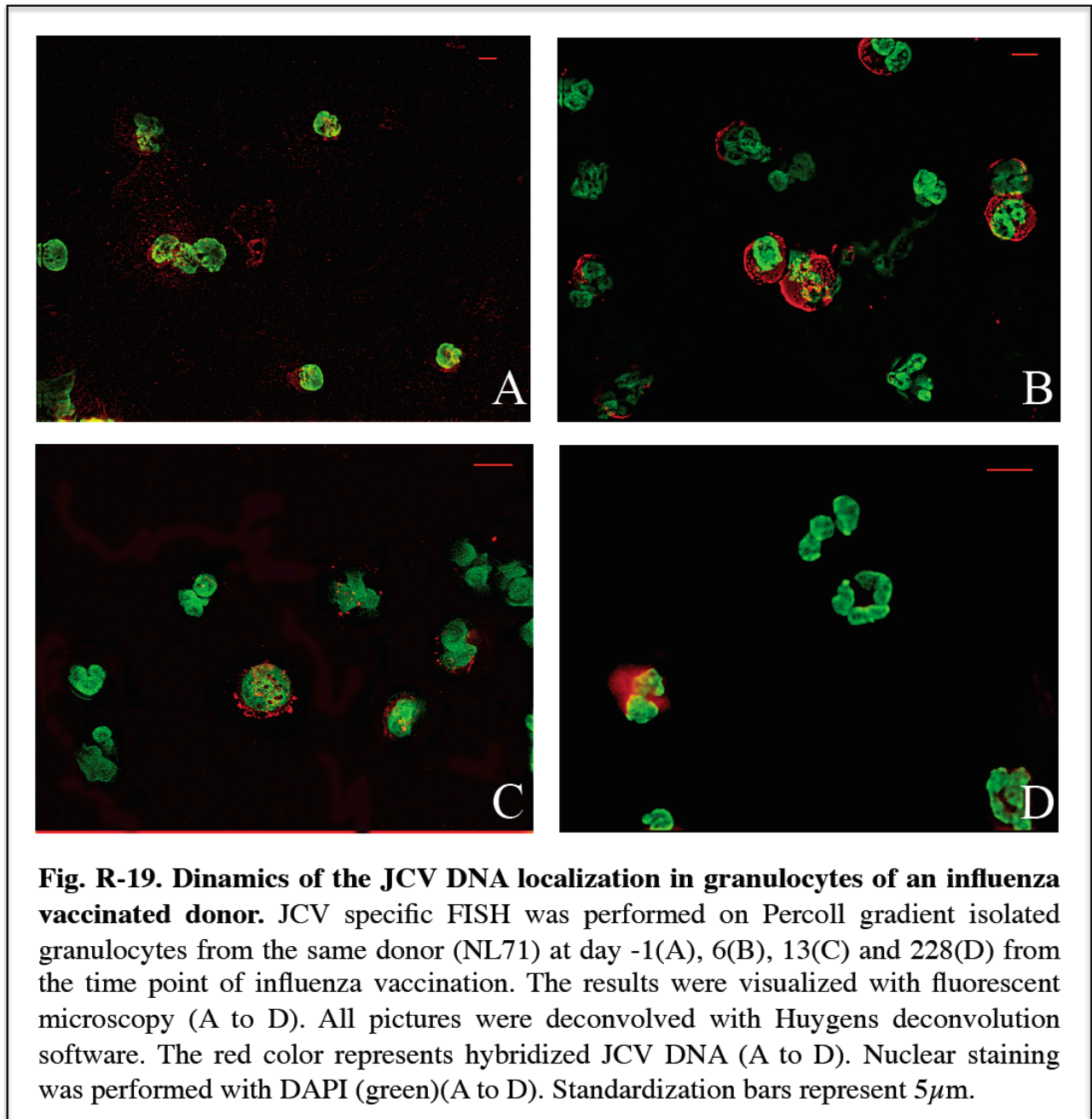


retroviral therapies. However, until now, no one addressed the question of the possible influence of sporadic immune disturbances on JCV modulation in the periphery. Therefore we wanted to further detail the JCV-PBC association in the context of a subtle modulation of the immune system. Activation of the immune response to vaccination is changing the intracellular environment of the circulating cells (Lee and Burckart 1998; Baxter and Hodgkin 2002) for a defined period of time after which it reverts to the status quo before the vaccination. Therefore we studied the time course of JCV association from donors after vaccination against influenza virus.

Blood samples were collected as described from 3 donors at day -1 before vaccination followed by collection of samples at day 6 and day 13 after vaccination. Additional samples were taken at day 140 and day 228 after vaccination when the effect of the immune stimulation was expected to have lost effect. The PBMCs and granulocytes were separated by Percoll gradient centrifugation. As the effect of vaccines is mainly on the B and T-cells, we wanted to analyse these two subpopulations more intensively, especially as JCV has been reported to be able to replicate in B-cell lines in vitro. Therefore, the PBMCs isolated from the three vaccinees at all time points were further separated by magnetic activated cell sorting (MACS) with specific CD antibodies in B cells (CD19), T cells (CD3) and monocytes (CD14) as described. FISH with chemical amplification was performed on all cell subpopulations including all the necessary controls (ACTA1, FIV). The result was assessed with fluorescence microscopy followed by deconvolution.

At any experimental time point, the different PBMC subpopulations (**Fig. R-18 A, B and C**) showed no difference between the B-cells, T-cells and monocytes regarding the sub-cellular localization and the rate of cells carrying JCV positive signals (**Table R-12**). Generally, the signals were cytoplasmic with 10/12(83%) B and T-cell samples and 7/12 (58%) monocyte samples carrying cytoplasmic JCV while the rate of positive cells was also very low, with an average of 1.8 ± 0.3 per 10^5 B-cells, $2.5 \pm 0.0.8$ per 10^5 T-cells and 8.4 ± 2.9 per 10^5 monocytes. Only one sample had higher rates of JCV affected cell (NL84) with 12 B-cells, 24 T-cells and 9 monocytes per 1000 counted cells associated with JCV.

In contrast to PBMC, within the granulocyte population 9/12 (75%) samples had nuclear associated JCV and 4/12 (33%) even exclusively nuclear, while all 12/12 (100%) granulocyte samples carried cells with cytoplasmic JCV (**Fig. R-18 D, Fig. R-19 A-D, Table R-12**). The rate of affected cells was also higher than in the PBMC with a mean value of 33.4 ± 9 for the cytoplasmic localization and 6.7 ± 2.5 for the perinuclear and nuclear localization.



However, when plotted against the vaccination time points, the rate of affected granulocytes did not show any significant correlation with the vaccination status of the patients (**Fig. R-20**) even though a temporal variation of the JCV DNA load could be observed. This suggests that JCV association with the cells of the peripheral blood system is rather not modulated by the limited activation of the immune system through vaccination.

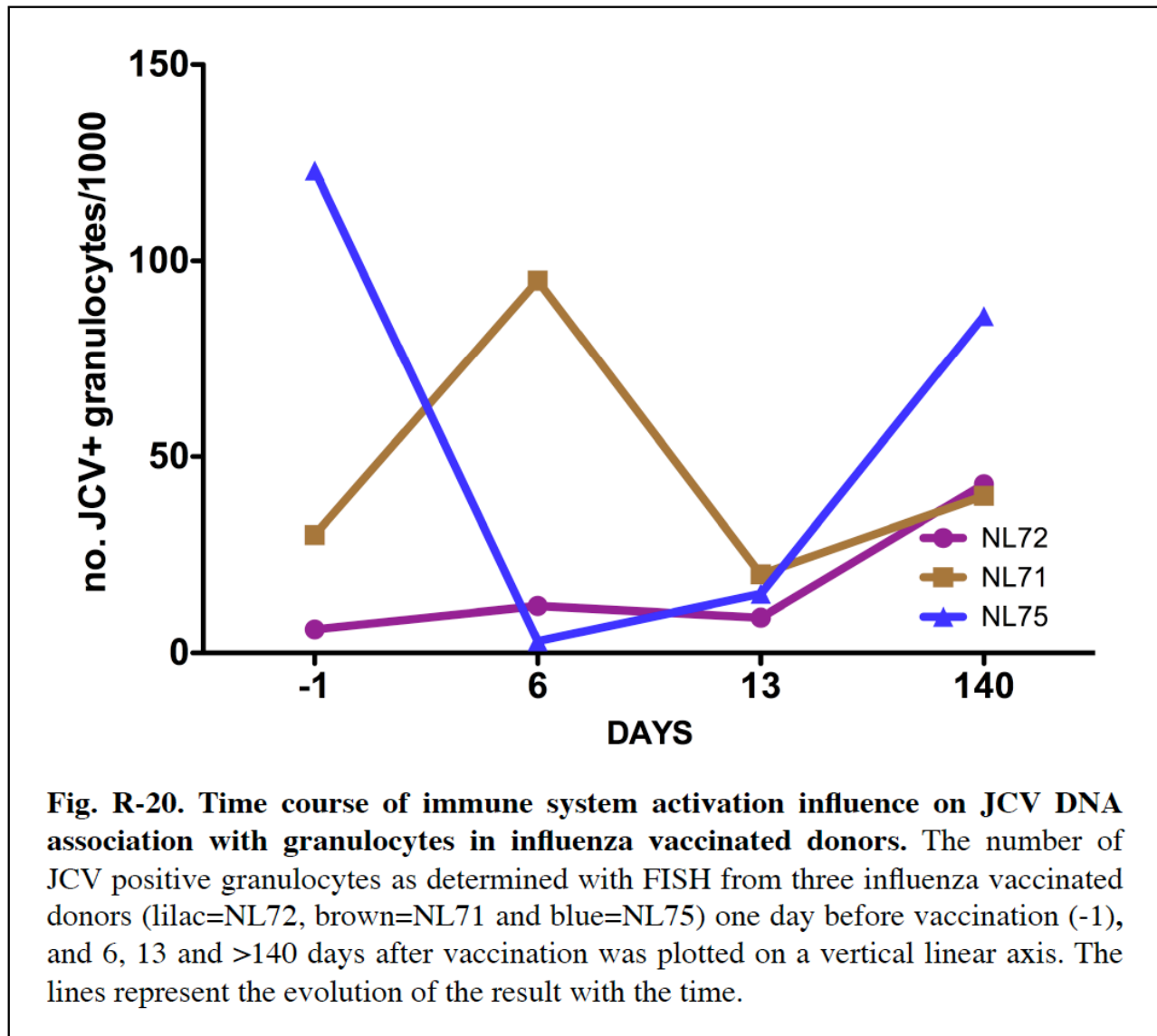


Table R-12. JCV FISH results on peripheral blood cell subpopulations of influenza vaccinees

		vacc	granulocytes				B-cells				T-cells				monocytes			
			no. gran affected /1000				no. B-cells affected /1000				no. T-cells affected /1000				no. monos affected / 1000			
probe	donor	dpV	total	cyto	c/n	nucl	total	cyto	c/n	nucl	total	cyto	c/n	nucl	total	cyto	c/n	nucl
NL 72	1	-1	6	6	0	0	0	0	0	0	1/h	1/h	0	0	0	0	0	0
NL 88	1	6	12	11	1	0	1/h	1/h	0	0	1/h	1/h	0	0	0	0	0	0
NL 89	1	13	9	9	0	0	0	0	0	0	0	0	0	0	0	0	0	0
NL 94	1	84	43	36	6	1	3/h	3/h	0	0	2/h	2/h	0	0	5/h	3/h	2/h	0
NL 71	2	-1	30	23	7	0	1/h	1/h	0	0	1/h	1/h	0	0	1/h	1/h	0	0
NL 84	2	6	95	76	17	2	12	11	1	0	24	20	4	0	9	9	0	0
NL 96	2	13	20	19	1	0	1/h	1/h	0	0	1/h	1/h	0	0	1/h	1/h	0	0
NL 97	2	224	40	37	3	0	1/h	1/h	0	0	0	0	0	0	0	0	0	0
NL 75	3	6	123	98	23	2	3/h	3/h	0	0	2/h	2/h	0	0	5/h	5/h	0	0
NL 76	3	-1	3	3	0	0	1.5/h	1.5/h	0	0	9/h	8/h	1/h	0	25/h	22/h	3/h	0
NL 79	3	13	15	14	1	0	3/h	3/h	0	0	6/h	6/h	0	0	13/h	12/h	1/h	0
NL 92	3	140	86	69	14	3	2/h	2/h	0	0	1/h	1/h	0	0	13/h	13/h	0	0

FISH with JCV specific probe and chemical amplification was performed on peripheral blood cell subpopulations of 3 laboratory workers that received influenza vaccination. The collection time points of the blood samples were one day before and 6, 13 and between 84 and 224 days after vaccination. The hybridized virus was visualized by classical fluorescence microscopy and documented using QFluoro software (Leica, Wetzlar, Germany). 5×10^4 cells were counted and the number of JCV positive cells as was reported to 1000 cells counted. After deconvolution (Huygens Essential deconvolution software, SVI, The Netherlands) the intracellular localization of the virus was assayed and the number of cells carrying exclusively cytoplasmic (cyto), cytoplasmic and nuclear (cyto/nucl.) and exclusively nuclear (nucl.) JCV signals were reported to 1000 total counted cells. The number of virus particles in the cell was not possible to assess due to the chemical amplification of the signal.

NL= normal leukocytes sample number

/h= per hundred thousand cells

dpV= days post-vaccination

4. Summary and discussions

With the advent in the 1980s of the human immunodeficiency virus (HIV-1) epidemic and, in more recent years, of the large-scale employment of immunosuppressive drugs in the treatment of autoimmune diseases, the rate of progressive multifocal leukoencephalopathy (PML) patients increased dramatically but until now no specific therapy against JC virus has been yet developed. Therefore, more knowledge is required about both, the active JCV infection which leads to the establishment of PML and about the mechanism of virus entry and persistence in the human organism. However, in contrast to PML, the knowledge on JCV persistent infection in healthy individuals is limited. A recent discovery was the detection of JCV in cells of the hematopoietic system, both in lymphoid tissues like hematopoietic progenitor cells and tonsillar stromal cells but also in peripheral blood leukocytes (PBL). This finding may play a crucial role in the understanding of JCV trafficking in the human organism, its transport from the entrance site to the site of infection, the CNS, irrespective whether it is the gastrointestinal or the nasopharyngeal tract.

Based on the fact that JCV persistence is characterized by episomal presence of viral DNA in cell nuclei, our aim was to characterize the type of JCV interaction with peripheral blood cells (PBC). As it is not yet clarified which cells of the immune system are associated with JCV (Koralnik, Schmitz et al. 1999; Shimizu, Imamura et al. 1999; Dorries, Sbiera et al. 2003), our focus was the determination of the specific cell population affected and also the type of virus-cell association. While presence of JCV DNA in blood cells of healthy donors was reported before (Doerries 2006) and has been associated with persistent infection, the situation in patients with HIV-1 infections, the group with the highest risk of developing the JCV end-stage disease PML, was not evaluated yet. However, a differential analysis of JCV association with the PBCs in these patients compared with healthy donors might shed light into the early events leading to the establishment of PML. Therefore, in our experiments we have compared the JCV association with PBC from healthy donors (professional blood donors and laboratory personnel) with PBC from a HIV-1 infected risk group both without active JCV infection in the CNS and with established PML. In order to assess if not only severe immunodeficiency but also subtle modulation of the immune system is able to influence the virus status in the PBC we also analyzed, in a separate setting, a group of healthy donors which received influenza vaccination treatment.

Several leukocyte populations have been suggested to be mostly affected by JCV, most prominently the granulocytes (Doerries 2006). Therefore, in the healthy blood donors and HIV-1 infected patients we selected the granulocyte population and the peripheral blood mononuclear cells

(PBMC), as major constituents of the leukocytes, as our target cells to analyze their association with JCV. The cells studied had been purified from whole blood using Percoll density gradient centrifugation and the purity of the resulting cells was analyzed by specific cell surface molecules fluorescent activated cell sorting FACS. The cells resulting from Percoll density gradient centrifugation of the whole blood proved to be of high purity, the contaminating cells being under 1% of the total cells separated, therefore suitable for further molecular analyses (Serrano, Roman et al. 2000; Hotfilder, Rottgers et al. 2002). The contaminant cells, either in the PBMC or in the granulocyte population could be furthermore differentiated *in situ* due to their specific cellular and nuclear phenotype. This was very important in preliminary experiments to determine the cellular lineage more often associated with JCV DNA.

PBMCs are constituted of heterogenous populations, both phenotypically and functionally. The different functional role of the cell populations is associated with different expression patterns of the respective cells and this is of a crucial importance along all the steps of the JC virus life cycle from virus entry to expression (Kumar, Tang et al. 1996; Shinohara, Nagashima et al. 1997; Monaco, Sabath et al. 2001). The cell specific expression pattern can be of great importance especially for subtle influences induced in the immune system during vaccination. Therefore, for the experiments performed on PBC of the vaccinee group, further separation of the PBMCs in the constitutive components B-cells, T-cells and monocytes, respectively, was performed using magnetic activated cell sorting (MACS). Specific surface proteins based separation of the different subpopulations using magnetic beads coated with the respective antibodies is known to result in an enrichment of the cells of interest (CD19 for B-cells, CD3 for T-cells, CD14 for monocytes and CD66b for granulocytes)(Manyonda, Soltys et al. 1992; Semple, Allen et al. 1993). The homogeneity of the MACS separated populations was determined by FACS using the established cellular markers. However, due to the competition between magnetic separation and fluorescent determination antibodies for the same surface molecules, the purity of the cells as measured in FACS was lower than the purity of cells separated by Percoll gradient, being under 90%. However, by determining in FACS the amount of cells still carrying the magnetic purification antibodies after isolation, the determined purity of the MACS isolated cells increased to 90-99%.

Relating these results with other published molecular biological analyses of MACS separated cells (Nielsen, Nielsen et al. 1997; Draube, Pfister et al. 2001) the purity of cellular preparations obtained was considered sufficient that possible contaminant cells could not interfere in determining the exact cell population affected by JCV in our experimental analyses in the peripheral leukocytes (de Wynter, Coutinho et al. 1995).

The presence of JCV DNA in different populations of peripheral blood cells of healthy and diseased individuals was reported before (Tornatore, Berger et al. 1992; Azzi, De Santis et al. 1996). However, the estimated amount of virus in the PBCs was assumed to be very low (Dorries, Sbiera et al. 2003). Therefore the first analyses to determine the PBC population most predominantly associated with JCV DNA were performed with highly sensitive and specific PCR and Southern blot hybridization. The strategy for PCR included standard first PCR (sPCR) followed by sensitivity as well as specificity enhancement by nested PCR (nPCR) technique and radioactive Southern blot hybridization analysis.

As JCV is sharing 70% of its genome with the other primate polyomaviruses BKV and SV40, in a first step, JCV genomic sequence specific amplification and hybridization oligonucleotides were designed using the Oligo 6.0 software. These primers were analyzed for their amplification sensitivity using cloned JCV target DNA dilutions from 12 genome equivalents (GE) to 12×10^3 GE and for their specificity using cloned BKV target DNA dilutions from 12 GE to 12×10^7 GE. In PCR experiments, the lower amplification limit of the JCV oligonucleotides for JCV DNA was determined to be between 12 and 120 copies and for BKV DNA between 12×10^6 and 12×10^7 . This demonstrated that the oligonucleotides used for PCR detection of JCV DNA were highly sensitive (12 GE detection) and had a 10^6 fold higher affinity for the JCV than for the BKV DNA sequences. This high specificity of the primers for the JCV DNA sequences compared to BKV render the chances of PCR cross-detecting the related BKV associated with the PBCs were statistically insignificant.

While the regions encoding for the early (TAg, tAg) and late (VP1, VP2, agno) virus proteins is largely conserved in all JCV strains, often occurring modifications and rearrangements have been published for the regulatory control region (CR) depending on the tissue from which the JCV DNA was extracted but especially in the JCV strains isolated from the CNS during PML (Ferrante, Delbue et al. 2003). Although these rearrangements have been also found in peripheral tissues it has been postulated that these rearrangements could be responsible for the neural tropism during active infection (Ciappi, Azzi et al. 1999). Therefore, in our experimental settings the PCR primers have been chosen from both, the late viral capsid protein VP1 encoding region and the CR. Standard PCR (sPCR), nested PCR (nPCR) and Southern blot hybridization (SB) was performed for both these regions in the matched PBMC and granulocyte samples from the healthy blood donors and the HIV-1 infected patients.

Molecular analyses by PCR on peripheral blood cells revealed the presence of JCV DNA at a rate depending on the sensitivity of the PCR techniques used. Detection was JCV specific and there was no contamination of the probes with aerosolic DNA as the negative controls, using water

as template, remained negative. Several unspecific amplification bands could be observed after sPCR, however, they were visible at different lengths than the specific products in the electrophoresis and were not confirmed in the JCV specific Southern blot hybridization. For the VP1 late region, after the sPCR amplification rates of JCV DNA in PBMCs and granulocytes from healthy blood donors and laboratory personnel were 9 and 58%, respectively, whereas after Southern blot analysis products were found in 55 and 79% of the probes respectively. Increasing the sensitivity by nested PCR and Southern blot hybridization of these products revealed presence of JCV DNA in 100% of the samples, both PBMC and granulocytes. Interestingly, the PBMC samples from the patients with HIV-1 infection were associated with JCV VP1 DNA at similar or even lower levels as the healthy donors, as 33% of the samples were positive after the sPCR and 60% after the nested PCR and only 87% after Southern blot hybridization. However, in the granulocyte samples the situation was different, as after the sPCR already 67% of the granulocyte samples were positive, 80% after the nPCR and 100% after Southern blot hybridization.

As the sensitivity of detection increases 10 to 100 fold between each step (sPCR, nPCR and SB)(Evans, Joss et al. 1995; Ogawa, Setiyono et al. 2004), this demonstrates that the level of JCV VP1 DNA in PBC is generally very low. From the number of samples that were negative in sPCR we can conclude that 58% of the PBMC samples of healthy donors (blood donors and laboratory personnel combined) and 67% of samples of HIV-1 infected patients had low levels of JCV VP1 DNA. The number of granulocyte samples with low JCV VP1 presence was much lower in the HIV-1 infected patients (23%) than those of healthy donors (48% for both, blood donors and laboratory personnel combined) meaning that the JCV DNA-granulocyte association in HIV-1 patients is higher than in healthy donors

Additionally, using the same methodology, the presence of archetype JCV control region was assessed in matched PBMC and granulocyte samples of healthy blood donors and laboratory personnel. Compared to the late region, the levels of JCV DNA association with the PBCs was much lower, no PBMC and granulocyte samples were positive after the sPCR and only 67% and 43% of the PBMC and 73% and 43% of the granulocyte samples were positive after the Southern blot hybridization of the nPCR products in the healthy blood donors and laboratory personnel, respectively. This suggests that, as reported before(Ciappi, Azzi et al. 1999; Pietropaolo, Videtta et al. 2003), control region suffers frequent rearrangements as compared with the archetype also in the PBC of healthy donors.

The JCV DNA analysis by PCR and Southern blot in the PBC of both healthy donors and HIV-1 infected patients revealed that while both the PBMC and granulocytes were widely associated with JCV DNA, the distribution between the two populations in the same blood sample

and the amount of JCV DNA in individual populations varied from sample to sample. Although the findings varied widely among individuals, it became clear that the granulocyte is the preferred cell type for harbouring JCV DNA, and especially in the HIV-1 infected patients group the rate of association was higher. The variable amplification pattern suggests a rather complex interaction of the virus with different types of hematopoietic cells. This may include persistent virus infection as well as attachment to cellular membranes or phagocytosis of virus particles, thus it could be that the virus binds abortively on cell surfaces but does not mediate JCV infection. In case of Fc receptor mediated viral phagocytosis, JCV DNA would be localized on the membrane or in the cytoplasm traveling from the cell surface through the phagocytotic pathway. In contrast, peripheral blood cells might be infected by circulating virus or maybe by JCV at the stage of hematopoietic precursor cells (Monaco, Atwood et al. 1996; Monaco, Sabath et al. 2001) and would be associated with intranuclear presence of the viral genome.

However, in contrast to the PCR method, which is based on whole cell DNA extraction, the question of JCV DNA localization at subcellular level can only be revealed by an *in situ* hybridization method. In order to clarify the type of virus-cell association the localization of the JCV DNA to a particular subcellular compartment in the single cell affected was addressed. Until the late 1970s radioisotopes were the only labels available for nucleic acid probes and radiography was the only means to detect *in-situ* hybridized sequences (Gall and Pardue 1969). With the time, the radioisotopes have been replaced by the safer alternative, fluorescent labels (Rudkin and Stollar 1977). The fluorescent *in situ* hybridization (FISH) was able to overcome the inconveniences of radioactive hybridization like the relatively cumbersome safety measures, the limited shelf-life of radioisotopes which restricted the length of time a probe could be used, and the long exposure times required for autoradiography (Levsky and Singer 2003). In the same time it permitted co-localization with other cellular structures through multiple fluorescent labelling (Speel, Herbergs et al. 1994). However, FISH also had its disadvantages, like lower sensitivity and the size of the probe sequence needed, which was much bigger than for the *in situ* radioactive hybridization. However, the sensitivity of the fluorescent probes has improved over time with the use of PCR labelling instead of terminal labelling, which permitted integration of more labelled molecules in the detection sequence and the development of chemically based signal amplification technologies. Fluorescence *in situ* hybridization techniques (FISH) were already published before to be a reliable and sensitive tool in detecting low amounts of virus DNA (Wagner and Bloom 1997) with combined DNA probes. While JCV specific radioactive *in situ* hybridization has been used successfully before (Dorries, Sbiera et al. 2003), no specific FISH method was yet developed for

JCV, which would permit the subcellular localization of the viral DNA in the peripheral blood cells.

Therefore a JCV adapted FISH procedure was developed taking into account the fixation and permeabilization conditions necessary for the work with primary cells, the sensitivity and specificity of the probe due to the expected low virus concentration in the peripheral blood cells and the cross-reactivity between the main polyomaviruses species, and finally the hybridization conditions.

In the first phase of experiments it became clear that introduction of a FISH probe into the cytoplasm and nuclei of primary cells could not be achieved with standard fixation and permeabilization protocols for *in situ* hybridization in cultured cells or tissue sections. The conditions of fixation included maintenance of the cell structure during the hybridization procedure and the permeability of the cytoplasmic and nuclear membranes in order to insure the equal distribution of the probes and antibodies to all the cellular levels, in case of the JCV to be able to detect the episomal viral DNA at nuclear level, a prerequisite of JCV infection.

Combining the two requirements of the fixation method for FISH, several fixatives, surfactant agents and proteolytic substances as well as reaction buffers, salt concentration and pH were optimized (Looi and Cheah 1992; Shibuya, Miwa et al. 1992; Macville, Van Dorp et al. 1995; Nuovo 1995; Suthipintawong, Leong et al. 1996). As an indicator of cell permeability a commercial FITC marker developed for permeability analysis was used and the localization of the fluorescence signal at different cellular levels was followed in fluorescence microscopy. The initial experimental setting envisaged a parallel detection of both the JCV DNA using FISH and detection of the viral proteins using immune-fluorescence (IF). Therefore we compared in a first step the methanol/acetic acid (Me/Ac 3:1) fixation, as the only fixation published which would permit both these methods to be performed in parallel (Nuovo 1995), with two other fixatives published as suitable for FISH alone, acetone and methanol/acetic acid. However, it became soon clear that the double FISH and IF staining could not be achieved as the methanol/acetic acid fixation, even performed at different temperatures and times proved to lead to cellular structure loss and therefore unsuitable for FISH. Unsuitable for FISH proved to be also the acetone fixation, but in this case the effect was opposite to the Me/Ac as the cells structures were cluttered and no nuclear permeabilization, as visualized with the FITC marker, was achieved even under variation of concentration, temperature and time. The best conditions were achieved with the paraformaldehyde fixation, however, this method alone could only deliver perinuclear localization of the marker, raising the idea that permeabilization could be improved by postfixation treatment of cells with either surfactants or proteolytic substances. From the surfactants, Triton X-100 treatment lead to

cell structure disintegration, and only saponine treatment (0.5% for 60 minutes) achieved nuclear permeabilization. However, due to the reversibility of saponine effect (Francis, Kerem et al. 2002) subsequent use in all the buffers was needed, which was incompatible with the FISH technology due to inhibition of DNA-DNA binding (Simons, Morrissey et al. 2006). For the proteolytic treatment we have chosen the two most often used enzymes for permeabilization enhancement in FISH, pepsine and proteinase K, both individually and in combined treatment. In the same time we varied the treatment concentration and time but also the pH as it has been reported to have an important influence in their activity (Farinas, Bulter et al. 2001). While individually the enzymes were not so effective, with the combined enzymatic treatment at low pH the desired nuclear permeabilization was achieved, probably because the two enzymes have effect on different classes of proteins in the membrane (Hedstrom 2002). Finally, the best treatment conditions for the peripheral blood leukocytes were determined to be a fixation step of 15 minutes at 4°C with 4% paraformaldehyde in PBS with air drying for at least 30 minutes followed by a 5 minutes treatment at 37°C with a mixture consisting of 1µg/µl proteinase K, 0.25% pepsin and 0.1N HCl in PBS . Important at this stage was that Ca⁺⁺ and Mg⁺⁺ were omitted in the phosphate buffer. This fixation/permeabilization procedure permitted the FITC marker to localize at the subcellular level as demonstrated by colocalization staining with the nuclear DNA marker DAPI.

The principle of *in situ* hybridization is the specific annealing of two complementary single strands of DNA, the double stranded DNA being unable to hybridize. In order to permit the JCV specific DNA probe to anneal to the complementary sequence of the viral DNA in the cell, both the probe and the cellular DNA had to be denatured. As the probe consists only of nucleic acids the normal denaturation process (Weil 1963) of 10 minutes heating at 100°C and the subsequent shock cooling at 4°C was used. However, the same procedure could not be used to denature the genomic DNA *in situ* because of danger of destroying the cellular structures consisting of lipids and proteins (Nash and Plaut 1964). Therefore we had to avoid the strong denaturation of the cellular structures by decreasing the melting temperature of the cellular DNA from 100°C to 65°C by using 95% formamide solution with 0.1xSSC as denaturation buffer (Fu and Gruenwedel 1976; Rauch, Wolf et al. 2000).

In order to specifically detect the possible intracellular JCV DNA a JCV specific DNA hybridization probe mixture was designed (Staratschek-Jox, Kotkowski et al. 2000) consisting of 16 individual DNA probes summing 2811 base pairs covering 55% of the viral genome. The distribution of the individual probes was spanning all the functional regions of the JCV, 2 probes were situated in the non-coding, control region (CR), 7 probes in the late viral capsid protein (VP) region and 7 in the early tumor antigen (TA_g) region. The individual probes were PCR labeled with

digoxigenin (DIG) tagged dUTP given the high integration rate of 1 DIG-dUTP to every 15 bases on each strand of the DNA (Chevalier, Yi et al. 1997). The common hybridization temperature for the probe mix had to be adjusted to meet physiological levels that would minimize the denaturation and loss of cellular structures but in the same time to keep the specificity and sensitivity of its binding to the complementary JCV sequences. This was achieved by increasing the salt concentration to 5xSSC in order to attain a stringent hybridization temperature of melting point (T_m) -20°C and subsequently decreasing the hybridization temperature by using 50% formamide solution in the hybridization buffer. The final hybridization temperature reached 37°C from the mean melting temperature of the individual probes of 72.8°C .

In dot-blot experiments, the sensitivity of each JCV probe and of the combined probe mix were analyzed. It was determined that the detection sensitivity of 20 ng of the individual probes was in a similar range, between 200fg and 200 pg of blotted JCV plasmid DNA. This range of sensitivity was probably due to the hybridization at the mean hybridization temperature calculated, which was not optimal for every individual probe. However, more importantly, the combined probe mix was as sensitive as the most sensitive of the individual probes (200fg) showing that the mean temperature used for hybridization was adequate for the use with the JCV probe mix. 20ng is the amount of probe recommended for FISH experiments (Leitch and Heslop-Harrison 1994). As membrane hybridization conditions are different from the *in situ* detection conditions, the specificity of the probe mix was also analyzed in two cell-lines, on one hand the JCV transformed hamster glial cell-line HJC-16 (Wold, Green et al. 1980) and as a cross-reactivity control the BKV infected (and not infected) green-monkey kidney cell-line Vero (Rhim, Schell et al. 1969). In addition, PBMC and granulocyte samples from healthy blood donors were used.

The amount of JCV DNA in the PBCs was expected to be low, as demonstrated by the PCR results on the same samples, therefore we developed a FISH method involving a chemical amplification step. This involves the hybridization of the digoxigenin labeled probe to the specific complementary sequences in the cells, followed by a detection of the DIG labeled sequence with a peroxidase labeled anti-digoxigenin monoclonal antibody. The peroxidase signals were further amplified by a chemical reaction with biotinylated tyramide. This created a deposit of precipitated tyramide around the hybridization site, with free biotin. This signal was further amplified by binding of streptavidin labeled with the fluorophore Texas red to the free biotin. Biotin to streptavidin binding is one of the strongest non-covalent interactions known in nature (Green 1975), therefore this reaction is practically irreversible, making FISH with chemical amplification a very stable and reproducible method. The only drawback is that animal cells contain endogenously biotin and peroxide they need in their metabolic processes. This lead at the beginning to unspecific

JCV signals, for example in the uninfected and BKV infected Vero cells. However, after quenching the endogenous biotin and peroxidase using tyramide OHCl and water peroxide, respectively, the unspecific signals in the Vero cells disappeared while the JCV probe hybridized 100% of the HJC cells. This indicated that the specificity of the DIG probe *in situ* remained very high, even in the presence of high amounts of related virus as found in the BKV infected Veros cells (Flaegstad and Traavik 1987).

To further detect the sensitivity of the hybridization technique a house keeping gene control for human cells was developed. A human skeletal alpha actin gene (ACTA1) specific probe mixture was created, consisting of 14 PCR DIG labeled DNA fragments, with a total length of 2194bp, covering approximately 58% of the gene total length. The use of the alpha actin gene had the advantage that the gene is only expressed in the skeletal myocytes and not in the blood cells, eliminating the possibility of hybridizing cytoplasmic ACTA1 mRNA. The ACTA1 probe was used as a permanent control in all the FISH experiments performed. In the fluorescence *in situ* hybridization on PBMC and granulocytes from all the different donors studied the probe hybridized each of the gene alleles, proving the method capability to determine the specific DNA at one gene level.

Due to the fact that the DNA has a certain amount of electromagnetic charge (Doerfler 1980), the DNA-DNA hybridization could take place due to electrical attraction between the different DNA molecules, as such enhancing the level of unspecific binding. Even if an acetylation step was included in the procedure in order to diminish the electrical charge, unspecific hybridization could still take place. Therefore a hybridization probe specific for DNA sequences non-existent in the analyzed cells, and not related to the JCV sequence was necessary. As an unspecific hybridization control, a feline immunodeficiency virus (FIV) probe mixture of 11 individual probes summing 1955 base pairs, approximately 21% of the viral genome, was synthesized. FIV was specifically chosen because viral DNA sequences are generally very different from the animal sequences, so that similar sequences with the very big genomic DNA were avoided. As FIV belongs to the retrovirus family its possible sequence similarities with JCV are improbable. As hoped, the FIV digoxigenin labeled probe did not hybridize in the JCV transformed cell line HJC and neither in any of the peripheral blood cell samples studied therefore in our study the digoxigenin labeled DNA probes are not unspecifically hybridizing unrelated DNA.

In conclusion the analyses of the newly developed JCV FISH methodology proved that this method is able to detect highly specific JC virus DNA intracellularly in JCV transformed cell-lines and is highly sensitive, being able to detect the DNA at one gene allele level in the case of the

house keeping gene ACTA-1. However, the fluorescent signals appeared highly intense and diffuse, due partly to the chemical amplification of the signal but also to the intrinsic nature of fluorescence. While the exact location of JCV to subcellular levels is of outmost importance in clarifying the type of virus-cell association, the fluorescent glow could be an impediment as one could not differentiate between epi-nuclear and nuclear localization. We bypassed this problem by using a deconvolution software to post-process the digital recordings of the FISH. Based on the nearest-neighbor algorithm, this software is able to eliminate the artificial fluorescent glow, revealing the real source of the signal. In addition, we improved the localization possibility by artificially changing the color of the nuclear signals from blue to green. The areas where JCV colocalized with the nuclei became orange a color much better identified than the blue-red overlap in the original pictures.

Having the methodology at hand, the question of JCV localization as tool for persistent infection detection in peripheral blood cells was analyzed in the two main groups of donors that were also analyzed using the PCR technology. The first group was formed of healthy donors, professional blood donors and healthy laboratory personnel. and as a comparison a second group, the risk group, constituted of HIV-1 infected patients either without active JCV infection in the CNS or with clinically established PML. The localization of the JCV positive signals within the studied cells was observed after FISH with chemical amplification followed by classical fluorescence microscopy. However, it became clear that the chemical amplification method is not suited for detecting JCV in the HIV-1 infected patients as the PBC of these patients, especially the granulocyte population, were highly affected. This made recognition of different localization possibilities very difficult as epi-nuclear signals masked the real nuclear signals (Fay, Taneja et al. 1997).

The problem was solved by omitting the chemical amplification from the FISH procedure and using confocal microscopy instead of the classical fluorescence microscopy. This eliminated the intensive fluorescence glow of the tyramide amplification technique and confocal microscopy increased the detection sensitivity by the visualization of a single cell at different depth levels situated at around 20 nm distance from another, without backlighting from the other levels. This was a great advantage in discerning between nuclear and cytoplasmic localization, without fluorescence interference. In the case of both, the PBMC and granulocytes, the intracellular analysis revealed three types of localization: cytoplasmic, overlapping cytoplasmic and nuclear as well as nuclear localization alone. In the cytoplasmic localization, the JCV signals were restricted to the cytoplasm. Here we could also distinguish between a distal and a proximal localization in

report to the nucleus. The distal signals were located in the outer layer, corresponding to the internal or external part of the cell membrane . This pattern suggested mainly a membrane attachment either by virus specific receptors followed by active mechanisms of cellular entry (Pho, Ashok et al. 2000) or by unspecific binding of antibody opsonized virus particles followed by phagocytosis. It could also represent virus particles being on their final stage from being excreted from the cell.

However, as this localization was not accompanied by nuclear JCV, which would signify virus replication, the theory of virus excretion is not viable. In the proximal localization, the specific signals were either filling the cytoplasm or were located close to the nuclei, however, without overlapping it. This suggested either a more advanced state of phagocytosis, when the phagosomes are approaching the endoplasmic reticulum (ER) in order to be recycled. Some virus particles could have escaped this mechanism, attached to the nuclear membrane and started their transfer to the nucleus, which would explain the overlapping cytoplasmic-nuclear signals also found in the PBC. However, this type of localization would also suggest active replication in the cell nucleus followed by exit and assembly in the cytoplasm. This theory is also supported by the presence of cells with exclusive nuclear localization of JCV DNA.

The ubiquitous presence of JCV DNA at different intracellular levels did not allow to differentiate between the states of active virus replication and phagocytosis. However, the rate of distribution types was clearly different regarding both either the cell type affected or the health status of the host. 97% of all the donors carried exclusive cytoplasmic JCV in their PBMC, 43% had overlapping cytoplasmic-nuclear signals and only one donor, an HIV-1 infected patient had PBMC with exclusive nuclear signal suggesting that for the PBMC the opsonisation/phagocytosis process is prevalent.

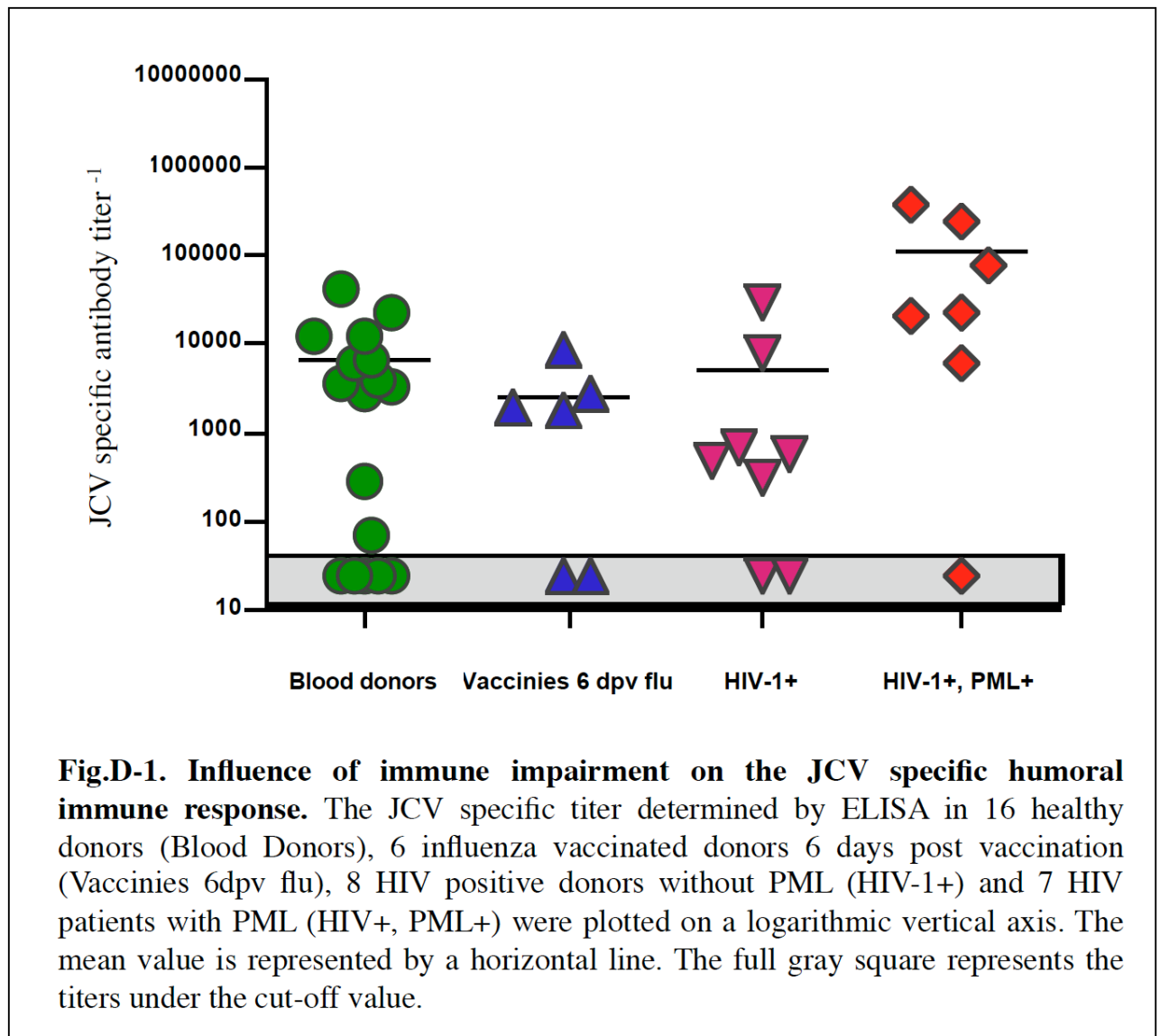
In the same line was the low rate of affected cells per donor, where in average only 2.5 PBMCs of healthy donors and 14.5 PBMCs of HIV-1 infected patients in 1000 carried JCV DNA. Interestingly, the rate of cells affected was directly correlated with the localization, so the more cells were positive for JCV DNA the localization shifted from exclusive cytoplasmic to overlapping cytoplasmic-nuclear signals. For the opsonisation/phagocytosis theory this would suggest that with an increased number of circulating free virus particles in the HIV-1 infected patients, the number of PBMC affected by JCV increases also. This would lead to more viruses being able to escape the phagocytosis process and to migrate to the nucleus. However, this process is probably abortive in the PBMC as almost none of the PBMCs carried exclusive nuclear JCV. In addition, the number of virus particles per cell, as determined in the PBMC of the HIV-1 infected patients by confocal microscopy technology, was very low. In contrast, the PBMC of PML patients

carried in average 6.6 copies per cell and only 40% of these signals were associated with the nucleus. This data, corroborated with the data from the PCR analyses and already published data (Dorries, Sbiera et al. 2003) makes the mononuclear cells the least likely population of PBC to harbor a persistent JCV infection. This is despite active JCV replication could be shown by other groups in the case of B-lymphocytes in vitro (Atwood, Amemiya et al. 1992; Rieckmann, Michel et al. 1994).

Analyzing the localization of JCV DNA in the granulocyte populations of the same individuals, the situation presented itself more complex than in the PBMCs. Except the exclusive cytoplasmic localization of JCV, which could be found in all the donors studied, the percentage of donors carrying granulocytes with cytoplasmic-nuclear JCV increased to 73%. More notably, 49% of the donors had granulocytes with exclusive nuclear JCV, this percentage increased even to 100% when we restricted for the HIV-1 infected patients only. This indicates that, compared to the PBMC, in the granulocytes there might be DNA replication or even virion assembly, even though the main form of virus-cell association still remained the phagocytotic pathway. As in the case of the PBMC, the tendency to nuclear association was directly correlated with the rate of cell positivity. This was especially high in the HIV-1 infected patients where almost all granulocytes were affected by JCV (92.6%). Interestingly, the PML status did not seem to make a significant difference, with the rate of affected granulocytes in PML patients even a bit lower (87.3%) than in HIV-1 patients without PML. In contrast, in the healthy donors the rate was much lower, with only in average 40 granulocytes affected in 1000, however, still higher than the PBMCs of the same donors.

The high number of affected granulocytes, especially in the HIV-1 infected patients, associated with the increase preponderance of exclusively nuclear virus DNA would support the theory that initial phagocytosis of the virus might be followed by virus activation and replication in the nucleus as is the case with the murine polyomavirus (Mannova and Forstova 2003; Liebl, Difato et al. 2006). However, this infection might be limited, as the number of virus particles per cells was in average only 20.3 for the PML patients and slightly lower (13.1) in the patients without PML, and from this, the percentage of nuclear copies was only 38 and 18% respectively. Even as such, this contradicts with the short life of normal circulating granulocytes of only 10 hours (Carlson and Kaneko 1975) that would not permit a full replication cycle of the JC virus (Sweet, Del Valle et al. 2002). However, JCV early tumor antigen (TAg) has been shown to interfere with the anti-apoptotic mechanisms of the cells (O'Neill, Frisque et al. 1995; Khalili, Del Valle et al. 2003). Together with the fact that the migration to the tissues prolongs the granulocyte life-span by

48 hours (Mc and Opeskin 1998) it would not be surprising if JCV persistently infected granulocytes would be the carrier for JCV infection to the CNS during HIV-1 immunosuppression. However, it seems that the PML status of the patients is not a determining factor. This data is also supported by the fact that JCV antibody titers in PML patients are not significantly different, even though slightly higher, than in the other study groups (Fig. D-1, laboratory data, unpublished).



From our data we could observe that the JCV association with the cells of the peripheral blood is highly influenced by the immune status of the host. HIV-1 infection represents a strong deregulation of the immune system and has, as we could demonstrate, a great influence on the JCV localization in the periphery. However, as it was reported before that short-time changes in immune system activation have a proliferative effect on the JCV (Andrews, Daniel et al. 1983; Atwood,

Wang et al. 1995), we also wanted to address the question of the JCV modulation by the immune system in a more subtle system.

We therefore performed a JCV FISH analysis on the PBCs of three healthy donors that received an influenza vaccination. Several time points have been set for material collection, including the day 6 after vaccination when the immune response is highest (Lambkin, Oxford et al. 2000). As the changes induced by the modulation of the immune system might be too subtle to detect in the bulk of mononuclear cells, the PBMCs of these donors were further separated in the respective subpopulations, the B-cells, T-cells and monocytes. JCV FISH and sub-cellular localization in the leukocyte subpopulations of the influenza vaccinees revealed the same pattern as with the PBCs of the healthy blood donors. The rate of affected cells was also very low, with an average of 1.8 B-cells, 2.5 T-cells and 8.4 monocytes per 10^5 carrying the JCV genome. 83% of all the B and T-cell and 58% of all the monocyte samples had exclusive cytoplasmic localization of JCV and none presented exclusive nuclear localization. The granulocyte patterns were also comparable to those from healthy blood donors, with rates of 33.4 positive cells per 1000 and 33% of the samples with nuclear signals. In addition, when plotted against the vaccination time-points it became obvious that the modulation of the immune system through vaccination with influenza virus vaccine did not lead to a recognizable pattern of JCV-cell association in any cell population of the peripheral blood.

From all data gathered we are proposing the following JCV infection pattern model (**Fig. D-2**). JC virus enters the human body either through the respiratory or the digestive system and establishes a persistent infection in the respiratory proximal nodes or the gut. Both this organs are highly irrigated by the circulatory system (Love, Matthews et al. 1972; Davidson, Fletch et al. 1973). Low amounts of JCV are continuously produced asymptotically and enter the blood flow. Oponised virus is phagocytosed by the cells of the immune system and the JC virus occasionally reaches the nucleus but the replication is abortive both in the PBMC and granulocytes. During immunosuppression as found during HIV-1 infection the JCV persistent infection escapes the immunological control of the T-lymphocytes (Koralnik 2002) and reaches the blood stream. Increased JC virus load in the serum leads to an increase of the virus load mainly in the specialized phagocytes the granulocytes. JCV thus may escape the immunological control mechanisms and might be able to establish a persistent infection in these cells. Wether this is leading to a dormant state or is followed by virus replication under as yet unknown conditions remains to be studied. However, in the cases where opportunistic CNS diseases occur, the granulocytes as members of the

immune response are the first to cross the blood-brain barrier, and as such carrying JCV to and potentiating infection in the CNS.

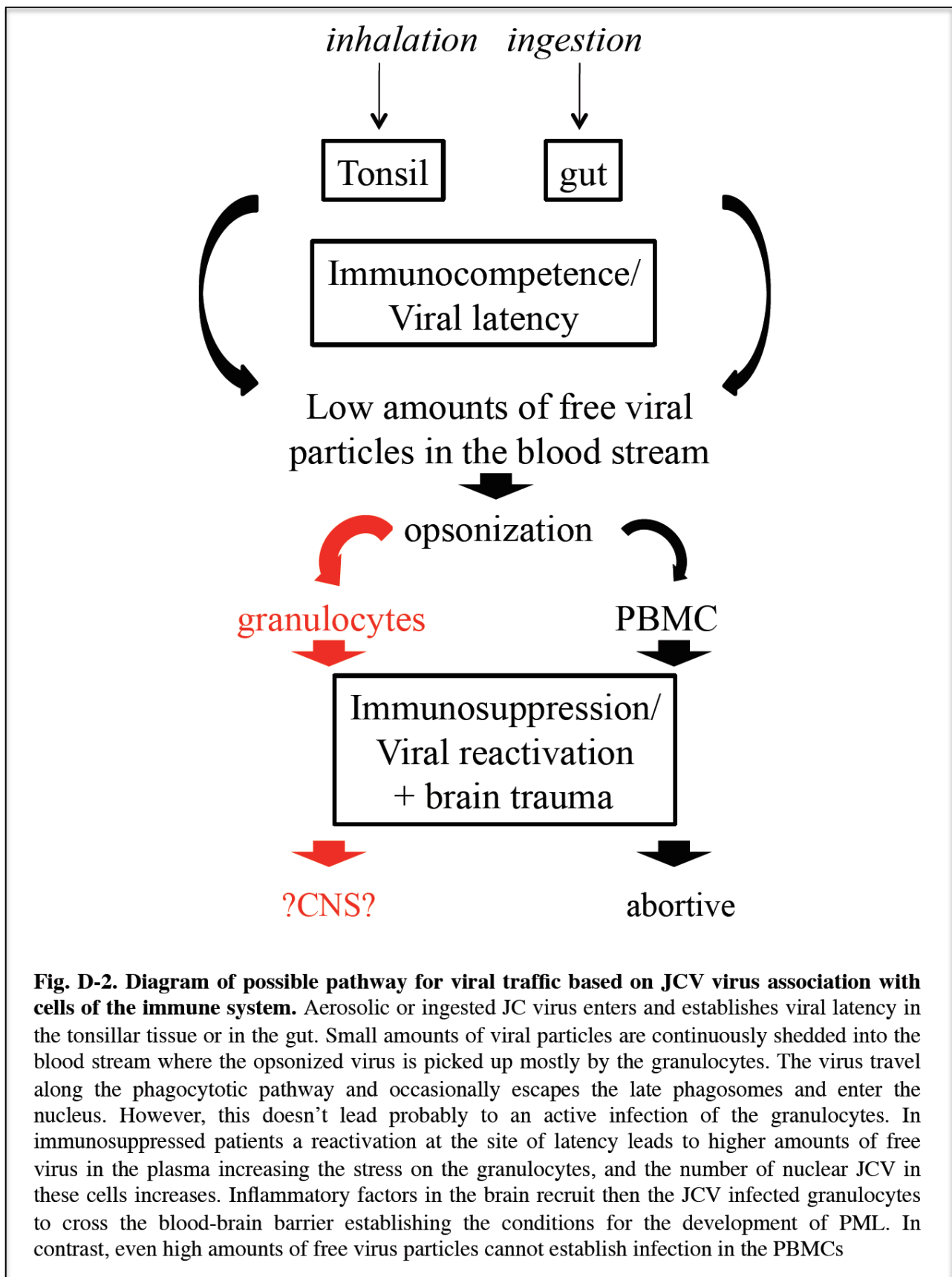


Fig. D-2. Diagram of possible pathway for viral traffic based on JCV virus association with cells of the immune system. Aerosolic or ingested JC virus enters and establishes viral latency in the tonsillar tissue or in the gut. Small amounts of viral particles are continuously shed into the blood stream where the opsonized virus is picked up mostly by the granulocytes. The virus travel along the phagocytotic pathway and occasionally escapes the late phagosomes and enter the nucleus. However, this doesn't lead probably to an active infection of the granulocytes. In immunosuppressed patients a reactivation at the site of latency leads to higher amounts of free virus in the plasma increasing the stress on the granulocytes, and the number of nuclear JCV in these cells increases. Inflammatory factors in the brain recruit then the JCV infected granulocytes to cross the blood-brain barrier establishing the conditions for the development of PML. In contrast, even high amounts of free virus particles cannot establish infection in the PBMCs

5. Bibliography

- Altschuler, E. L. (2000). "Is JC polyoma virus the cause of ulcerative colitis and multiple sclerosis?" Med Hypotheses **55**(4): 335-6.
- An, S. F., D. Franklin, et al. (1992). "Generation of digoxigenin-labelled double-stranded and single-stranded probes using the polymerase chain reaction." Mol Cell Probes **6**(3): 193-200.
- Andrews, C. A., R. W. Daniel, et al. (1983). "Serologic studies of papovavirus infections in pregnant women and renal transplant recipients." Prog Clin Biol Res **105**: 133-41.
- Andrews, C. A., K. V. Shah, et al. (1988). "A serological investigation of BK virus and JC virus infections in recipients of renal allografts." J Infect Dis **158**(1): 176-81.
- Arthur, R. R., S. Dagostin, et al. (1989). "Detection of BK virus and JC virus in urine and brain tissue by the polymerase chain reaction." J Clin Microbiol **27**(6): 1174-9.
- Arthur, R. R., K. V. Shah, et al. (1988). "BK and JC virus infections in recipients of bone marrow transplants." J Infect Dis **158**(3): 563-9.
- Astrom, K. E., E. L. Mancall, et al. (1958). "Progressive multifocal leuco-encephalopathy; a hitherto unrecognized complication of chronic lymphatic leukaemia and Hodgkin's disease." Brain **81**(1): 93-111.
- Atwood, W. J., K. Amemiya, et al. (1992). "Interaction of the human polyomavirus, JCV, with human B-lymphocytes." Virology **190**(2): 716-23.
- Atwood, W. J., L. Wang, et al. (1995). "Evaluation of the role of cytokine activation in the multiplication of JC virus (JCV) in human fetal glial cells." J Neurovirol **1**(1): 40-9.
- Azzi, A., R. De Santis, et al. (1996). "Human polyomaviruses DNA detection in peripheral blood leukocytes from immunocompetent and immunocompromised individuals." J Neurovirol **2**(6): 411-6.
- Baxter, A. G. and P. D. Hodgkin (2002). "Activation rules: the two-signal theories of immune activation." Nat Rev Immunol **2**(6): 439-46.
- Beckmann, A. M., K. V. Shah, et al. (1985). "Genetic heterogeneity of the human papovaviruses BK and JC." J Med Virol **15**(3): 239-50.
- Berger, J. R. and E. O. Major (1999). "Progressive multifocal leukoencephalopathy." Semin Neurol **19**(2): 193-200.
- Berger, L. C., D. B. Smith, et al. (1996). "Interaction between T antigen and TEA domain of the factor TEF-1 derepresses simian virus 40 late promoter in vitro: identification of T-antigen domains important for transcription control." J Virol **70**(2): 1203-12.

- Black, P. H., W. P. Rowe, et al. (1963). "A Specific Complement-Fixing Antigen Present In Sv40 Tumor And Transformed Cells." Proc Natl Acad Sci U S A **50**: 1148-56.
- Blumberg, B. M., D. J. Mock, et al. (2000). "The HHV6 paradox: ubiquitous commensal or insidious pathogen? A two-step in situ PCR approach." J Clin Virol **16**(3): 159-78.
- Bofill-Mas, S., M. Formiga-Cruz, et al. (2001). "Potential transmission of human polyomaviruses through the gastrointestinal tract after exposure to virions or viral DNA." J Virol **75**(21): 10290-9.
- Bofill-Mas, S. and R. Girones (2001). "Excretion and transmission of JCV in human populations." J Neurovirol **7**(4): 345-9.
- Boubenider, S., C. Hiesse, et al. (1999). "Post-transplantation polyomavirus infections." J Nephrol **12**(1): 24-9.
- Brew, B. J., N. W. Davies, et al. (2010). "Progressive multifocal leukoencephalopathy and other forms of JC virus disease." Nat Rev Neurol **6**(12): 667-79.
- Caldarelli-Stefano, R., L. Vago, et al. (1999). "Detection and typing of JC virus in autopsy brains and extraneural organs of AIDS patients and non-immunocompromised individuals." J Neurovirol **5**(2): 125-33.
- Carlson, G. P. and J. J. Kaneko (1975). "Intravascular granulocyte kinetics in developing calves." Am J Vet Res **36**(4 Pt.1): 421-5.
- Casareale, D., R. Pottathil, et al. (1992). "Improved blood sample processing for PCR." PCR Methods Appl **2**(2): 149-53.
- Chen, N. N., C. F. Chang, et al. (1995). "Cooperative action of cellular proteins YB-1 and Pur alpha with the tumor antigen of the human JC polyomavirus determines their interaction with the viral lytic control element." Proc Natl Acad Sci U S A **92**(4): 1087-91.
- Chevalier, J., J. Yi, et al. (1997). "Biotin and digoxigenin as labels for light and electron microscopy in situ hybridization probes: where do we stand?" J Histochem Cytochem **45**(4): 481-91.
- Ciappi, S., A. Azzi, et al. (1999). "Archetypal and rearranged sequences of human polyomavirus JC transcription control region in peripheral blood leukocytes and in cerebrospinal fluid." J Gen Virol **80** (Pt 4): 1017-23.
- Cinque, P., I. J. Koralnik, et al. (2009). "Progressive multifocal leukoencephalopathy in HIV-1 infection." Lancet Infect Dis **9**(10): 625-36.
- Daniel, D. C., M. J. Wortman, et al. (2001). "Coordinate effects of human immunodeficiency virus type 1 protein Tat and cellular protein Puralpha on DNA replication initiated at the JC virus origin." J Gen Virol **82**(Pt 7): 1543-53.

- Davidson, J. W., A. L. Fletch, et al. (1973). "The technique and applications of lymphography." Can J Comp Med **37**(2): 130-8.
- de Wynter, E. A., L. H. Coutinho, et al. (1995). "Comparison of purity and enrichment of CD34+ cells from bone marrow, umbilical cord and peripheral blood (primed for apheresis) using five separation systems." Stem Cells **13**(5): 524-32.
- Degener, A. M., V. Pietropaolo, et al. (1997). "Detection of JC and BK viral genome in specimens of HIV-1 infected subjects." New Microbiol **20**(2): 115-22.
- Del Valle, L. and K. Khalili (2010). "Detection of human polyomavirus proteins, T-antigen and agnoprotein, in human tumor tissue arrays." J Med Virol **82**(5): 806-11.
- Doerfler, W. (1980). "Surface charge patterns as recognition signals in nucleic acid molecules." Med Hypotheses **6**(11): 1171-5.
- Doerries, K. (2006). "Human polyomavirus JC and BK persistent infection." Adv Exp Med Biol **577**: 102-16.
- Dolei, A., V. Pietropaolo, et al. (2000). "Polyomavirus persistence in lymphocytes: prevalence in lymphocytes from blood donors and healthy personnel of a blood transfusion centre." J Gen Virol **81**(Pt 8): 1967-73.
- Dorries, K., S. Sbierra, et al. (2003). "Association of human polyomavirus JC with peripheral blood of immunoiapaired and healthy individuals." J Neurovirol **9 Suppl 1**: 81-7.
- Dorries, K., E. Vogel, et al. (1994). "Infection of human polyomaviruses JC and BK in peripheral blood leukocytes from immunocompetent individuals." Virology **198**(1): 59-70.
- Dourmashkin, R. R., R. M. Dougherty, et al. (1962). "Electron microscopic observations on Rous sarcoma virus and cell membranes." Nature **194**: 1116-9.
- Draube, A., R. Pfister, et al. (2001). "Immunomagnetic enrichment of CD138 positive cells from weakly infiltrated myeloma patients samples enables the determination of the tumor clone specific IgH rearrangement." Ann Hematol **80**(2): 83-9.
- Dubois, V., H. Dutronc, et al. (1997). "Latency and reactivation of JC virus in peripheral blood of human immunodeficiency virus type 1-infected patients." J Clin Microbiol **35**(9): 2288-92.
- Durm, M., F. M. Haar, et al. (1996). "Optimization of fast-fluorescence in situ hybridization with repetitive alpha-satellite probes." Z Naturforsch [C] **51**(3-4): 253-61.
- Durm, M., I. Sorokine-Durm, et al. (1998). "Fast-FISH technique for rapid, simultaneous labeling of all human centromeres." Cytometry **31**(3): 153-62.
- Ebeling, W., N. Hennrich, et al. (1974). "Proteinase K from Tritirachium album Limber." Eur J Biochem **47**(1): 91-7.

- Eggleton, P., R. Gargan, et al. (1989). "Rapid method for the isolation of neutrophils in high yield without the use of dextran or density gradient polymers." J Immunol Methods **121**(1): 105-13.
- Eldred, W. D., C. Zucker, et al. (1983). "Comparison of fixation and penetration enhancement techniques for use in ultrastructural immunocytochemistry." J Histochem Cytochem **31**(2): 285-92.
- Elsner, C. and K. Dorries (1992). "Evidence of human polyomavirus BK and JC infection in normal brain tissue." Virology **191**(1): 72-80.
- Elsner, C. and K. Dorries (1998). "Human polyomavirus JC control region variants in persistently infected CNS and kidney tissue." J Gen Virol **79** (Pt 4): 789-99.
- Evans, M. F., H. A. Aliesky, et al. (2003). "Optimization of biotinyl-tyramide-based in situ hybridization for sensitive background-free applications on formalin-fixed, paraffin-embedded tissue specimens." BMC Clin Pathol **3**(1): 2.
- Evans, R., A. W. Joss, et al. (1995). "The use of a nested polymerase chain reaction for detecting *Pneumocystis carinii* from lung and blood in rat and human infection." J Med Microbiol **42**(3): 209-13.
- Farinas, E. T., T. Bulter, et al. (2001). "Directed enzyme evolution." Curr Opin Biotechnol **12**(6): 545-51.
- Fay, F. S., K. L. Taneja, et al. (1997). "Quantitative digital analysis of diffuse and concentrated nuclear distributions of nascent transcripts, SC35 and poly(A)." Exp Cell Res **231**(1): 27-37.
- Ferrante, A. and Y. H. Thong (1982). "Separation of mononuclear and polymorphonuclear leucocytes from human blood by the one-step Hypaque-Ficoll method is dependent on blood column height." J Immunol Methods **48**(1): 81-5.
- Ferrante, P., S. Delbue, et al. (2003). "Analysis of JC virus genotype distribution and transcriptional control region rearrangements in human immunodeficiency virus-positive progressive multifocal leukoencephalopathy patients with and without highly active antiretroviral treatment." J Neurovirol **9 Suppl 1**: 42-6.
- Fisher, J. H., J. F. Gusella, et al. (1984). "Molecular hybridization under conditions of high stringency permits cloned DNA segments containing reiterated DNA sequences to be assigned to specific chromosomal locations." Proc Natl Acad Sci U S A **81**(2): 520-4.
- Flaegstad, T. and T. Traavik (1987). "BK virus in cell culture: infectivity quantitation and sequential expression of antigens detected by immunoperoxidase staining." J Virol Methods **16**(1-2): 139-46.

- Forstova, J., N. Krauzewicz, et al. (1993). "Cooperation of structural proteins during late events in the life cycle of polyomavirus." J Virol **67**(3): 1405-13.
- Francis, G., Z. Kerem, et al. (2002). "The biological action of saponins in animal systems: a review." Br J Nutr **88**(6): 587-605.
- Frisque, R. J. (1983). "Regulatory sequences and virus-cell interactions of JC virus." Prog Clin Biol Res **105**: 41-59.
- Frisque, R. J., G. L. Bream, et al. (1984). "Human polyomavirus JC virus genome." J Virol **51**(2): 458-69.
- Fu, J. C. and D. W. Gruenwedel (1976). "Salt effects on the denaturation of DNA. V. Preferential interactions of native and denatured calf thymus DNA in Na₂SO₄ solutions of varying ionic strength." Biopolymers **15**(2): 265-82.
- Gall, J. G. and M. L. Pardue (1969). "Formation and detection of RNA-DNA hybrid molecules in cytological preparations." Proc Natl Acad Sci U S A **63**(2): 378-83.
- Gardner, M. B. and P. A. Luciw (1989). "Animal models of AIDS." Faseb J **3**(14): 2593-606.
- Glasova, M., E. Konikova, et al. (1995). "Evaluation of different fixation-permeabilization methods for simultaneous detection of surface, cytoplasmic markers and DNA analysis by flow cytometry in some human hematopoietic cell lines." Neoplasma **42**(6): 337-46.
- Goldmann, C., H. Petry, et al. (1999). "Molecular cloning and expression of major structural protein VP1 of the human polyomavirus JC virus: formation of virus-like particles useful for immunological and therapeutic studies." J Virol **73**(5): 4465-9.
- Graham, F. L., J. Smiley, et al. (1977). "Characteristics of a human cell line transformed by DNA from human adenovirus type 5." J Gen Virol **36**(1): 59-74.
- Green, N. M. (1975). "Avidin." Adv Protein Chem **29**: 85-133.
- Greenlee, J. E., O. Narayan, et al. (1977). "Induction of brain tumors in hamsters with BK virus, a human papovavirus." Lab Invest **36**(6): 636-41.
- Gruda, M. C., J. M. Zabolotny, et al. (1993). "Transcriptional activation by simian virus 40 large T antigen: interactions with multiple components of the transcription complex." Mol Cell Biol **13**(2): 961-9.
- Hasui, K., T. Takatsuka, et al. (2002). "Improvement of supersensitive immunohistochemistry with an autostainer: a simplified catalysed signal amplification system." Histochem J **34**(5): 215-22.
- Hedstrom, L. (2002). "Serine protease mechanism and specificity." Chem Rev **102**(12): 4501-24.
- Hinuma, Y. and J. T. Grace, Jr. (1967). "Cloning of immunoglobulin-producing human leukemic and lymphoma cells in long-term cultures." Proc Soc Exp Biol Med **124**(1): 107-11.

- Hirsch, H. H., C. B. Drachenberg, et al. (2006). "Polyomavirus-associated nephropathy in renal transplantation: critical issues of screening and management." Adv Exp Med Biol **577**: 160-73.
- Holland, M. S., C. D. Mackenzie, et al. (1996). "A comparative study of histological conditions suitable for both immunofluorescence and in situ hybridization in the detection of Herpesvirus and its antigens in chicken tissues." J Histochem Cytochem **44**(3): 259-65.
- Hotfilder, M., S. Rottgers, et al. (2002). "Immature CD34+CD19- progenitor/stem cells in TEL/AML1-positive acute lymphoblastic leukemia are genetically and functionally normal." Blood **100**(2): 640-6.
- Hou, J. and E. O. Major (2000). "Progressive multifocal leukoencephalopathy: JC virus induced demyelination in the immune compromised host." J Neurovirol **6 Suppl 2**: S98-S100.
- Houff, S. A., E. O. Major, et al. (1988). "Involvement of JC virus-infected mononuclear cells from the bone marrow and spleen in the pathogenesis of progressive multifocal leukoencephalopathy." N Engl J Med **318**(5): 301-5.
- Howley, P. M., F. Rentier-Delrue, et al. (1980). "Cloned human polyomavirus JC DNA can transform human amnion cells." J Virol **36**(3): 878-82.
- Ishaq, M. and G. L. Stoner (1994). "Differential expression of mRNAs for JC virus large and small tumor antigens in brain tissues from progressive multifocal leukoencephalopathy patients with and without AIDS." Proc Natl Acad Sci U S A **91**(17): 8283-7.
- Jacobs, N., M. P. Moutschen, et al. (1993). "Efficient immunoselection of cytolytic effectors with a magnetic cell sorter." Res Immunol **144**(2): 141-50.
- Jensen, F. C., A. J. Girardi, et al. (1964). "Infection of Human and Simian Tissue Cultures with Rous Sarcoma Virus." Proc Natl Acad Sci U S A **52**: 53-9.
- Kamen, R., J. Favaloro, et al. (1980). "Topography of the three late mRNA's of polyoma virus which encode the virion proteins." J Virol **33**(2): 637-51.
- Kenna, J. G., G. N. Major, et al. (1985). "Methods for reducing non-specific antibody binding in enzyme-linked immunosorbent assays." J Immunol Methods **85**(2): 409-19.
- Khaitlina, S. Y. (2001). "Functional specificity of actin isoforms." Int Rev Cytol **202**: 35-98.
- Khalili, K., L. Del Valle, et al. (2003). "Human neurotropic polyomavirus, JCV, and its role in carcinogenesis." Oncogene **22**(33): 5181-91.
- Khatri, B. O., S. Man, et al. (2009). "Effect of plasma exchange in accelerating natalizumab clearance and restoring leukocyte function." Neurology **72**(5): 402-9.
- Kitamura, T., C. Sugimoto, et al. (1997). "Persistent JC virus (JCV) infection is demonstrated by continuous shedding of the same JCV strains." J Clin Microbiol **35**(5): 1255-7.

- Kohler, A., B. Lauritzen, et al. (2000). "Signal amplification in immunohistochemistry at the light microscopic level using biotinylated tyramide and nanogold-silver staining." J Histochem Cytochem **48**(7): 933-41.
- Koralnik, I. J. (2002). "Overview of the cellular immunity against JC virus in progressive multifocal leukoencephalopathy." J Neurovirol **8 Suppl 2**: 59-65.
- Koralnik, I. J., D. Boden, et al. (1999). "JC virus DNA load in patients with and without progressive multifocal leukoencephalopathy." Neurology **52**(2): 253-60.
- Koralnik, I. J., J. E. Schmitz, et al. (1999). "Detection of JC virus DNA in peripheral blood cell subpopulations of HIV-1-infected individuals." J Neurovirol **5**(4): 430-5.
- Krejci, P., V. Kleinwachter, et al. (1976). "Interaction of DNA and deoxyribonucleoprotein with methylene blue after the treatment with fixation solutions used in chromosome G-banding techniques." Folia Biol (Praha) **12**(3): 201-8.
- Kumar, K. U., S. C. Tang, et al. (1996). "Glial and muscle embryonal carcinoma cell-specific independent regulation of expression of human JC virus early promoter by cyclic AMP response elements and adjacent nuclear factor 1 binding sites." J Med Virol **49**(3): 199-204.
- Kunitake, T., T. Kitamura, et al. (1995). "Parent-to-child transmission is relatively common in the spread of the human polyomavirus JC virus." J Clin Microbiol **33**(6): 1448-51.
- Laghi, L., A. E. Randolph, et al. (1999). "JC virus DNA is present in the mucosa of the human colon and in colorectal cancers." Proc Natl Acad Sci U S A **96**(13): 7484-9.
- Lalli, E., D. Gibellini, et al. (1992). "In situ hybridization in suspension and flow cytometry as a tool for the study of gene expression." Anal Biochem **207**(2): 298-303.
- Lambkin, R., J. S. Oxford, et al. (2000). "Rapid antibody response to influenza vaccination in "at risk" groups." Vaccine **18**(21): 2307-11.
- Lawrence, J. B., L. M. Marselle, et al. (1990). "Subcellular localization of low-abundance human immunodeficiency virus nucleic acid sequences visualized by fluorescence in situ hybridization." Proc Natl Acad Sci U S A **87**(14): 5420-4.
- Lee, J. I. and G. J. Burckart (1998). "Nuclear factor kappa B: important transcription factor and therapeutic target." J Clin Pharmacol **38**(11): 981-93.
- Leitch, I. J. and J. S. Heslop-Harrison (1994). "Detection of digoxigenin-labeled DNA probes hybridized to plant chromosomes in situ." Methods Mol Biol **28**: 177-85.
- Levsky, J. M. and R. H. Singer (2003). "Fluorescence in situ hybridization: past, present and future." J Cell Sci **116**(Pt 14): 2833-8.

- Liebl, D., F. Difato, et al. (2006). "Mouse polyomavirus enters early endosomes, requires their acidic pH for productive infection, and meets transferrin cargo in Rab11-positive endosomes." J Virol **80**(9): 4610-22.
- Linda, H., A. von Heijne, et al. (2009). "Progressive multifocal leukoencephalopathy after natalizumab monotherapy." N Engl J Med **361**(11): 1081-7.
- Loeber, G. and K. Dorries (1988). "DNA rearrangements in organ-specific variants of polyomavirus JC strain GS." J Virol **62**(5): 1730-5.
- Loken, M. R. and L. A. Herzenber (1975). "Analysis of cell populations with a fluorescence-activated cell sorter." Ann N Y Acad Sci **254**: 163-71.
- Looi, L. M. and P. L. Cheah (1992). "In situ hybridisation: principles and applications." Malays J Pathol **14**(2): 69-76.
- Love, A. H., J. G. Matthews, et al. (1972). "Intestinal blood flow and sodium transport." Gut **13**(10): 853-4.
- Macville, M. V., A. G. Van Dorp, et al. (1995). "Monitoring morphology and signal during non-radioactive in situ hybridization procedures by reflection-contrast microscopy and transmission electron microscopy." J Histochem Cytochem **43**(7): 665-74.
- Major, E. O. (2010). "Progressive multifocal leukoencephalopathy in patients on immunomodulatory therapies." Annu Rev Med **61**: 35-47.
- Major, E. O., K. Amemiya, et al. (1990). "Glial cells of the human developing brain and B cells of the immune system share a common DNA binding factor for recognition of the regulatory sequences of the human polyomavirus, JCV." J Neurosci Res **27**(4): 461-71.
- Major, E. O., K. Amemiya, et al. (1992). "Pathogenesis and molecular biology of progressive multifocal leukoencephalopathy, the JC virus-induced demyelinating disease of the human brain." Clin Microbiol Rev **5**(1): 49-73.
- Malm-Erjefalt, M., T. R. Stevens, et al. (2004). "Discontinuous Percoll gradient centrifugation combined with immunomagnetic separation obviates the need for erythrocyte lysis and yields isolated eosinophils with minimal granule abnormalities." J Immunol Methods **288**(1-2): 99-109.
- Mannova, P. and J. Forstova (2003). "Mouse polyomavirus utilizes recycling endosomes for a traffic pathway independent of COPI vesicle transport." J Virol **77**(3): 1672-81.
- Manyonda, I. T., A. J. Soltys, et al. (1992). "A critical evaluation of the magnetic cell sorter and its use in the positive and negative selection of CD45RO+ cells." J Immunol Methods **149**(1): 1-10.

- Manz, W., G. Arp, et al. (2000). "Widefield deconvolution epifluorescence microscopy combined with fluorescence in situ hybridization reveals the spatial arrangement of bacteria in sponge tissue." J Microbiol Methods **40**(2): 125-34.
- Martin, P. and T. Papayannopoulou (1982). "HEL cells: a new human erythroleukemia cell line with spontaneous and induced globin expression." Science **216**(4551): 1233-5.
- Matoba, T., Y. Orba, et al. (2008). "An siRNA against JC virus (JCV) agnoprotein inhibits JCV infection in JCV-producing cells inoculated in nude mice." Neuropathology **28**(3): 286-94.
- Mc, D. A. R. and K. Opeskin (1998). "Timing of early changes in brain trauma." Am J Forensic Med Pathol **19**(1): 1-9.
- McCance, D. J. (1983). "Persistence of animal and human papovaviruses in renal and nervous tissues." Prog Clin Biol Res **105**: 343-57.
- McNeil, J. A., C. V. Johnson, et al. (1991). "Localizing DNA and RNA within nuclei and chromosomes by fluorescence in situ hybridization." Genet Anal Tech Appl **8**(2): 41-58.
- Menezes, J., W. Leibold, et al. (1975). "Establishment and characterization of an Epstein-Barr virus (EBC)-negative lymphoblastoid B cell line (BJA-B) from an exceptional, EBV-genome-negative African Burkitt's lymphoma." Biomedicine **22**(4): 276-84.
- Merabova, N., D. Kaniowska, et al. (2008). "JC virus agnoprotein inhibits in vitro differentiation of oligodendrocytes and promotes apoptosis." J Virol **82**(3): 1558-69.
- Mergenthaler, H. G., F. G. Staber, et al. (1982). "The response of murine splenic granulocyte-macrophage colony-forming cells to lipid A in vivo." Exp Hematol **10**(8): 637-49.
- Min, T. and J. Swansbury (2003). "Cytogenetic studies using FISH: background." Methods Mol Biol **220**: 173-91.
- Monaco, M. C., W. J. Atwood, et al. (1996). "JC virus infection of hematopoietic progenitor cells, primary B lymphocytes, and tonsillar stromal cells: implications for viral latency." J Virol **70**(10): 7004-12.
- Monaco, M. C., P. N. Jensen, et al. (1998). "Detection of JC virus DNA in human tonsil tissue: evidence for site of initial viral infection." J Virol **72**(12): 9918-23.
- Monaco, M. C., B. F. Sabath, et al. (2001). "JC virus multiplication in human hematopoietic progenitor cells requires the NF-1 class D transcription factor." J Virol **75**(20): 9687-95.
- Mueller, C., A. Graessmann, et al. (1978). "Mapping of early SV40-specific functions by microinjection of different early viral DNA fragments." Cell **15**(2): 579-85.
- Muhlegger, K., E. Huber, et al. (1990). "Non-radioactive labeling and detection of nucleic acids. IV. Synthesis and properties of digoxigenin-modified 2'-deoxyuridine-5'-triphosphates and a

- photoactivatable analog of digoxigenin (photodigoxigenin)." Biol Chem Hoppe Seyler **371**(10): 953-65.
- Murakami, T., T. Hagiwara, et al. (2001). "A novel method for detecting HIV-1 by non-radioactive in situ hybridization: application of a peptide nucleic acid probe and catalysed signal amplification." J Pathol **194**(1): 130-5.
- Nash, D. and W. Plaut (1964). "On the Denaturation of Chromosomal DNA in Situ." Proc Natl Acad Sci U S A **51**: 731-5.
- Nath, J. and K. L. Johnson (1998). "Fluorescence in situ hybridization (FISH): DNA probe production and hybridization criteria." Biotech Histochem **73**(1): 6-22.
- Nielsen, S. D., J. O. Nielsen, et al. (1997). "In vitro separation and expansion of CD4 lymphocytes from HIV-infected individuals without activation of HIV infection." J Immunol Methods **200**(1-2): 107-12.
- Norbury, C. J. and M. Fried (1987). "Polyomavirus early region alternative poly(A) site: 3'-end heterogeneity and altered splicing pattern." J Virol **61**(12): 3754-8.
- Nuovo, G. J. (1995). "In situ PCR: protocols and applications." PCR Methods Appl **4**(4): S151-67.
- O'Neill, F. J., R. J. Frisque, et al. (1995). "Immortalization of human cells by mutant and chimeric primate polyomavirus T-antigen genes." Oncogene **10**(6): 1131-9.
- Ogawa, M., A. Setiyono, et al. (2004). "Evaluation of PCR and nested PCR assays currently used for detection of *Coxiella burnetii* in Japan." Southeast Asian J Trop Med Public Health **35**(4): 852-5.
- Olmsted, R. A., A. K. Barnes, et al. (1989). "Molecular cloning of feline immunodeficiency virus." Proc Natl Acad Sci U S A **86**(7): 2448-52.
- Padgett, B. L., C. M. Rogers, et al. (1977). "JC virus, a human polyomavirus associated with progressive multifocal leukoencephalopathy: additional biological characteristics and antigenic relationships." Infect Immun **15**(2): 656-62.
- Padgett, B. L., D. L. Walker, et al. (1971). "Cultivation of papova-like virus from human brain with progressive multifocal leukoencephalopathy." Lancet **1**(7712): 1257-60.
- Pattanapanyasat, K., D. E. Kyle, et al. (1994). "Flow cytometric immunophenotyping of lymphocyte subsets in samples that contain a high proportion of non-lymphoid cells." Cytometry **18**(4): 199-208.
- Paz, A., U. Fiszler, et al. (1999). "Phenotyping analysis of peripheral blood leukocytes in patients with multiple sclerosis." Eur J Neurol **6**(3): 347-52.
- Pho, M. T., A. Ashok, et al. (2000). "JC virus enters human glial cells by clathrin-dependent receptor-mediated endocytosis." J Virol **74**(5): 2288-92.

- Pichon, C., M. Monsigny, et al. (1999). "Intracellular localization of oligonucleotides: influence of fixative protocols." Antisense Nucleic Acid Drug Dev **9**(1): 89-93.
- Pietro Paolo, V., D. Fioriti, et al. (2003). "Detection and sequence analysis of human polyomaviruses DNA from autoptic samples of HIV-1 positive and negative subjects." Int J Immunopathol Pharmacol **16**(3): 269-76.
- Pietro Paolo, V., M. Videtta, et al. (2003). "Rearrangement patterns of JC virus noncoding control region from different biological samples." J Neurovirol **9**(6): 603-11.
- Pollard, K., D. Lunny, et al. (1987). "Fixation, processing, and immunochemical reagent effects on preservation of T-lymphocyte surface membrane antigens in paraffin-embedded tissue." J Histochem Cytochem **35**(11): 1329-38.
- Pulvertaft, J. V. (1965). "A Study Of Malignant Tumours In Nigeria By Short-Term Tissue Culture." J Clin Pathol **18**: 261-73.
- Raap, A. K. (1998). "Advances in fluorescence in situ hybridization." Mutat Res **400**(1-2): 287-98.
- Randhawa, P., F. Baksh, et al. (2001). "JC virus infection in allograft kidneys: analysis by polymerase chain reaction and immunohistochemistry." Transplantation **71**(9): 1300-3.
- Randhawa, P., R. Shapiro, et al. (2005). "Quantitation of DNA of polyomaviruses BK and JC in human kidneys." J Infect Dis **192**(3): 504-9.
- Ranganathan, P. N. and K. Khalili (1993). "The transcriptional enhancer element, kappa B, regulates promoter activity of the human neurotropic virus, JCV, in cells derived from the CNS." Nucleic Acids Res **21**(8): 1959-64.
- Rauch, J., D. Wolf, et al. (2000). "The influence of formamide on thermal denaturation profiles of DNA and metaphase chromosomes in suspension." Z Naturforsch [C] **55**(9-10): 737-46.
- Rhim, J. S., K. Schell, et al. (1969). "Biological characteristics and viral susceptibility of an African green monkey kidney cell line (Vero)." Proc Soc Exp Biol Med **132**(2): 670-8.
- Ricciardiello, L., L. Laghi, et al. (2000). "JC virus DNA sequences are frequently present in the human upper and lower gastrointestinal tract." Gastroenterology **119**(5): 1228-35.
- Rieckmann, P., U. Michel, et al. (1994). "Regulation of JC virus expression in B lymphocytes." J Virol **68**(1): 217-22.
- Rudkin, G. T. and B. D. Stollar (1977). "High resolution detection of DNA-RNA hybrids in situ by indirect immunofluorescence." Nature **265**(5593): 472-3.
- Sabath, B. F. and E. O. Major (2002). "Traffic of JC virus from sites of initial infection to the brain: the path to progressive multifocal leukoencephalopathy." J Infect Dis **186 Suppl 2**: S180-6.
- Sadowska, B., R. Barrucco, et al. (2003). "Regulation of human polyomavirus JC virus gene transcription by AP-1 in glial cells." J Virol **77**(1): 665-72.

- Safak, M., G. L. Gallia, et al. (1999). "Physical and functional interaction between the Y-box binding protein YB-1 and human polyomavirus JC virus large T antigen." J Virol **73**(12): 10146-57.
- Safak, M., G. L. Gallia, et al. (1999). "A 23-bp sequence element from human neurotropic JC virus is responsive to NF-kappa B subunits." Virology **262**(1): 178-89.
- Safak, M., G. L. Gallia, et al. (1999). "Reciprocal interaction between two cellular proteins, Puralpha and YB-1, modulates transcriptional activity of JCVCY in glial cells." Mol Cell Biol **19**(4): 2712-23.
- Salunke, D. M., D. L. Caspar, et al. (1986). "Self-assembly of purified polyomavirus capsid protein VP1." Cell **46**(6): 895-904.
- Sandalon, Z. and A. Oppenheim (1997). "Self-assembly and protein-protein interactions between the SV40 capsid proteins produced in insect cells." Virology **237**(2): 414-21.
- Sano, T., T. Hikino, et al. (1998). "In situ hybridization with biotinylated tyramide amplification: detection of human papillomavirus DNA in cervical neoplastic lesions." Mod Pathol **11**(1): 19-23.
- Saribas, A. S., B. T. Arachea, et al. (2011). "Human polyomavirus JC small regulatory agnoprotein forms highly stable dimers and oligomers: implications for their roles in agnoprotein function." Virology **420**(1): 51-65.
- Sariyer, I. K., A. S. Saribas, et al. (2011). "Infection by agnoprotein-negative mutants of polyomavirus JC and SV40 results in the release of virions that are mostly deficient in DNA content." Virol J **8**: 255.
- Schatzl, H. M., E. Sieger, et al. (1994). "Detection by PCR of human polyomaviruses BK and JC in immunocompromised individuals and partial sequencing of control regions." J Med Virol **42**(2): 138-45.
- Schmid, H., H. Nitschko, et al. (2005). "Polyomavirus DNA and RNA detection in renal allograft biopsies: results from a European multicenter study." Transplantation **80**(5): 600-4.
- Schneider, E., S. Whitmore, et al. (2008). "Revised surveillance case definitions for HIV infection among adults, adolescents, and children aged <18 months and for HIV infection and AIDS among children aged 18 months to <13 years--United States, 2008." MMWR Recomm Rep **57**(RR-10): 1-12.
- Schneider, U., H. U. Schwenk, et al. (1977). "Characterization of EBV-genome negative "null" and "T" cell lines derived from children with acute lymphoblastic leukemia and leukemic transformed non-Hodgkin lymphoma." Int J Cancer **19**(5): 621-6.

- Semple, J. W., D. Allen, et al. (1993). "Rapid separation of CD4+ and CD19+ lymphocyte populations from human peripheral blood by a magnetic activated cell sorter (MACS)." Cytometry **14**(8): 955-60.
- Serrano, J., J. Roman, et al. (2000). "Molecular analysis of lineage-specific chimerism and minimal residual disease by RT-PCR of p210(BCR-ABL) and p190(BCR-ABL) after allogeneic bone marrow transplantation for chronic myeloid leukemia: increasing mixed myeloid chimerism and p190(BCR-ABL) detection precede cytogenetic relapse." Blood **95**(8): 2659-65.
- Shadan, F. F., C. Cunningham, et al. (2002). "JC virus: a biomarker for colorectal cancer?" Med Hypotheses **59**(6): 667-9.
- Shibuya, M., T. Miwa, et al. (1992). "Embedding and fixation techniques for immunohistochemical staining with anti-DNA polymerase alpha and Ki-67 monoclonal antibodies to analyze the proliferative potential of tumors." Biotech Histochem **67**(3): 161-4.
- Shimizu, N., A. Imamura, et al. (1999). "Distribution of JC virus DNA in peripheral blood lymphocytes of hematological disease cases." Intern Med **38**(12): 932-7.
- Shinohara, T., K. Nagashima, et al. (1997). "Propagation of the human polyomavirus, JCV, in human neuroblastoma cell lines." Virology **228**(2): 269-77.
- Shishido-Hara, Y., Y. Hara, et al. (2000). "Analysis of capsid formation of human polyomavirus JC (Tokyo-1 strain) by a eukaryotic expression system: splicing of late RNAs, translation and nuclear transport of major capsid protein VP1, and capsid assembly." J Virol **74**(4): 1840-53.
- Simons, V., J. P. Morrissey, et al. (2006). "Dual effects of plant steroidal alkaloids on *Saccharomyces cerevisiae*." Antimicrob Agents Chemother **50**(8): 2732-40.
- Smith, G. E., M. D. Summers, et al. (1983). "Production of human beta interferon in insect cells infected with a baculovirus expression vector." Mol Cell Biol **3**(12): 2156-65.
- Sock, E., M. Wegner, et al. (1991). "DNA replication of human polyomavirus JC is stimulated by NF-I in vivo." Virology **182**(1): 298-308.
- Speel, E. J., J. Herbergs, et al. (1994). "Combined immunocytochemistry and fluorescence in situ hybridization for simultaneous tricolor detection of cell cycle, genomic, and phenotypic parameters of tumor cells." J Histochem Cytochem **42**(7): 961-6.
- Staratschek-Jox, A., S. Kotkowski, et al. (2000). "Detection of Epstein-Barr virus in Hodgkin-Reed-Sternberg cells : no evidence for the persistence of integrated viral fragments in Latent membrane protein-1 (LMP-1)-negative classical Hodgkin's disease." Am J Pathol **156**(1): 209-16.

- Strober, W. (2001). "Trypan blue exclusion test of cell viability." Curr Protoc Immunol **Appendix 3**: Appendix 3B.
- Stuckenholz, C., Y. Kageyama, et al. (1999). "Guilt by association: non-coding RNAs, chromosome-specific proteins and dosage compensation in *Drosophila*." Trends Genet **15**(11): 454-8.
- Sundsfjord, A., T. Flaegstad, et al. (1994). "BK and JC viruses in human immunodeficiency virus type 1-infected persons: prevalence, excretion, viremia, and viral regulatory regions." J Infect Dis **169**(3): 485-90.
- Sundsfjord, A., A. R. Spein, et al. (1994). "Detection of BK virus DNA in nasopharyngeal aspirates from children with respiratory infections but not in saliva from immunodeficient and immunocompetent adult patients." J Clin Microbiol **32**(5): 1390-4.
- Suthipintawong, C., A. S. Leong, et al. (1996). "Immunostaining of cell preparations: a comparative evaluation of common fixatives and protocols." Diagn Cytopathol **15**(2): 167-74.
- Suzuki, T., Y. Orba, et al. (2010). "The human polyoma JC virus agnoprotein acts as a viroporin." PLoS Pathog **6**(3): e1000801.
- Sweet, T. M., L. Del Valle, et al. (2002). "Molecular biology and immunoregulation of human neurotropic JC virus in CNS." J Cell Physiol **191**(3): 249-56.
- Tada, H., M. Lashgari, et al. (1989). "Cell type-specific expression of JC virus early promoter is determined by positive and negative regulation." J Virol **63**(1): 463-6.
- Tada, H., M. S. Lashgari, et al. (1991). "Regulation of JC virus late promoter function: evidence that a pentanucleotide "silencer" repeat sequence AGGGAAGGGA down-regulates transcription of the JC virus late promoter." Virology **180**(1): 327-38.
- Tada, H., J. Rappaport, et al. (1990). "Trans-activation of the JC virus late promoter by the tat protein of type 1 human immunodeficiency virus in glial cells." Proc Natl Acad Sci U S A **87**(9): 3479-83.
- Tamura, T., T. Inoue, et al. (1988). "Enhancer of human polyoma JC virus contains nuclear factor I-binding sequences; analysis using mouse brain nuclear extracts." Biochem Biophys Res Commun **157**(2): 419-25.
- Tavazzi, E., P. Ferrante, et al. (2011). "Progressive multifocal leukoencephalopathy: an unexpected complication of modern therapeutic monoclonal antibody therapies." Clin Microbiol Infect **17**(12): 1776-80.
- Taylor, A., H. P. Erba, et al. (1988). "Nucleotide sequence and expression of the human skeletal alpha-actin gene: evolution of functional regulatory domains." Genomics **3**(4): 323-36.

- To, L. T. and S. Bernard (1992). "Effect of fixation on the detection of transmissible gastroenteritis coronavirus antigens by the fixed-cell immunoperoxidase technique." J Immunol Methods **154**(2): 195-204.
- Tollerud, D. J., J. W. Clark, et al. (1989). "The influence of age, race, and gender on peripheral blood mononuclear-cell subsets in healthy nonsmokers." J Clin Immunol **9**(3): 214-22.
- Tornatore, C., J. R. Berger, et al. (1992). "Detection of JC virus DNA in peripheral lymphocytes from patients with and without progressive multifocal leukoencephalopathy." Ann Neurol **31**(4): 454-62.
- Truong, K., J. Boenders, et al. (1997). "Signal amplification of FISH for automated detection using image cytometry." Anal Cell Pathol **13**(3): 137-46.
- Vago, L., P. Cinque, et al. (1996). "JCV-DNA and BKV-DNA in the CNS tissue and CSF of AIDS patients and normal subjects. Study of 41 cases and review of the literature." J Acquir Immune Defic Syndr Hum Retrovirol **12**(2): 139-46.
- Vandekerckhove, J. and K. Weber (1978). "At least six different actins are expressed in a higher mammal: an analysis based on the amino acid sequence of the amino-terminal tryptic peptide." J Mol Biol **126**(4): 783-802.
- Viscidi, R. P., D. E. Rollison, et al. (2003). "Serological cross-reactivities between antibodies to simian virus 40, BK virus, and JC virus assessed by virus-like-particle-based enzyme immunoassays." Clin Diagn Lab Immunol **10**(2): 278-85.
- von Giesen, H. J., E. Neuen-Jacob, et al. (1997). "Diagnostic criteria and clinical procedures in HIV-1 associated progressive multifocal leukoencephalopathy." J Neurol Sci **147**(1): 63-72.
- Wagner, E. K. and D. C. Bloom (1997). "Experimental investigation of herpes simplex virus latency." Clin Microbiol Rev **10**(3): 419-43.
- Walker, D. L. and B. L. Padgett (1983). "The epidemiology of human polyomaviruses." Prog Clin Biol Res **105**: 99-106.
- Walker, D. L., B. L. Padgett, et al. (1973). "Human papovavirus (JC): induction of brain tumors in hamsters." Science **181**(100): 674-6.
- Weber, T. (2008). "Progressive multifocal leukoencephalopathy." Neurol Clin **26**(3): 833-54, x-xi.
- Weber, T. and E. O. Major (1997). "Progressive multifocal leukoencephalopathy: molecular biology, pathogenesis and clinical impact." Intervirol **40**(2-3): 98-111.
- Wei, G., C. K. Liu, et al. (2000). "JC virus binds to primary human glial cells, tonsillar stromal cells, and B-lymphocytes, but not to T lymphocytes." J Neurovirol **6**(2): 127-36.
- Weil, R. (1963). "The denaturation and the renaturation of the DNA of polyoma virus." Proc Natl Acad Sci U S A **49**: 480-7.

- Weiss, D. J., R. Kraemer, et al. (1989). "Isolation of granulocytes and mononuclear cells from the blood of dogs, cats, horses and cattle." Vet Clin Pathol **18**(2): 33-6.
- Weissert, R. (2011). "Progressive multifocal leukoencephalopathy." J Neuroimmunol **231**(1-2): 73-7.
- White, F. A., 3rd, M. Ishaq, et al. (1992). "JC virus DNA is present in many human brain samples from patients without progressive multifocal leukoencephalopathy." J Virol **66**(10): 5726-34.
- White, M. K. and K. Khalili (2011). "Pathogenesis of progressive multifocal leukoencephalopathy--revisited." J Infect Dis **203**(5): 578-86.
- Wikstrom, A. C., O. Bakke, et al. (1987). "Intracellular localization of the glucocorticoid receptor: evidence for cytoplasmic and nuclear localization." Endocrinology **120**(4): 1232-42.
- Wold, W. S., M. Green, et al. (1980). "Integration pattern of human JC virus sequences in two clones of a cell line established from a JC virus-induced hamster brain tumor." J Virol **33**(3): 1225-8.
- Xu, K., T. Huang, et al. (1998). "Improving the fixation method for preimplantation genetic diagnosis by fluorescent in situ hybridization." J Assist Reprod Genet **15**(9): 570-4.
- Yamamoto, J. K., E. Ho, et al. (1986). "A feline retrovirus induced T-lymphoblastoid cell-line that produces an atypical alpha type of interferon." Vet Immunol Immunopathol **11**(1): 1-19.
- Yasumura, Y. and M. Kawakita (1963). "The research for the SV40 by means of tissue culture technique." Nippon Rinsho **21**(6): 1201-1219.
- Zambrano, A., M. Kalantari, et al. (2002). "Detection of human polyomaviruses and papillomaviruses in prostatic tissue reveals the prostate as a habitat for multiple viral infections." Prostate **53**(4): 263-76.
- Zentgraf, H., W. Keller, et al. (1978). "The structure of SV 40 chromatin." Philos Trans R Soc Lond B Biol Sci **283**(997): 299-303.
- Zipursky, A., E. Bow, et al. (1976). "Leukocyte density and volume in normal subjects and in patients with acute lymphoblastic leukemia." Blood **48**(3): 361-71.
- Zurhein, G. and S. M. Chou (1965). "Particles Resembling Papova Viruses In Human Cerebral Demyelinating Disease." Science **148**: 1477-9.

6. Abbreviations

Ab	Antibody
ACTA1	Human skeletal alpha-actin gene
AIDS	Acquired Immunodeficiency Syndrome
BKV	BK virus
bp	base pairs (DNA length)
BSA	Bovine Serum Albumine
cAMP	cyclic adenosine monophosphate
CD	Cluster Designation
CMV	Human Cytomegalo Virus
CNS	Central Nervous System
DAPI	4',6-diamidino-2-phenylindole, dihydrochloride
dATP	desoxyadenosine triphosphate
dCTP	desoxycytidine triphosphate
dGTP	desoxyguanine triphosphate
dTTP	desoxythymidine triphosphate
dUTP	desoxy uracil triphosphate
DIG	Digoxigenin
DMSO	Dimethyl sulphoxide
DNA	Desoxyribonucleic Acid
EDTA	Ethylene diamine tetraacetic acid
ELISA	Enzyme Linked Immunosorbent Assay
FA	Formamide
FACS	Fluorescence Activated Cell Sorter
FCS	Fetal Calf Serum
FISH	Fluorescence <i>in situ</i> Hybridization
FITC	Fluoresceine isothiocyanate
FIV	Feline Immunodeficiency Virus
GE	Genomic Equivalents
HHV6	Human Herpes Virus 6
HIV-1	Human Immunodeficiency Virus
HRP	Horseradish Peroxidase
ISH	<i>In situ</i> Hybridization

ISPCR	<i>In situ</i> Polymerase Chain Reaction
JCV	JC Virus
kb	kilobases (nucleic acids length)
LB medium	Luria Broth medium
mAb	Monoclonal Antibody
MACS	Magnetic Microbeads Cell Separation
MEM	Minimal Essential Medium
NF- κ B	Nuclear Factor κ -B-cell
OD	Optical Density
PBL	Peripheral Blood Leukocytes
PBMC	Peripheral Blood Mononuclear Cells
PBS	Phosphate Buffered Saline
PCR	Polymerase Chain Reaction
PE	Phycoerythrine
PFA	Paraformaldehyde
PMNL	Polymorphonuclear Leukocytes
RH	Radioactive Hybridization
RNA	Ribonucleic Acid
rpm	Rotations per minute
RT	Room Temperature
RTPCR	Reverse Transcription Polymerase Chain Reaction
SDS	Sodium dodecyl sulphate
SV40	Simian Virus 40
TAg	Tumor Antigen
Taq Pol	<i>Thermophilus aquaticus</i> DNA polymerase
TCR	Transcriptional Control Region
TdT	Terminal Desoxynucleotide Transferase
TN	Tris-Natrium chloride Buffer
TO-PRO-3	Quinolinium, 4-[3-(3-methyl-2(3H)- benzothiazolylidene)-1-propenyl]-1-[3-(trimethylammonio)propyl]-, diiodide
Tris	Tris(hydroxymethyl)aminomethan
UV	Ultraviolet rays
VP	Viral capsid protein
xg	x fold the gravitational force

7. English abstract

Primary contact with human polyomaviruses is followed by lifelong asymptomatic persistence of viral DNA. Under severe immunosuppression JCV activation may lead to unrestricted virus growth in the CNS followed by development of progressive multifocal leukoencephalopathy (PML). Besides the kidney and the brain, target cells of persistent infection were also found in the hematopoietic system. This included the presence of JCV genomes in peripheral blood cells (PBCs). In the attempt to understand the role of PBCs for the JCV infection in humans, we asked for the type of cells affected as well as for virus interaction with PBCs.

Analysis of separated subpopulations by highly sensitive and specific polymerase chain reaction and Southern blot hybridization revealed the presence of JCV DNA mostly in circulating granulocytes. These cells have important functions in innate immunity and are professional phagocytes. This suggested that PCR amplified DNA might be the result of an extranuclear association of the virus due to membrane attachment or phagocytosis rather than JCV infection with presence of viral DNA in the nucleus.

In the attempt to answer this question JCV DNA was subcellularly localized in the blood of 22 healthy donors by JCV specific fluorescence *in situ* hybridization (FISH). Granulocytes and peripheral blood mononuclear cells (PBMCs) were separated by Percoll gradient centrifugation. Intracellular JCV DNA was hybridized with Digoxigenin-labeled JCV specific DNA probes covering half of the viral genome. As the sensitivity of the anti-digoxigenin antibody system was lower than the PCR detection level, a chemical amplification step was included consisting of peroxidase labeled secondary antibody precipitating biotinylated tyramide followed by detection with streptavidin-Texas-Red and fluorescence microscopy. Comparison of the number of cells affected in healthy individuals with 15 HIV-1 infected patients with and without PML revealed that the rate of affected PBMCs was comparable in both groups (2.5 ± 0.4 and 14.5 ± 0.9 per 1000). In contrast, the rate of JCV positive granulocytes in the immunosuppressed group was $92.6 \pm 1.7\%$ compared to $4 \pm 1.4\%$ in healthy donors thus confirming that granulocytes are the major group of circulating cells affected by JCV and that HIV-1 associated immune impairment has an important effect on the virus-cell association.

Localization revealed that JCV DNA was predominantly located within the cytoplasm, although hybridizing signals occasionally covered the nuclear compartment. The fluorescent glow of chemical amplification combined with classical fluorescence microscopy did not allow an unequivocal localization of viral DNA. However, confocal microscopy of 24 sections through single cells combined with FISH without chemical amplification confirmed cytoplasmic

localization of JCV DNA in a large number of cells. Additionally, it clearly demonstrated that JCV DNA was also located in the nucleus and nuclear localization directly correlated with the number of cells affected. Calculation of the virus load in subcellular compartments revealed that up to 50% of the JCV genomes were located in the nucleus thus pointing to viral infection at least in the granulocytes of HIV-1 infected patients. This may contribute to the distribution of the virus from sites of peripheral infection to the CNS and may promote the development of active PML in the severely immune impaired patients.

8. German abstract

Primärer Kontakt mit dem humanen Polyomavirus JC führt zu lebenslanger asymptomatischer Persistenz der viralen DNA in den Zielorganen der Infektion insbesondere der Niere und dem ZNS. Unter schwerer Immunsuppression kann die Aktivierung des JCV zu uneingeschränkter Vermehrung des Virus im ZNS und zur Entwicklung einer zentralnervösen Erkrankung, der progressiven multifokalen Leukoenzephalopathie (PML) führen. Neuerdings wurde JCV DNA auch in Zellen des blutbildenden Systems insbesondere in peripheren Blutzellen (PBCs) beschrieben. Um die Rolle der PBCs für die JCV-Infektion beim Menschen besser zu verstehen, sollte der virus-assoziierte Zelltyp bestimmt und die Virus-Zell Interaktion näher untersucht werden.

Die Analyse von isolierten Blutzellsubpopulationen durch eine sensitive und spezifische Polymerase-Kettenreaktion mit folgender Southern Blot-Hybridisierung ergab die Präsenz von JCV-DNA zumeist in zirkulierenden Granulozyten. Diese Zellen haben eine wichtige Funktion in der angeborenen Immunität und sind professionelle Phagozyten. Dies legt nahe, dass die PCR-amplifizierte DNA eher das Ergebnis einer extranukleären Assoziation des Virus durch Membranassoziation oder Phagozytose als einer JCV-Infektion ist, die durch Virus-DNA im Kern charakterisiert ist.

Bei dem Versuch, diese Frage zu klären, wurde JCV-DNA in Blutzellen von gesunden Spendern mittels JCV-spezifischer Fluoreszenz *in situ* Hybridisierung (FISH) subzellulär lokalisiert. Granulozyten und periphere mononukleäre Blutzellen (PBMCs) wurden isoliert und intrazelluläre JCV-DNA mit Digoxigenin-markierten JCV DNA-Sonden, die die Hälfte des viralen Genoms repräsentierten, hybridisiert. Da die Empfindlichkeit des Anti-Digoxigenin-Antikörpersystems niedriger war als die PCR-Nachweisgrenze, wurde ein chemischer Amplifikationsschritt benutzt, das sogenannte Tyramidsystem, um die Sensitivität der FISH in Kombination mit der klassischen Fluoreszenzmikroskopie zu erhöhen. Der Vergleich der Anzahl von JCV betroffenen Zellen in gesunden Individuen mit Zellen von HIV-1-infizierten Patienten mit und ohne PML zeigte, dass die Rate der betroffenen PBMCs in beiden Gruppen ($2,5 \pm 0,4$ und $14,5 \pm 0,9$ pro 1000) vergleichbar war. Im Gegensatz dazu war die Rate der JCV positiven Granulozyten in der immunsupprimierten Gruppe, $92,6 \pm 1,7\%$, im Vergleich zu denen bei gesunden Spendern $4 \pm 1,4\%$ deutlich höher. Dies bestätigte, dass mit den Granulozyten die größte Gruppe von zirkulierenden Zellen von JCV betroffen sind und dass die schwere Beeinträchtigung der immunologischen Kompetenz durch die HIV-1 Infektion einen bedeutenden Einfluss auf die Virus-Zell Interaktion hat.

Die intrazelluläre Lokalisation der viralen DNA ergab, dass die Signale überwiegend im Zytoplasma lokalisiert waren, wenngleich gelegentlich auch nukleäre Kompartimente betroffen waren. Durch die chemischen Verstärkung der Fluoreszenzsignale in Kombination mit klassischer Fluoreszenzmikroskopie war es jedoch nicht möglich eine eindeutige Lokalisierung der viralen DNA zu erreichen. Erst die Anwendung der konfokalen Mikroskopie bestätigte die predominant zytoplasmatische Lokalisierung von JCV-DNA in einer großen Anzahl von Zellen und hat eindeutig gezeigt, dass JCV-DNA zusätzlich im Kern lokalisiert ist. Die Kern Lokalisation korreliert direkt mit der Anzahl der betroffenen Zellen. Berechnung der Viruslast in subzellulären Kompartimenten hat gezeigt, dass bis zu 50% der JCV Genome im Kern von Granulozyten von HIV-1 Patienten lokalisiert waren. Dies deutet auf eine virale Infektion der Granulozyten hin und lässt vermuten, dass sie unter der HIV-1 Infektion an der Disseminierung des JC Virus aus den Organen der peripheren Infektion in das ZNS beteiligt sind und in der Konsequenz auch bei der Entwicklung der PML eine wesentliche Rolle spielen könnten.

9. Curriculum vitae

Name: Sbiera
 Vorname: Silviu
 Geburts -Datum/-Ort: 18/02/1976, Radauti, Rumänien

Schulbildung

Grundschule: 09/1982 – 06/1990, Grundschule Nr. 3, Suceava, Rumänien
 Gymnasium: 09/1990 – 06/1994, Colegiul National “Stefan cel Mare”, Suceava, Rumänien
 Gymnasium Abschluss 24/07/1994, Abitur

Hochschule: 1994 – 1998, Ökologie und Umweltschutz, Biologische Fakultät, “Al.I.Cuza” Universität, Iasi, Rumänien
 Preise: Erster Preis für wissenschaftliche Aktivität im Universitätsjahr 1996-1997
 Diplom: “Explorative Untersuchungen in Bezug auf die Wasserqualität des Flusses Bistrita unter Verwendung vom Globalen Biologischen Verzeichnis (AFNOR, Essais des eaux)”
 Hochschulabschluss: 06/1998, Biologie Diplom

Auslandsstudien: 19/04/1999 – 07/05/1999, Ökologische Restauration, Lelystad, Niederlande
 Postgraduierte Training: 01/05/2000 – 31/07/2006, Doktorand an dem Institut für Virologie und Immunbiologie der Universität Würzburg
 Promotionsthema: Interaktion zwischen JC Polyomavirus und Zellen des peripheren hämatopoietischen System
 Stipendien: 01/05/2000– 01/05/2003, Graduiertenkolleg “Immunmodulation”, Universität Würzburg

Berufliche Werdegang: 01/07/1998 – 30/04/2000, Biologe bei der Rumänisch Nationale Wassergesellschaft, Iasi, Rumänien

01/05/2000 – 31/07/2006, Doktorand am Institut für Virologie und Immunbiologie der Universität Würzburg

01/08/2006 – jetzt, wissenschaftliche Mitarbeiter, Schwerpunkt Endokrinologie und Diabetologie, Universitätsklinikum Würzburg

Gutachterliche Tätigkeit

Zeitschriften

- Endocrine
- Endocrine Related Cancer
- Molecular and Cellular Endocrinology
- Onkologie
- PLoS ONE

Publikationen

K. Dörries, **S. Sbiera**, K. Drews, G. Arendt, C. Eggers and R. Dörries “Human Polyomavirus DNA in peripheral blood of persistently infected individuals” *Journal of Neurovirology*, 2003, 9, Supplement 1: 81-87

S. Sbiera, S. Wortmann and M. Fassnacht “Dendritic cell based immunotherapy, a promising therapeutic approach for endocrine malignancies”, review, *Hormone and Metabolic Research*, 2008, 40 (2): 89-98

C.L. Ronchi, **S. Sbiera**, L. Kraus, S. Wortmann, S. Johansen, P. Adam, H.S. Willenberg, S. Hahner, B. Allolio and M. Fassnacht “Expression of excision repair cross complementing group 1 and prognosis in adrenocortical carcinoma patients treated with platinum based chemotherapy” *Endocrine Related Cancer*, 2009, 16 (3):907-18

Sbiera S, Schull S, Assie G, Voelker HU, Kraus L, Beyer M, Ragazzon B, Beuschlein F, Willenberg HS, Hahner S, Saeger W, Bertherat J, Allolio B, Fassnacht M “High diagnostic and prognostic value of steroidogenic factor-1 expression in adrenal tumors.” *J Clin Endocrinol Metab*, 2010, 95 (10):E161-71

Adam P, Hahner S, Hartmann M, Heinrich B, Quinkler M, Willenberg HS, Saeger W, **Sbiera S**, Schull S, Voelker HU, Ströbel P, Allolio B, Fassnacht M “Epidermal growth factor receptor in adrenocortical tumors: analysis of gene sequence, protein expression and correlation with clinical outcome” *Modern Pathology*, 2010, 23(12):1596-604

Gaujoux S, Grabar S, Fassnacht M, Ragazzon B, Launay P, Libé R, Chokri I, Audebourg A, Royer B, **Sbiera S**, Vacher-Lavenu MC, Dousset B, Bertagna X, Allolio B, Bertherat J, Tissier F “ β -catenin activation is associated with specific clinical and pathologic characteristics and a poor outcome in adrenocortical carcinoma” *Clinical Cancer Research*, 2011, 17(2):328-36

Sbiera S, Dexneit T, Reichardt SD, Michel KD, van den Brandt J, Schull S, Kraus L, Beyer M, Mlynski R, Wortmann S, Allolio B, Reichardt HM, Fassnacht M “Influence of short-term glucocorticoid therapy on regulatory T cells in vivo“ PLoS One, 2011, 6(9):e24345

Kroiss M, Reuss M, Kühner D, Johansen S, Beyer M, Zink M, Hartmann MF, Dhir V, Wudy SA, Arlt W, **Sbiera S**, Allolio B, Fassnacht M “Sunitinib inhibits cell proliferation and alters steroidogenesis by downregulation of HSD3B2 in adrenocortical carcinoma cells” Frontiers in Endocrinology, 2011, September 9th, volume 2, doi: 10.3389/fendo.2011.00027

Cristina L. Ronchi*, Ellen Leich*, **Silviu Sbiera**, Dirk Weismann, Andreas Rosenwald, Bruno Allolio, Martin Fassnacht “Single nucleotide polymorphism microarray analysis in cortisol-secreting adrenocortical adenomas identifies new candidate genes and pathways” Neoplasia, 2012, 14(3):206-18

Marco Volante, Massimo Terzolo, Martin Fassnacht, Ida Rapa, Antonina Germano, **Silviu Sbiera**, Fulvia Daffara, Paola Sperone, Giorgio Scagliotti, Bruno Allolio, Mauro Papotti, and Alfredo Berruti ” Ribonucleotide reductase large subunit (RRM1) gene expression predicts efficacy of adjuvant mitotane in adrenocortical cancer” Clinical Cancer Research, 2012, 18(12):3452-61

Cristina L. Ronchi*, **Silviu Sbiera**, Sonja Steinhauer, Andreas Rosenwald, Martin Fassnacht, Bruno Allolio “Low SGK1 expression in human adrenocortical tumors is associated with autonomous glucocorticoid secretion and poor prognosis” J Clin Endocrinol Metab, 2012, *in press*

Silviu Sbiera, Matthias Kroiss, Tabitha Thamm, Melanie Beyer, Dorothee Kuehner, Marion Wobser, Jürgen Becker, Patrick Adam, Bruno Allolio, Martin Fassnacht “Survivin in adrenocortical tumors – pathophysiological implications and therapeutic potential” Hormone and Metabolic Research, 2012, *in press*

Vorträge und Posters (Auswahl)

K. Dörries, **S. Sbiera**, K. Drews, T. Bashir, C. Eggers and G. Arendt “CNS and the hematopoietic system are targets for persistent human polyomavirus infection in immun impaired and healthy individuals” DNA Tumour Virus Meeting, Juli 24-29, 2001, Churchill College, Cambridge, UK

S. Sbiera, K. Drews, C. Eggers, G. Arendt and K. Dörries “Human polyomavirus infection in peripheral blood of immun impaired and healthy individuals” 4th International Symposium on Neurovirology and 10th Conference on Neuroscience of HIV Infection, Juni 19-22, 2002, Düsseldorf, Deutschland

S. Sbiera and K. Dörries “Human Polyomavirus JC association with peripheral blood cells” First International Conference Polyomaviruses and Human Diseases: Basic and Clinical Perspectives, Mai 8-10, 2003, Pozzolatice, Florenz, Italien (Journal of Neurovirology, 9, Supplement 2, 68)

K. Dörries, **S. Sbiera**, C. Eggers, G. Arendt and R. Dörries “JCV persistence in peripheral blood and the CNS” First International Conference Polyomaviruses and Human Diseases: Basic and Clinical Perspectives, Mai 8-10, 2003, Pozzolatice, Florenz, Italien (Journal of Neurovirology, 9, Supplement 2, 51)

K. Dörries, **S. Sbiera** and R. Dörries “JCV persistence in the CNS and peripheral blood of immunocompetent individuals” 2nd International EMBO Workshop on the structural biology of small DNA tumor viruses, April 22-27, 2003, Abbazia di Pontignano, Sienna, Italien

K. Dörries, **S. Sbiera**, G. Arendt and R. Dörries “Human polyomavirus infection in serum and peripheral blood cells of immun impaired and healthy individuals” ICGEB DNA Tumor Virus Meeting, Juli 15-20, 2003, International Centre for Genetic Engineering and Biotechnology, Stazione Marittima Congress Centre, Trieste, Italien

K. Dörries, **S. Sbiera**, G. Arendt and R. Dörries “Interaction of human polyomaviruses with cells of the hematopoietic system” 2nd International Symposium Polyomaviruses and Human Diseases and 4th International Symposium for Zoonosis Control: Emerging Virus Infections”, Juni 11-13, 2004, Sapporo, Japan

K. Dörries, **S. Sbiera** and R. Dörries “HuPyV JC regularly circulates in peripheral blood of persistently infected individuals” DNA Tumor Viruses Conference, Juli 13-18, 2004, University of Wisconsin, Madison, USA

A. Welcker, **S. Sbiera**, G. Arendt, I.W. Husstedt and K. Dörries “Transcriptional activity of the human polyomavirus JC in peripheral blood cells” Jahrestagung der Gesellschaft für Virologie, März 16-19, 2005, Hannover, Deutschland

K. Dörries, **S. Sbiera**, A. Welcker and R. Dörries “Association or infection: intracellular localization of human polyomavirus DNA in peripheral blood cell subpopulations” EMBO Workshop: Structural Basis of Papovavirus Biology, April 11-16, Abbazia di Pontignano, Siena, Italien

K. Dörries, **S. Sbiera**, A. Welcker and R. Dörries “Human Polyomavirus JC in hematopoietic cells” International Workshop on JC Virus, PML and Multiple Sclerosis, Juni 3-4, 2005, Temple University, Philadelphia, USA

S. Sbiera, A. Welcker and K. Dörries “Circulating hematopoietic cells as targets for JCV persistent infection” DNA Tumor Virus Meeting, Juli 19-24, 2005, Cambridge, UK

K. Dörries, **S. Sbiera**, I.W. Husstedt, G. Arendt and R. Dörries “Association of human polyomavirus DNA with peripheral blood cell subpopulations” 3rd International Conference Polyomaviruses and Human Diseases: Basic and Clinical Perspectives, September 12-14, 2005, Providence, USA

S. Wortmann, **S. Sbiera**, D. Kühner, M. Wobser, P. Adam, L. Kraus, J.C. Becker, B. Allolio and M. Fassnacht “Survivin, ein erfolgsversprechender Angriffspunkt für eine Immuntherapie bei Patienten mit Nebennierenkarzinom” 51 Symposium der Deutsche Gesellschaft für Endokrinologie (DGE) und 12 Jahrestagung der Österreichischen Gesellschaft für Endokrinologie und Stoffwechsel (ÖGES), März 7-10, 2007, Salzburg, Österreich

S. Sbiera, S. Wortmann, L. Kraus, D. Kühner, P. Adam, B. Allolio and M. Fassnacht “Fibroblast Activation Protein (FAP) as target antigen in ACC immunotherapy” 5th Bad Brückenaauer Wintertagung, März 16-17, 2007, Bad Brückenaau, Deutschland

S. Sbiera, S. Wortmann, L. Kraus, T. Thamm, D. Kühner, M. Wobser, J.C. Becker, P. Adam, B. Allolio and M. Fassnacht “Survivin: candidate protein for immunotherapy in patients with adrenocortical carcinoma” 9th Annual Meeting Young Active Research, November 5-7, 2007, Lübeck, Deutschland

S. Sbiera, S. Wortmann, L. Kraus, T. Thamm, D. Kühner, S. Schull, M. Wobser, J.C. Becker, P. Adam, B. Allolio and M. Fassnacht “Survivin as potential target-protein for immunotherapy in patients with adrenocortical carcinoma” Cancer Immunotherapy (CIMT) Annual Meeting, Mai 15-16, 2008, Mainz, Deutschland

S. Sbiera, S. Schull, H.U. Voelker, L. Kraus, F. Beuschlein, H.S. Willenberg, S. Hahner, B. Allolio, M. Fassnacht “Steroidogenic factor 1 - a valuable diagnostic and prognostic tool in patients with adrenocortical carcinoma“ 11th European Congress of Endocrinology, April 25-29, Istanbul, Türkei

S. Sbiera, D. Kühner, S. Wortmann, P. Adam, H.U. Voelker, L. Kraus, M. Beyer, M. Quinkler, H.S. Willenberg, U. Flierl, D. Weismann, S. Hahner, B. Allolio, M. Fassnacht “Endocrine gland-derived vascular endothelial growth factor (EG-VEGF) and its receptors in adrenocortical carcinoma“ 11th European Congress of Endocrinology, April 25-29, 2009, Istanbul, Türkei

S. Sbiera, S. Schull, G. Assie, H.U. Voelker, L. Kraus, F. Beuschlein, H.S. Willenberg, S. Hahner, J. Bertherat, B. Allolio and M. Fassnacht “Diagnostic and Prognostic Value of Steroidogenic Factor 1 (SF-1) in Adrenal Tumors“ 9. Deutsche Nebennierenkonferenz und Tagung der Sektion Nebenniere, Hypertonie und Steroide der Deutschen Gesellschaft für Endokrinologie, Januar 15-16, 2010, Berlin, Deutschland

S. Sbiera, M. Beyer, S. Schull, L. Kraus, M. Quinkler, F. Beuschlein, B. Allolio and M. Fassnacht “Individualized streptozotocin therapy in adrenocortical carcinoma: The role of GLUT-2 and MGMT“ 53 Symposium der Deutsche Gesellschaft für Endokrinologie (DGE) und Jahrestagung der Slowakischen Gesellschaft für Endokrinologie, März 3-6, 2010, Leipzig, Deutschland

T. Dexneit, **S. Sbiera**, S. Schnull, J. van den Brandt, L. Kraus, M. Beyer, R. Mlynski, S. Wortmann, H.M. Reichardt, B. Allolio and M Fassnacht "Influence of short-term glucocorticoid therapy on regulatory T cells" 53 Symposium der Deutsche Gesellschaft für Endokrinologie (DGE) und Jahrestagung der Slowakischen Gesellschaft für Endokrinologie, März 3-6, 2010, Leipzig, Deutschland

S. Sbiera, M. Kroiss, Melanie Beyer, Felix Gardill, Laura Wiemer, Martina Zink, S. Hahner, T. van der Merwe, A. Schirbel, B. Allolio and M. Fassnacht "Towards the elucidation of mitotane action – results from an *in vitro* approach", 54 Symposium der Deutsche Gesellschaft für Endokrinologie (DGE), März 30-April 2, 2011, Hamburg, Deutschland

Silviu Sbiera, Thomas Dexneit, Sebastian Schnull, Hans-Ulrich Voelker, Luitgard Kraus, Sonja Steinhauer, Bruno Allolio and Martin Fassnacht "The role of circulating and tumor infiltrating T-cells on clinical outcome in adrenocortical carcinoma", Joint 15th International Congress of Endocrinology and 14th European Congress of Endocrinology, Mai 5-9, 2012, Florenz, Italien

Würzburg,